THE GAS CHROMATOGRAPHY OF AMMONIA:

Heterogeneous systems containing silver ammines

A thesis submitted to the University of Cape Town

for the degree of Doctor of Philosophy

by

AARON LOUIS RUTENBERG

1963

PREFACE

I would like to express my gratitude and thanks to Dr. A.H. Spong for offering me the chance to do the work described in this thesis, and for giving me his advice and help throughout its course.

My thanks are also due to Mr. M. Kort for allowing me to use his quickfit glassware for the distillation of solvents, and to Mr. B. Harris for his assistance in the drawing of the illustrations.

To Francois du Bois Sadie, and Ralph Torrington, my appreciations, for their interest and help in this work.

A.L. Rutenberg.

Department of Chemistry,
University of Cape Town,
October, 1963.

SUMMARY

The gas-liquid chromatography of ammonia on fixed phases consisting of silver salts dissolved in high boiling organic liquids, yielded chromatograms showing a peak followed by a plateau or plateaux of decreasing height. This phenomenon was ascribed by du Plessis to the formation of solid ammine complexes, the plateau height being some function of the dissociation pressure of the complex. Calibration of the detector response to ammonia, enabled the dissociation pressures of the complexes to be computed from the plateau heights.

Certain silver salt-solvent systems gave chromatograms, whose plateaux showed decay of the rear end, or whose heights divided into two levels. This was attributed to rate-effects caused by slow decomposition of the complex.

Kinetic considerations and phase rule interpretation of the plateau portion of the chromatogram, yielded quantitative information about the complexes, while the investigation of temperature effects gave a measure of the bond strength between the ammonia and silver. A modified tensimetric experiment gave results supporting the quantitative information derived from the chromatograms.

Freshly prepared columns absorbed ammonia due to the formation of a solid complex, whose dissociation pressure lay below the limits of the detector response. The ratio of the absorbed ammonia to the amount of silver in the column gave the apparent molar composition of the complex.

The work described in this thesis has shown that the chromatographic flow system affects the apparent values of the thermodynamic quantities associated with the complexes, and this has been accounted for.

This work also showed that the process underlying solid complex formation in the liquid phase is the same as for homogeneous

complex formation in the liquid phase, which has been reported in the literature. The appearance of a plateau in the case of solid complexes is due to an invariant state prevailing under constant temperature conditions, since the number of phases formed is sufficient to yield this state, and hence define the pressure variable. The information obtained from the literature, enabled an alternative chromatographic method of investigating solid ammine complexes to be proposed for future work.

Finally the chromatography of ammonia on the toluidine isomers as liquid substrates was carried out in order to investigate possible hydrogen bonding effects.

CONTENTS

SUMMARY

The gas-liquid chromatography of ammonia on fixed phases consisting of silver salts dissolved in high boiling organic liquids, yielded chromatograms showing a peak followed by a plateau or plateaux of decreasing height. This phenomenon was ascribed by du Plessis to the formation of solid ammine complexes, the plateau height being some function of the dissociation pressure of the complex. Calibration of the detector response to ammonia, enabled the dissociation pressures of the complexes to be computed from the plateau heights.

Certain silver salt-solvent systems gave chromatograms, whose plateaux showed decay of the rear end, or whose heights divided into two levels. This was attributed to rate-effects caused by slow decomposition of the complex.

Kinetic considerations and phase rule interpretation of the plateau portion of the chromatogram, yielded quantitative information about the complexes, while the investigation of temperature effects gave a measure of the bond strength between the ammonia and silver. A modified tensimetric experiment gave results supporting the quantitative information derived from the chromatograms.

Freshly prepared columns absorbed ammonia due to the formation of a solid complex, whose dissociation pressure lay below the limits of the detector response. The ratio of the absorbed ammonia to the amount of silver in the column gave the apparent molar composition of the complex.

The work described in this thesis has shown that the chromatographic flow system affects the apparent values of the thermodynamic quantities associated with the complexes, and this has been accounted for.

This work also showed that the process underlying solid complex formation in the liquid phase is the same as for homogeneous

complex formation in the liquid phase, which has been reported in the literature. The appearance of a plateau in the case of solid complexes is due to an invariant state prevailing under constant temperature conditions, since the number of phases formed is sufficient to yield this state, and hence define the pressure variable. The information obtained from the literature, enabled an alternative chromatographic method of investigating solid ammine complexes to be proposed for future work.

Finally the chromatography of ammonia on the toluidine isomers as liquid substrates was carried out in order to investigate possible hydrogen bonding effects.

INTRODUCTION

The work done in this thesis was carried on directly from work submitted by du Plessis for the Ph.D. degree.

Originally, the gas chromatography of ammonia was started in an attempt to separate $N^{14}H_3$ and $N^{15}H_3$. However the discovery of plateau type chromatograms led du Plessis to the conclusion, that the elucidation of these chromatogram characteristics was a necessary prelude to the isotope separation.

His findings were not conclusive and the work undertaken in this thesis was an attempt to unravel the problem further.

Section 1 of this thesis gives a brief survey of gas chromatography, and shows its application to the study of chemical reactions. Section 2 gives the theory for the interpretation of the experimental results in section 4, while section 3 describes the apparatus and procedures used. In section 5, the results are correlated and the work done discussed. Proposals for future work are suggested.

SECTION 1

HISTORICAL

1.1 Survey of gas chromatography

The use of chromatography as an analytical tool is based on the differences in the values of the partition coefficients of substances between two phases, one of which is stationary, and usually of great surface area, the other a moving fluid phase. This technique was first truly realized in 1903, when Tswett[1] separated the extract of green leaves into several components. In the separation, he obtained several bands having various shades of green and yellow, and these coloured bands led him to misname the process "chromatography". It was not until 1931 that the idea of chromatography was revived, when Kuhn and Lederer[2] used it to separate α and β - carotene. Till then elution chromatography was confined to a static solid adsorbent and a flowing liquid.

The extention of chromatography to liquid-liquid and gas-liquid phase systems was introduced by Martin and Synge[3] in 1941, but the gas-liquid concept was only put to the experimental test for the first time by James and Martin[4] in 1952.

Between 1941 and 1952 displacement and frontal chromatography were realized. Displacement chromatography pioneered by Tiselius[5] and Claesson[6], is a form of chromatography where solutes or adsorbates compete with a displacer vapour, the partition coefficient of the vapour between the phases being greater than any of the solutes or adsorbates. This results in the vapour displacing the mixture of solutes or adsorbates from the stationary phase, each component of the mixture displacing the components with a smaller partition coefficient than its own. When the column is saturated by the displacer, a series of

adjacent zones of components emerge from the column, the zone length being proportional to the amount of the corresponding component. Displacement chromatography has several times been used with success in gas-solid systems.[7 - 10]

Frontal chromatography applied by Claesson[9] in 1946 to gas-solid systems has also been extended to gas-liquid systems.[7,8] In this method the components of the mixture emerge in a series of zones, the first zone containing the least strongly retained component, which emerges at the same concentration as it entered the column. Subsequent components appear in turn contaminated by the preceding substances.

Since 1952, gas chromatography has undergone a prodigious development. Its analytical application embraces an immense variety of substances, ranging from complex hydrocarbon mixtures, to analysis for example of the gaseous emanation products of the onion.[11]

Gas-liquid chromatography has far outstripped gas-solid chromatography as an analytical tool, as obviously gas-liquid interactions afforded far greater variety in obtaining separations of components than gas-solid interactions. Furthermore, retention times are generally very much greater for adsorption than for solution, while non-linear adsorption isotherms are extremely common. Solid adsorbents have properties dependent on origin, precolumn treatment and subsequent history. Catalytic activity of the adsorbent also gives rise to problems. These objections are met with to a far lesser extent in gas-liquid systems.

Efficient separations of mixtures in gas-liquid chromatography have been greatly increased with the introduction of such theories as put forward by van Deemter, Zuiderweg and Klinkenberg[12], where the factors affecting zone spreading have

been outlined, and a measure of the column efficiency, height equivalent to a theoretical plate (H.E.T.P.) has been computed, while Golay, following his theoretical studies[13,14] showed that with capillary type columns[15] one could obtain in practice, extremely efficient separations.

Gas chromatography has also been utilized for non-analytical purposes. Studies in thermodynamics, kinetics and diffusion are some of the fields in which it has been fruitfully employed.

1.2 Study of chemical reactions by gas chromatography

The wide analytical application of gas-liquid chromatography led to the idea of utilizing unusual solute-solvent interactions for specific types of separations[16 - 22]. Thus Langer, Zahn and Pantazoplos[20] for instance, used tetrahalophthalate esters for aromatic separations, suggesting charge-transfer interactions as being responsible for the selectivities observed.

Extension of this idea to the use of metals dissolved in the liquid phase and forming adducts with specific compound types[23 - 32] led logically to the use of gas chromatography as a means of studying these complexes. One method[24] consisted of comparing the retention times of substances on metal containing liquid substrates (complexes of the transition metals) with the retention times for liquids of very similar chemical composition, but containing either no metal atom, or one which has far weaker complexing properties. Thus the specific complex interaction between the metal and ligand could be examined.

In a large number of instances silver salt solutions have been used for preferential retardation of unsaturated hydrocarbons and other organic compounds, as a result of the complexing properties of silver[25 - 32], and this has led to the determination of equilibrium constants of silver-olefin complexes by gas-liquid chromatography[33, 34].

Muhs and Weiss[33] using silver nitrate ethylene glycol columns obtained equilibrium data for the reaction

$$\left[U_{(l)}\right] + \left[AgNO_{3(l)}\right] \rightleftharpoons \left[(AgNO_3 \cdot U)_{(l)}\right] \quad \ldots\ldots\ldots\ldots \quad (A)$$

where $\left[U_{(l)}\right]$ = concentration of the unsaturated hydrocarbon in the ethylene glycol.

$\left[AgNO_{3(l)}\right]$ = concentration of silver nitrate.

$\left[(AgNO_3 \cdot U)_{(l)}\right]$ = concentration of complex formed.

The unsaturated hydrocarbons ranged from aliphatic and alicyclic olefines to alkynes and aromatic compounds.

They assumed instantaneous equilibration of reaction (A), as well as a 1 : 1 molar ratio of the hydrocarbon to silver nitrate, on the basis of previous studies of these complexes.

The apparent partition coefficient, K', is defined as

$$K' = \frac{\left[U_{(l)}\right] + \left[(AgNO_3 \cdot U)_{(l)}\right]}{\left[U_{(g)}\right]}$$

where $\left[U_{(g)}\right]$ = concentration of hydrocarbon in the gas phase

K' can be written as

$$K' = K + K \cdot K_{(l)} \cdot \left[AgNO_{3(l)}\right] \quad \ldots\ldots\ldots\ldots\ldots\ldots \quad (1)$$

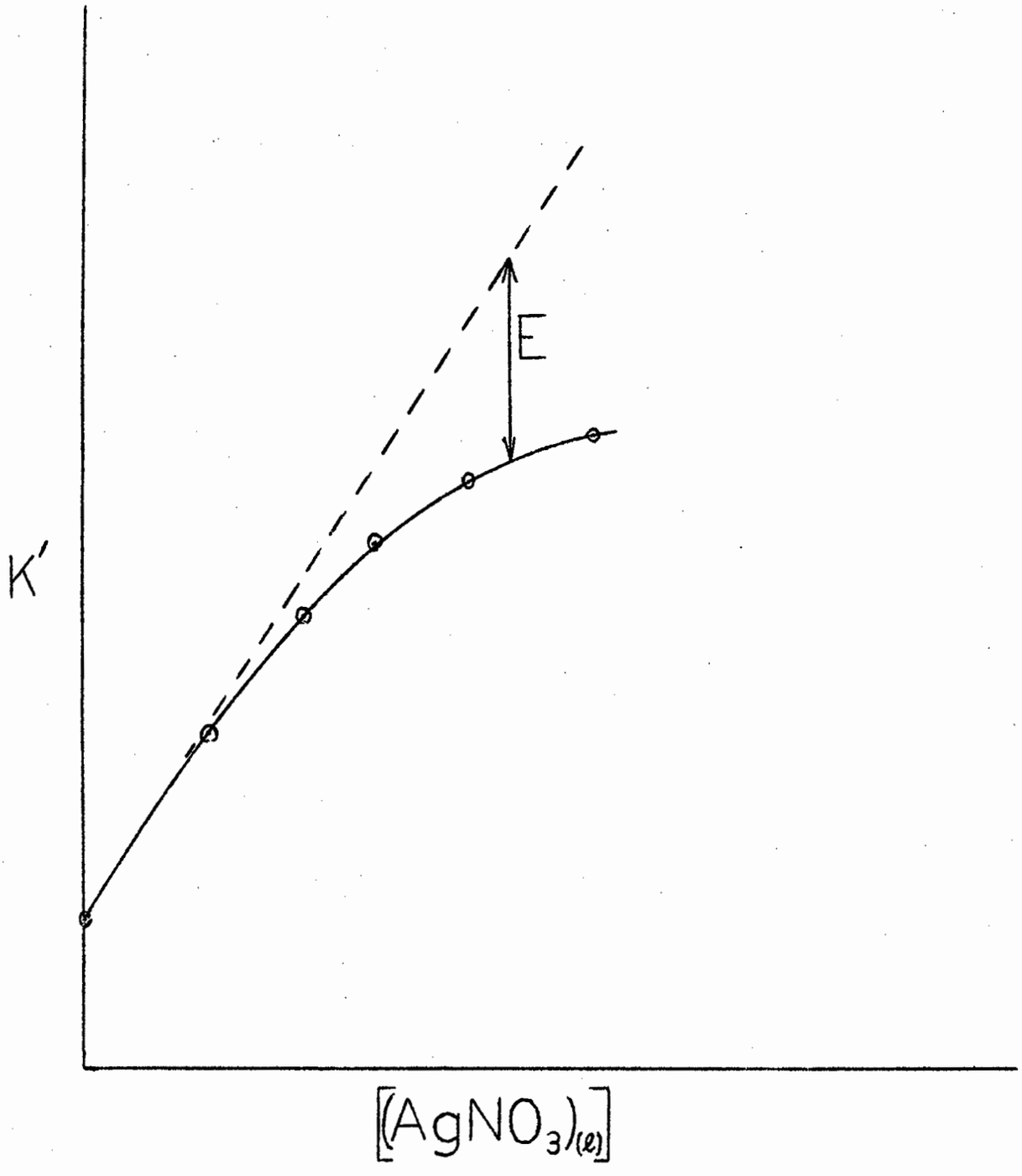

FIGURE 1. SALTING-OUT EFFECT OF SILVER NITRATE.

where K = partition coefficient of the hydrocarbon between the gas phase and pure liquid substrate.

$K_{(1)}$ = equilibrium constant for reaction (A)

K' is related to the retention volume of the peak maximum of the elution curve (see 2.2 p.16) by the relationship

$$K' = \frac{V^{o}_{R'}}{V_F}$$

where $V^{o}_{R'}$ = retention volume of peak maximum in the stationary phase.

V_F = volume of liquid stationary phase in the column.

$V^{o}_{R'}$ will increase with increasing silver nitrate concentration as more of the hydrocarbon is complexed. Utilizing this variation of $V^{o}_{R'}$, a plot of K' as a function of $[Ag\ NO_{3(1)}]$ should have given a linear relationship with a slope $K\ K_{(1)}$ and an intercept K (K is actually obtained experimentally).

However a salting-out effect due to the ionic effect of the silver salt in solution resulted in a curvature as shown in fig. 1.

It was empirically observed that the error involved, E, in using (1) conformed to the relationship

$$E = v.[Ag\ NO_{3(1)}]^{w}$$

where v and w are empirically determined constants

Thus (1) became

$$K' = K + K\ K_{(1)}[Ag\ NO_{3(1)}] - v[Ag\ NO_{3(1)}]^{w} \quad \ldots\ldots(2)$$

Equation (2) was used for determining $K_{(1)}$

Gil-av and Herling[34] also using silver nitrate in ethylene glycol, determined $K_{(1)}$ in an identical fashion for unsaturated hydrocarbons, but took into account the salting-out effect by measuring the retention volumes of the hydrocarbons on a column containing sodium nitrate in ethylene glycol at the same concentration as the silver solution.

The system postulated in determining $K_{(1)}$ is the same as the one used in considering the silver ammine complexes in this thesis (2.3).

Kinetic studies by gas-liquid chromatography have been shown to be feasible. This has been achieved by using the chromatographic column as the reaction chamber[35]. Aliphatic dienes were passed over chloromaleic anhydride as the column liquid to form non-volatile addition products. The unreacted amount of diene was measured from the chromatogram, while the conversion rate of the reaction was obtained by varying the flow-rate, and hence the contact time.

Emmett and others[36 - 41] have shown that connecting a catalytic reaction chamber to the head of a chromatographic column and sweeping the reactant through the chamber over the catalyst, and then directly into the column together with the subsequent products for analysis, enabled studies of catalytic reactions to be made.

Tamaru[41] suggested using the chromatographic column itself as the reaction chamber, with the solid support as the catalyst. He showed that this idea offered a method for studying adsorption under reaction conditions.

Tamaru's suggestion was put into effect by Bassett and Habgood[43] who investigated the case of a first order surface catalysed reaction, with the surface reaction as the

rate controlling step. This method permitted them to determine the extent of adsorption under reaction conditions, and hence ascertain the rate constant for the reaction on the catalyst surface, the activation energy of the surface reaction, as well as the heat of adsorption on the catalyst.

1.3 Elucidation of solid complexes by non-chromatographic methods

Equilibrium pressure data of solid complexes are usually obtained by manometric measurements in a tensimeter, while the composition of the complex is determined separately by analysis[44 - 51]. Elucidation of crystalline silver nitrate-olefin complexes and copper-olefin complexes has been achieved by tensimetric and analytical studies[52 - 62].

du Plessis[63] investigated solid silver ammine complexes tensimetrically and found agreement with chromatographic measurements.

1.4 Prior investigation of solid ammine complexes

The gas chromatography of ammonia on certain high boiling organic liquid substrates, in which silver nitrate or silver perchlorate had been previously dissolved, resulted in chromatograms consisting of a peak followed by a plateau or a series of plateaux of progressively decreasing height. This phenomenon was first investigated by du Plessis and Spong[64,65].

They suggested that the normal gas liquid distribution of ammonia was distorted by the formation of a solid ammine complex which only began to decompose once the value of the ammonia gas pressure dropped to the dissociation pressure value of the solid complex, as a result of the removal of the ammonia in the gas phase by the carrier gas. Thus as the

ammonia band traversed the column, it began to separate out into two parts, the peak followed by the plateau or plateaux, each plateau height being determined by the dissociation pressure of the complex.

The growth of the plateau at the expense of the peak as the ammonia band progressed through the column, naturally led to the eventual disappearance of the peak into the plateau, when the variables such as column length, flow-rate, silver concentration and sample size of ammonia injected, attained certain values. For an ammonia sample size below a critical value, no plateau was discerned as the amount of complex formed was so small that the ammonia pressure never attained the dissociation pressure value.

Freshly prepared columns absorbed ammonia due to the formation of a solid ammine complex with a dissociation pressure below the detection limits of the katharometer. Further addition of ammonia resulted in the emergence of a plateau type chromatogram, with an appreciable dissociation pressure.

du Plessis postulated the following process for the complexing reactions:

$$Ag\,X_{(l)} + x\,NH_{3(g)} \rightleftharpoons Ag\,X\,(NH_3)_{x(s)} \qquad \text{pd - very low}$$

$$Ag\,X\,(NH_3)_{x(s)} + y\,NH_{3(g)} \rightleftharpoons Ag\,X\,(NH_3)_{(x+y)(s)} \qquad \text{pd - appreciable}$$

By deriving formulae for the length of column occupied by the plateau zone, he computed the amount of silver in that length of column. The response of the detector to ammonia was calibrated, to enable the amount of ammonia in

the plateau zone to be calculated. The molar ratio of ammonia to silver was then determined on the assumptions that the concentration of complex throughout the plateau zone was constant, and that instantaneous equilibration of the complex occurred.

The values of y that were obtained, gave inconclusive results, and seemed to be dependent on sample size of ammonia and silver concentration of the column.

SECTION 2

THEORETICAL CONSIDERATIONS

2.1 Symbols used

All symbols are defined where they are introduced. The symbols used in this section are listed below, in alphabetical order, for easy reference:-

A	Area of chromatogram
Ag X	Silver salt
$Ag\ X(NH_3)_x(s)$	Complex I
$Ag\ X(NH_3)_{(x+y)}(s)$	Complex II
a	Average interstitial column area
C	Calibration constant of katharometer
C_I and C_{II}	Geometrical constants relating the surface areas of complex I and complex II to their mole numbers
c	Recorder chart speed
F (K)	Equilibrium function
F'(K)	Apparent equilibrium function
ΔH	Overall heat of reaction of complex II
ΔH_1	Heat of solution of ammonia in the organic solvent
ΔH_2	Heat of reaction of complex II
h	Height of experimental chromatogram at any instant
K	Partition coefficient
k_1, k_2 etc.	Rate constants of the reactions
L	Length of column

L_1	Length of zone II(a)
L'_1	Length of zone II(a) as it starts emerging from the column
n	Sample size of ammonia in μmoles
n_g	Moles of ammonia in the gas phase
n_l	Moles of ammonia in the liquid phase
n_{NH_3}	Initial number of moles of ammonia associated with the reaction forming complex II
n_I	Initial number of moles of complex I
n_{II}	Moles of complex II formed
p_d	Dissociation pressure of complex I or II
p_{NH_3}	Pressure of ammonia
p	Pressure of carrier gas
p_i	Value of p at column inlet
p_L	Value of p at distance L'_1 from column outlet
p_o	Value of p at column outlet
R	Gas constant
S_I	Surface area of solid complex I
S_{II}	Surface area of solid complex II
T	Absolute temperature
t	Time after sample injection
t_b	Value of t when zone II(a) starts emerging
t_e	Value of t when emergence of zone II(a) is complete.
t_e'	Value of t when emergence of corrected zone II(a) is complete

t_f	Residence time of migrant zone in the stationary phase
t_g	Residence time of carrier gas
t_r	Residence time of migrant zone in the column
V_c	Linear velocity of concentration zone
V_f	Volume of liquid fixed phase in column.
V_g	Interstitial volume of column
V_1	Linear carrier gas velocity
V_1'	Linear carrier gas velocity at column outlet
V_R	Retention volume of zone
V^o_R	Retention volume of zone corrected for carrier gas compressibility
$V^o_R{}'$	Retention volume of zone in stationary phase
V_t	Volumetric flow-rate of carrier gas
V_t'	Volumetric flow-rate of carrier gas at column outlet
$\bar{V}_t$	Average volumetric flow-rate of carrier gas across a length of column L_1
x	Molar ratio of NH_3 to Ag X in complex I
x_1	Distance from upstream end of column
y	Molar ratio of NH_3 to Ag $X(NH_3)_x$ in complex II
Δ	Moles of ammonia converted to complex II
ε	Error incurred in assumed y values

2.2 Determination of distribution functions and thermodynamic data by gas-liquid chromatography

Consider a perfectly uniform gas-liquid chromatographic

column, into which the substance under consideration is introduced. It will distribute itself between the moving gaseous and stationary liquid phases, in accordance with Henry's law. Molecules of the substance in each phase are considered to be in the same dynamic equilibrium with each other at all times, and thus the fraction of time spent by each mole of substance in the gaseous or liquid phase is proportional to its number of moles in that phase. Since molecules of the substance will only traverse the column when in the moving phase, the net rate of movement of such a dynamically equilibrated zone of substance, will be given by the expression:

$$V_c = V_l \cdot \frac{n_g}{n_g + n_l} \qquad \ldots\ldots\ldots\ldots\ldots\ldots\ldots\ldots \quad (3)$$

where V_c = linear velocity of concentration zone

V_l = linear velocity of carrier gas

n_g = number of moles of substance in the gas phase,

and n_l = number of moles of substance in the liquid phase.

The fundamental distribution function in chromatography, the partition coefficient, K, is defined for gas-liquid chromatography as,

$$K = \frac{n_l \cdot V_g}{n_g \cdot V_f} \qquad \ldots\ldots\ldots\ldots\ldots\ldots\ldots\ldots \quad (4)$$

where V_g = interstitial volume of column

V_f = volume of liquid fixed phase in the column

Substitution of (4) in (3) gives

$$V_c = V_l \cdot \left(\frac{1}{1 + \frac{K \cdot V_f}{V_g}} \right) \qquad \ldots\ldots\ldots\ldots\ldots\ldots\ldots\ldots \quad (5)$$

Now $V_c = \frac{L}{t_r}$ $\qquad \ldots\ldots\ldots\ldots\ldots\ldots\ldots\ldots \quad (6)$

and $V_l = \frac{V_t}{a}$ ..... (7)

where L = packed length of column

t_r = retention time of zone

a = interstitial area of column

V_t = volumetric flow-rate of carrier gas

Thus (5) becomes on substituting (6) and (7)

$$\frac{L}{t_r} = \frac{V_t}{a} \times \left(\frac{1}{1 + \frac{K \cdot V_f}{V_g}} \right) \quad \ldots\ldots (8)$$

Since $L \cdot a = V_g$ ..... (9)

$t_r \cdot V_t = V_R$ ..... (10)

and V_R = retention volume of the zone, which is equal to the volume of carrier gas swept through the column in time t_r, equation (8) becomes on substituting (9) and (10) and rearranging

$V_g + KV_f = V_R$

whence $K = \frac{V_R - V_g}{V_f}$ ..... (11)

The idealized column just described does not occur in practice as gases are highly compressible, and their volumetric flow-rates increase as they approach the column exit, due to the pressure drop across the column, while the assumption that K is independent of concentration is only true for ideal solutions. Furthermore, the ideal zone undergoes band-broadening, due to such causes as diffusion in the gas phase, liquid diffusion, finite rate of transfer of molecules of the zone between the phases, while the time spent by each molecule in the column will not be the same, as the devious paths in the packing have different lengths.

The compressibility of the gas can be taken into account[66] by assuming ideality for the gas phase, so that V_R is related to the ideal retention volume, V^o_R by

$$V^o_R = \frac{3\,(p_i/p_o)^2 - 1}{2\,(p_i/p_o)^3 - 1} \cdot V_R$$

where p_i = pressure of moving phase at column inlet

p_o = pressure of moving phase at column outlet

Equation (11) then becomes

$$K = \frac{V^o_R - V_g}{V_f} \qquad \ldots\ldots\ldots\ldots\ldots\ldots\ldots\ldots \quad (12)$$

Values of K (or related quantities) have often been reported in the literature[67 - 69], and their good agreement[67, 70 - 72] with values obtained by other techniques, has verified the soundness of the chromatographic method of determining K.

Now the retention time of the zone is composed of two parts, i.e., $t_r = t_g + t_f$

where t_g = residence time of carrier gas in the column

t_f = residence time of migrant zone in the stationary phase

As $V^o_R = V_t \cdot t_r = V_t\,(t_g + t_f) = V_g + V^o_R{}'$

where $V^o_R{}'$ = retention volume of zone in the stationary phase,

equation (12) thus becomes

$$K = \frac{V^o_R{}'}{V_f} \qquad \ldots\ldots\ldots\ldots\ldots\ldots\ldots\ldots \quad (13)$$

Equation (13) is more acceptable than (12) in determining K, as it has been pointed out[73], that V^o_R is influenced not only by the interstitial volume of the column, but by the void volumes of the sample injector and detector, and is hence of limited use.

The band-broadening factors mentioned, result in a peak-shaped differential chromatogram, which is symmetrical for ideal solutions, and whose peak maximum[67] obeys equation (13).

If cognizance is taken of the temperature dependence of V_f in equation (13), the temperature variation of K can be expressed in the usual form

$$\ln K = -\frac{\Delta H_1}{RT} + \text{constant} \quad \ldots\ldots\ldots\ldots\ldots\ldots \quad (14)$$

where ΔH_1 = heat of solution of solute in solvent

R = gas constant

T = absolute temperature

Thus relevant thermodynamic data can be obtained. Relationship (14) has been shown to hold to a good approximation for a large number of systems studied[67, 68, 74 - 78].

For non-ideal solutions, V^{o}_{R} becomes concentration dependent[68], and the peak shape asymmetrical. Two cases can be distinguished[67] :

(a) for "under-ideality", i.e., "negative" deviations from Raoults law ($\log \gamma < o$) where γ = activity coefficient, the value of K decreases with increasing concentration. Thus less concentrated regions of the band move more slowly than the higher concentrations, which results in a sharpening of the band front, and a broadening of the trailing edge of the band in its migration through the column. As the maximum concentration in the band falls, due to band-broadening, the net motion of the band becomes relatively slower, approaching that obtained in the limiting case of zero concentration in the solvent, and hence approaching ideality. Thus the

measured retention volume is less than the limiting value of V^{o}_{R}, and approaches it in the limiting case of a vanishingly small sample size.

(b) for "over-ideality" i.e., "positive" deviations from Raoults law ($\log \gamma > o$), the exact converse holds to case (a), the band having a diffuse front and a sharp rear, while the measured retention volume is greater than the limiting value of V^{o}_{R}, and approaches it with decrease in solute concentration.

A procedure for obtaining V^{o}_{R} for non-ideal systems has been proposed by Keulemans[79], based on the variation of the height equivalent to a theoretical plate (H.E.T.P.) with sample size, which has been reported to be linear[77, 80]. By extrapolation of the H.E.T.P. plot to zero sample size and utilization of the fact that the "final" or "initial" retention volume (which is independent of concentration and hence a constant) can be found from the intercept of the trailing rear end or broadened sloping front of the band with the time axis, the limiting value of V^{o}_{R} can be obtained. This is done by obtaining the hypothetical peak width, for a vanishingly small sample size from the extrapolated H.E.T.P. value. Subtracting or adding half the hypothetical peak width, either from the final, or to the initial retention volume, enables the limiting V^{o}_{R} value to be obtained. It has however also been reported[81], that the H.E.T.P. passes through a minimum contrary to the earlier reports[77, 80].

As the final or initial retention volume refers to the rate of motion of a zone of very low concentration at the edges of the solute band, the constancy of the retention volume is to be expected, as such a low concentration zone must be very

near ideality.

An alternative procedure to that of Keulemans has been put forward[67] in which the sample size introduced is the smallest possible, consistent with reproducibility and detector sensitivity. Under such low concentration conditions, the value of V^{o}_{R} obtained, is considered to be close enough to the true V^{o}_{R} value for its use to incur no serious error.

In measuring the values of K for ammonia in the various organic solvents (see section 4), this alternative procedure was used.

2.3 Processes by which solid ammine complexes can be formed

When ammonia is injected into a column containing a silver salt Ag X, dissolved in certain organic solvents, a solid complex, $Ag\ X\ (NH_3)_x(s)$ (complex I) is immediately formed. Practically all the silver is converted to the complex (see section 4, 4.5.2., 4.6.2., 4.7.2., 4.8.2.,) and it has a dissociation pressure p_d, too low to be detected. Additional injection of ammonia results in the formation of a further solid complex $Ag\ X\ (NH_3)_{(x+y)}(s)$ (complex II) with a discernible dissociation pressure, which manifests itself in a plateau type chromatogram.

Two possible processes are advanced in order to explain this phenomenon :

I
$$Ag\ X_{(l)} + xNH_{3(g)} \rightleftharpoons Ag\ X\ (NH_3)_x(s) \qquad p_d \text{ - very low}$$
$$Ag\ X\ (NH_3)_x(s) + y\ NH_{3(g)} \rightleftharpoons AgX(NH_3)_{(x+y)}(s) \qquad p_d \text{ - appreciable}$$

Alternatively,

II
$$NH_{3(g)} \rightleftharpoons NH_{3(l)}$$

$$AgX_{(l)} + x\,NH_{3(l)} \rightleftharpoons AgX(NH_3)_{x(s)} \qquad p_d \text{ - very low}$$

$$NH_{3(g)} \rightleftharpoons NH_{3(l)}$$

$$AgX(NH_3)_{x(s)} + y\,NH_{3(l)} \rightleftharpoons AgX(NH_3)_{(x+y)(s)}$$

$$p_d \text{ - appreciable}$$

Process I has already been discussed (see 1.4) and the stoichiometric results obtained by du Plessis were inconclusive. Controlled variation of the factors involved gave variable values of y, which indicated that process I is not a correct account of the reaction (see appendix I, p.118).

Process II has been assumed in this thesis, and the theoretical considerations in this section, coupled with the experimental results in section 4, tend to support the assumption.

2.3.1 Theoretical prediction of the shape of the ideal plateau type chromatogram

The normal gas-liquid distribution of ammonia is altered by the formation of a solid complex. As the ammonia migrates through the column, it begins to separate out into two parts, the head of the band, zone I, having the usual gas-liquid type distribution curve, the latter part of the band, zone II, having a gas-liquid distribution determined by the p_d value of the complex.

Zone I continually loses ammonia to zone II, which is only eluted from the liquid phase, once the ammonia gas pressure has dropped to the p_d value. If the residence time of the band in the column is long enough, all the ammonia in zone I

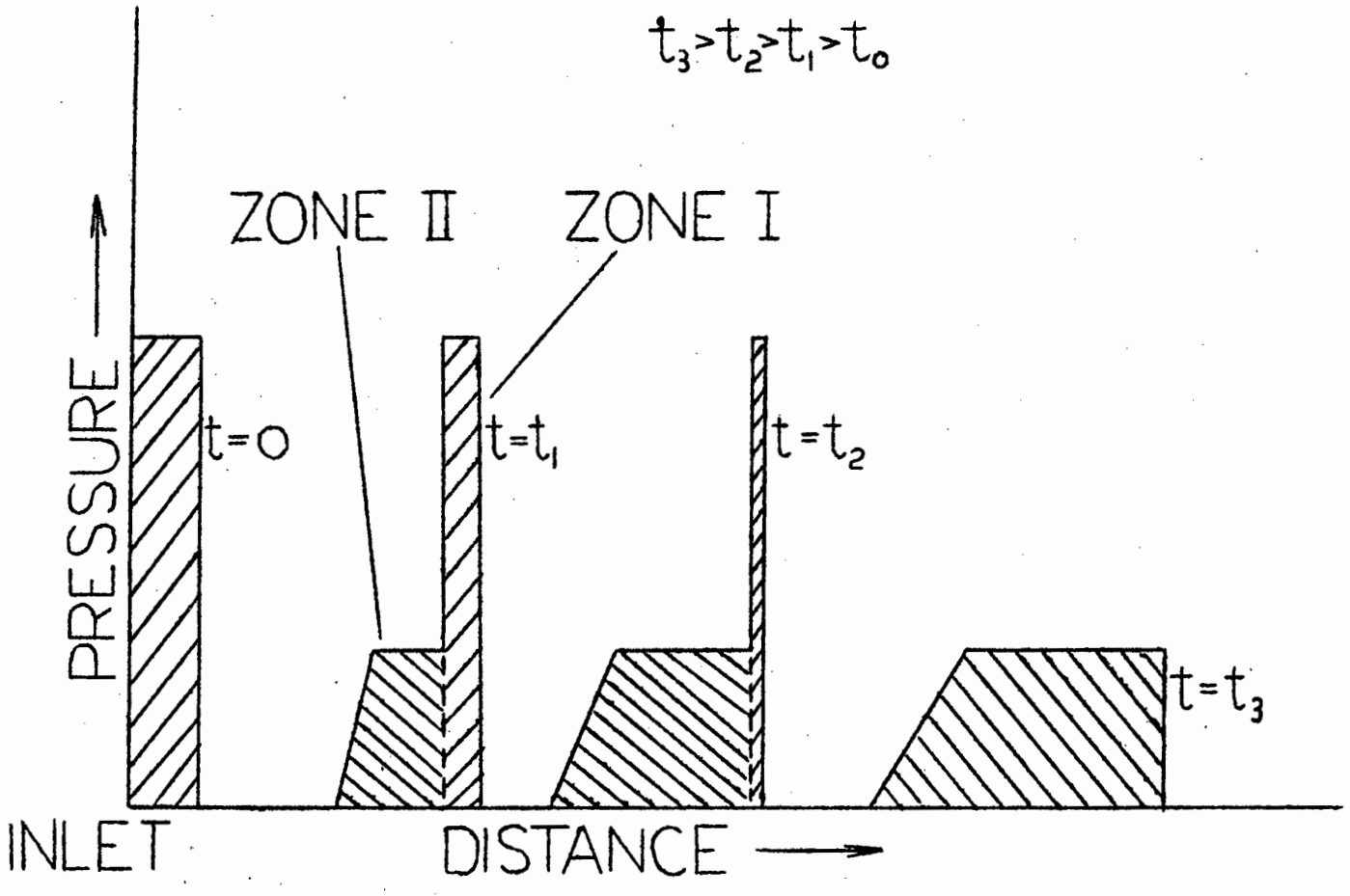

FIGURE 2. PLOT OF IDEAL AMMONIA BAND PRESSURE DISTRIBUTION AS A FUNCTION OF COLUMN DISTANCE TRAVERSED.

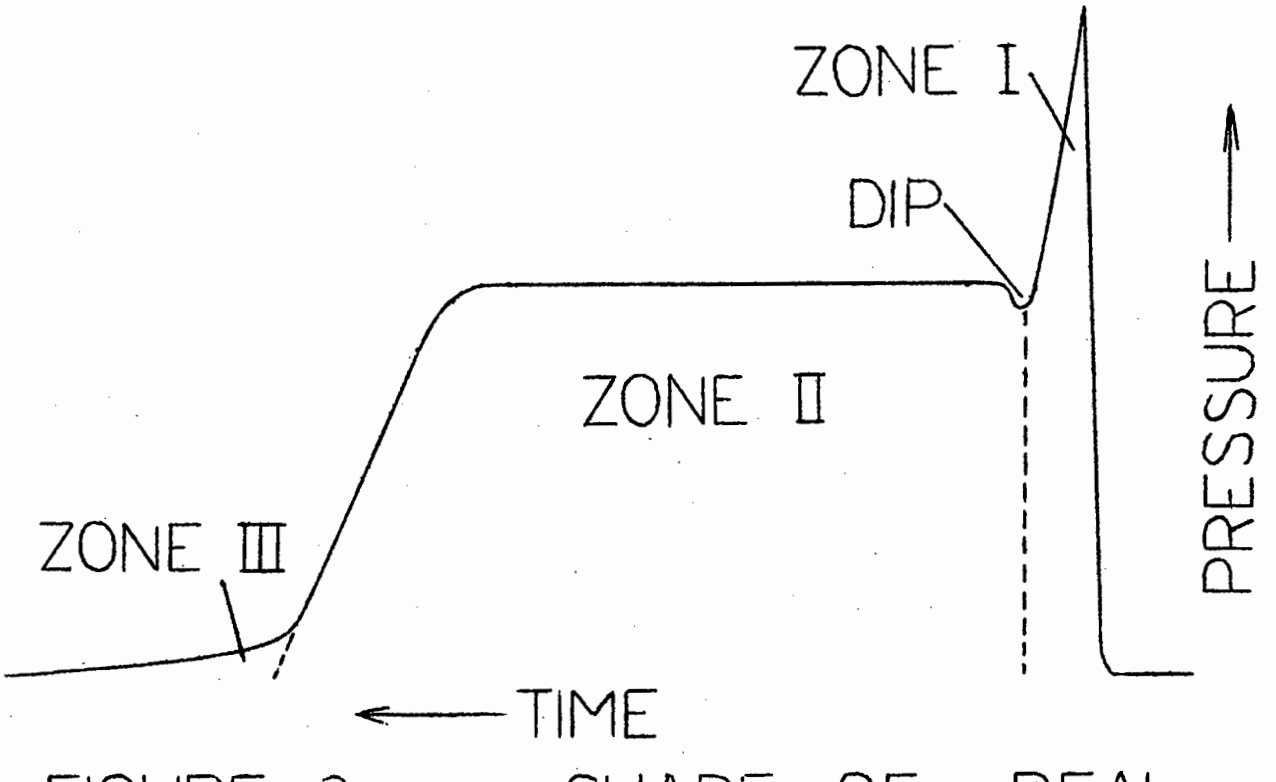

FIGURE 3. SHAPE OF REAL CHROMATOGRAM.

will be converted to zone II. The band will now be carried through the column at a rate determined by its new distribution value.

At the exit of the column, the ammonia will be eluted at the dissociation pressure value of the complex. Once complex II has disappeared, the pressure will begin to drop towards the baseline, as the remaining ammonia in the liquid phase is swept out.

If the band-broadening factors mentioned in 2.2 are assumed absent, the plot of ammonia pressure as a function of column distance traversed, will yield a series of curves as shown in fig. 2.

The effect of variables such as flow-rate, sample size, and silver concentration of the column, has already been discussed in 1.4.

2.3.2 Non-ideal chromatograms

In practice, the band-broadening causes mentioned in 2.2. are present. This results in a chromatogram of the shape shown in fig. 3. The straight edge followed by the trailing rear of zone I indicates "negative" deviations from ideality of the ammonia in the solvent (see 2.2 p. 17). The dip shown in the plateau is due to delayed decomposition of the complex and is explained in 4.5.3. Zone III is caused by the decay of zone II, this decay resulting from the band broadening causes (see 2.2. p.15).

2.4 Calibration of the katharometer

In order to obtain quantitative measurements of the chromatograms, the response of the katharometer to ammonia was calibrated, using columns containing silver nitrate dissolved

in m-toluidine as liquid substrate, as this system showed no permanent absorption of ammonia nor did it exhibit any complexing process (see 4.3 p.45).

The response of the katharometer was assumed to be proportional to n moles of ammonia present, or more conveniently to the pressure p_{NH_3}. This linearity has been reported in the literature[82].

Thus, $$p_{NH_3} = Ch \qquad (15)$$

where h is the chromatogram height,

and C is the calibration constant of the detector.

For an elemental time interval dt, the recorder chart moves a distance c dt, c being the chart speed, and a volume V_t' dt of gas leaves the column, V_t' being the volumetric flow-rate measured at the column outlet. The number of moles of ammonia, dn, in this volume is by the ideal gas law, $p_{NH_3} V_t' dt/RT$ mole.

Combining with equation (15) yields

$$dn = \frac{p_{NH_3} \cdot V_t' \cdot dt}{RT} = \frac{Ch\, V_t'\, dt}{RT}$$

whence, $$dn = \frac{CV_t'(h\, dt)}{RT} \simeq \frac{CV_t'\,(hc\, dt)}{cRT}$$

Now hc dt = dA, where dA is the elemental area under the curve traced by the recorder pen in time dt.

Thus, $$dn = \frac{CV_t' dA}{c\, RT}$$

$$\therefore \int dn = n = \frac{CV'_t A}{cRT}$$

Rearranging gives

$$C = \frac{n \cdot c\, RT}{V_t' \cdot A} \qquad (16)$$

The validity of (16) has already been established within certain ranges by du Plessis[83], while the values obtained in this work (see 4.3.3) support the proportionality assumption.

Equation (15) is used to measure the dissociation pressure, p_d.

When c = 24 inches $hr.^{-1}$, the chart speed most used, R = 82.05 cm^3. atmos. deg^{-1}. $mole^{-1}$., and n has μmole dimensions, (16) becomes

$$C = \frac{83.37 \cdot n \cdot T \cdot 10^{-6}}{V_t' A} \quad \text{atmos. cm}^{-1} \quad \ldots\ldots\ldots\ldots\ldots (17)$$

Equation (16) has been previously derived by du Plessis[84].

2.5 Determination of complex composition

In order to obtain y as indicated by process II in 2.3, the kinetics of the process must be considered as well as phase rule interpretation of the chromatograms.

2.5.1 Kinetics of complex formation in a flow system

Consider the reactions responsible for the plateau type chromatogram, viz.,

$$NH_3(g) \underset{k_2}{\overset{k_1}{\rightleftharpoons}} NH_3(l)$$

$$Ag\,X\,(NH_3)_x(s) + y\,NH_3(l) \underset{k_4}{\overset{k_3}{\rightleftharpoons}} AgX(NH_3)_{(x+y)}(s) \quad p_d \text{ - appreciable}$$

where k_1, k_2 etc., denote the specific rate constants of the reactions.

When complex II is dissociating at its dissociation pressure value under the flow conditions of the chromatogram,

two equations may be obtained. The first is

$$\frac{d\left[NH_{3(g)}\right]}{dt} = - k_1 \left[NH_{3(g)}\right] + k_2 \left[NH_{3(l)}\right] - \frac{\left[NH_{3(g)}\right]\bar{V}_t}{V_g \cdot \frac{L_1}{L}} \quad \ldots(18)$$

Equation (18) may be rewritten as

$$\frac{d\left[NH_{3(g)}\right]}{dt} = - k_1 \left[NH_{3(g)}\right] + k_2 \left[NH_{3(l)}\right] - \frac{\left[NH_{3(g)}\right]\bar{V}_t L}{V_g \cdot L_1} \quad \ldots(18a)$$

where [ ] indicates concentration terms, $\frac{\left[NH_{3(g)}\right]\bar{V}_t L}{V_g \cdot L_1}$ is the change in concentration of ammonia in unit time due to the removal of ammonia in the carrier gas, $\bar{V}_t$ is the average flow-rate of the carrier gas across the length of column, L_1 occupied by zone II.

Along the plateau region, $\left[NH_{3(g)}\right]$ is constant.

$\therefore \frac{d\left[NH_{3(g)}\right]}{dt} = 0$, and (18a) thus becomes

$$0 = - k_1 \left[NH_{3(g)}\right] + k_2 \left[NH_{3(l)}\right] - \frac{\left[NH_{3(g)}\right]\bar{V}_t \cdot L}{V_g \cdot L_1} \quad \ldots\ldots (19)$$

Rearranging (19) gives

$$\left[NH_{3(l)}\right] = \frac{\left[NH_{3(g)}\right](k_1 + \bar{V}_t \cdot L / V_g \cdot L_1)}{k_2} \quad \ldots\ldots\ldots\ldots (20)$$

Equation (20) indicates that for a particular flow-rate, $\left[NH_{3(l)}\right]$ = constant along the plateau region. Furthermore, when $\bar{V}_t = 0$, (20) is reduced to the normal static partition equilibrium. Thus

$$\frac{\left[NH_{3(l)}\right]}{\left[NH_{3(g)}\right]} = \frac{k_1}{k_2} = K$$

where K is the normal partition coefficient.

The second equation is hence given by

$$0 = \frac{d[NH_{3(l)}]}{dt} = - k_3 S_I [NH_{3(l)}]^y - k_2 [NH_{3(l)}] + k_1 [NH_{3(g)}] + k_4 \cdot S_{II} \quad \ldots\ldots\ldots\ldots\ldots\ldots\ldots\ldots\ldots\ldots\ldots\ldots\ldots\ldots (21)$$

where S_I denotes surface area of solid complex I

S_{II} denotes surface area of solid complex II

Adding (19) to (21) gives

$$0 = - k_3 S_I [NH_{3(l)}]^y - \frac{[NH_{3(g)}] \bar{V}_t L}{V_g \cdot L_1} + k_4 S_{II}$$

whence $$\bar{V}_t [NH_{3(g)}] = \frac{(k_4 S_{II} - k_3 S_I [NH_{3(l)}]^y) \cdot V_g L_1}{L} \quad \ldots\ldots (22)$$

At zero flow-rate (22) reduces to

$$0 = k_4 S_{II} - k_3 S_I [NH_{3(l)}]^y$$

whence,

$$\frac{k_3}{k_4} = \frac{S_{II}}{S_I [NH_{3(l)}]^y} \quad \ldots\ldots\ldots\ldots\ldots\ldots\ldots\ldots\ldots\ldots\ldots\ldots (23)$$

The surface areas of the solid complexes are unknown, but at a particular temperature are assumed to be linearly related to the respective number of moles of each by geometrical constants. This assumption is based on the fact that the value of the most concentrated silver solution used was about 0.4 moles per litre, spread over glass beads in a very thin layer, and packed along a chromatographic column of about 90 cm in length.

Thus, if n_{II} is the number of moles of complex II formed, and n_I is the initial number of moles of complex I present, then at static equilibrium (i.e., zero flow-rate)

$$S_{II} = C_{II} \cdot n_{II}$$

and $S_I = C_I \cdot (n_I - n_{II})$

where C_I and C_{II} are the respective geometric constants.

Equation (23) then becomes

$$\frac{k_3}{k_4} = \frac{C_{II}\ n_{II}}{C_I\ (n_I - n_{II}) \left[\frac{n_{NH_3} - y\ n_{II}}{V_f} \right]^y} \quad \ldots\ldots\ldots\ldots\ldots\ldots\ldots\ldots\ (24)$$

where n_{NH_3} is the initial number of moles of ammonia associated with the reaction.

Rearranging (24) yields

$$\frac{k_3}{k_4} \cdot \frac{C_I}{C_{II}} = F(K) = \frac{n_{II}}{(n_I - n_{II}) \left[\frac{n_{NH_3} - y\ n_{II}}{V_f} \right]^y} \text{ litre}^y \text{ mole}^{-y} \ldots\ (25)$$

where F (K) is some function of the equilibrium constant, and is designated the equilibrium function.

If the quantities of reacted and unreacted ammonia can be obtained at zero flow-rate, together with the amount of silver in the column associated with the reaction, F (K) can be evaluated for a series of columns, where the silver concentration is widely varied. By inserting in equation (25) values of y, until constancy is attained, the molar ratio of NH_3:Ag $X(NH_3)_x = y$, can be determined.

2.5.2 Effect of errors in the assumed value of y

The method of determining y described above is, in effect, a trial and error method. It is therefore desirable to examine the effect of an incorrect value of y on F (K).

Equation (25)

$$F(K) = \frac{n_{II}}{(n_I - n_{II}) \left[\frac{n_{NH_3} - y\ n_{II}}{V_f} \right]^y}$$

may be written as

$$F(K) = \frac{\frac{\Delta}{y}}{\left(n_I - \frac{\Delta}{y}\right)\left[\frac{n_{NH_3} - \Delta}{V_f}\right]^y} \text{ litre}^y \text{ mole}^{-y} \quad \ldots\ldots\ldots\ldots (26)$$

where Δ = number of moles of ammonia converted to complex II.

Rearranging (26) gives

$$F(K) = \frac{\Delta}{(y\, n_I - \Delta)\left[\frac{n_{NH_3} - \Delta}{V_f}\right]^y} \text{ litre}^y \text{ mole}^{-y} \quad \ldots\ldots\ldots\ldots (27)$$

For an incorrect assumption of y, say $y + \varepsilon$, (27) becomes

$$F'(K) = \frac{\Delta}{\left(n_I(y + \varepsilon) - \Delta\right)\left[\frac{n_{NH_3} - \Delta}{V_f}\right]^{y + \varepsilon}} \text{ litre}^{y + \varepsilon} \text{ mole}^{-(y + \varepsilon)} \quad \ldots\ldots\ldots\ldots (28)$$

where ε is the error in the assumed value of y

and $F'(K)$ = apparent equilibrium function.

Equation (28) can be written as

$$F'(K) = \frac{\Delta}{\left(n_I (y + \varepsilon) - \Delta\right)\left[\frac{n_{NH_3} - \Delta}{V_f}\right]^y \cdot \left[\frac{n_{NH_3} - \Delta}{V_f}\right]^{\varepsilon}} \quad \ldots\ldots (29)$$

Substituting (27) in (29) gives the relationship

$$F'(K) = F(K)\, \frac{(n_I y - \Delta)}{(n_I (y + \varepsilon) - \Delta)} \cdot \left[\frac{n_{NH_3} - \Delta}{V_f}\right]^{-\varepsilon} \quad \ldots\ldots (30)$$

ε occurs in two factors on the right hand side of (30). Its effect in the second of these is likely to be much greater than in the first, since in the second it appears as the exponent of a power to which the difference of two concentration terms is raised, while the first is merely the ratio of two very similar expressions. Therefore only the factor $\left[\frac{n_{NH_3} - \Delta}{V_f}\right]^{-\varepsilon}$ will be considered in detail.

The numerator of the fraction, $(n_{NH_3} - \Delta)$, is the number of moles of unreacted ammonia, and must decrease if n_I is increased while the injected sample and therefore $\frac{n_{NH_3}}{V_f}$, is kept constant. In practice, under chromatographic conditions, a constant sample injection does not give a constant $\frac{n_{NH_3}}{V_f}$ value. However this variation in the $\frac{n_{NH_3}}{V_f}$ value is found to be relatively small (e.g. in the benzonitrile system a six-fold decrease in n_I leads to a decrease of only 20% in $\frac{n_{NH_3}}{V_f}$).

Several consequences follow:-

(i) If ε is negative, $-\varepsilon$ is positive, and the factor $\left[\frac{n_{NH_3} - \Delta}{V_f}\right]^{-\varepsilon}$ will decrease as the silver loading of the column is increased and we may expect the same to be true of $F'(K)$. Further, the greater the magnitude of ε, the more marked this decrease will be.

(ii) If ε is positive, the factor $\left[\frac{n_{NH_3} - \Delta}{V_f}\right]^{-\varepsilon}$ and hence $F'(K)$ will increase with increase in the silver loading of the column. Again, the greater the magnitude of ε, the more marked the effect will be.

(iii) For $\varepsilon = 0$, $F'(K) = F(K)$ and no trend in the value of the equilibrium function with n_I should be observed.

This reversal of the trend of calculated F (K) values as the assumed value of y is increased has been observed (see section 4). This observation tends support to the assumption that when constancy of F (K) values for varied silver loading is found, the correct value of y has been inserted in the expression.

2.5.3 Calculation of the required quantities from the chromatograms

In order to determine F (K), the values of the amounts of

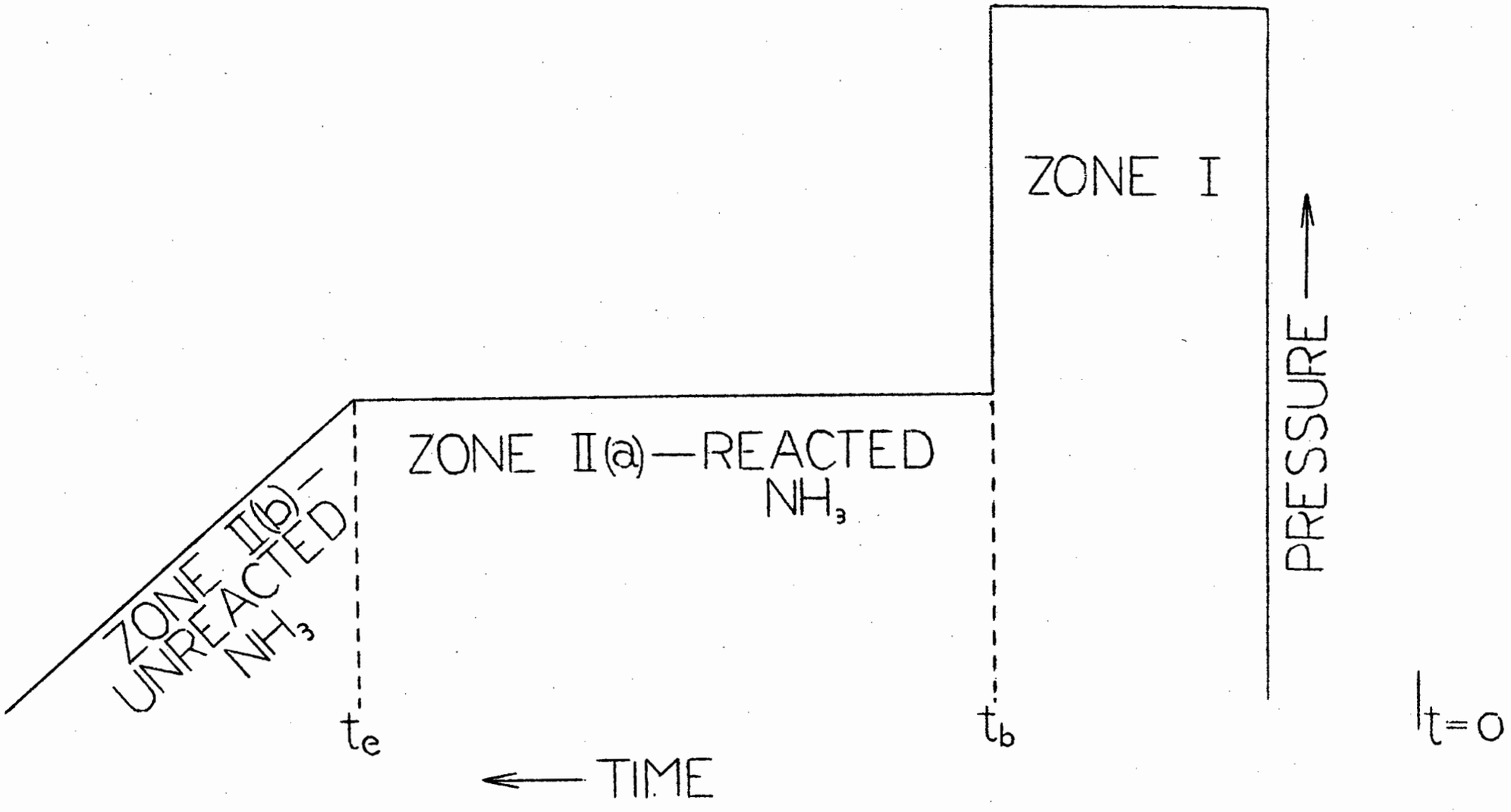

FIGURE 4. DETERMINATION OF REACTED AND UNREACTED AMOUNTS OF AMMONIA IN THE LIQUID PHASE FROM AN IDEAL CHROMATOGRAM.

reacted and unreacted ammonia at zero flow-rate must be obtained. However these quantities must first be measured under dynamic conditions by using the phase rule to interpret the plateau portion of the chromatogram.

Along the plateau portion, the complex is dissociating under constant temperature and pressure conditions, thus indicating a univariant state. When the solid complex has been completely dissociated, a phase has disappeared, the system becomes bivariant and the pressure drops towards the base-line.

The ammonia concentration in the gas phase is constant under plateau conditions and equation (20) shows that the same is true of the concentration in the liquid phase. Thus during elution of the plateau, ammonia eluted is replaced by ammonia from the dissociating complex. Hence the area of zone II(a) (fig. 4) represents reacted ammonia. When all of complex II has dissociated this can no longer occur and zone II(b) (fig. 4) represents unreacted ammonia. The dynamic values of reacted and unreacted amounts of ammonia are thus obtained from an ideal chromatogram as indicated in fig. 4.

Before the equivalent static amounts of reacted and unreacted ammonia can be obtained, the length of column, L'_1, occupied by the plateau just as it starts emerging has also to be determined. This also enables the amount of silver associated with the reaction to be computed.

L'_1 can be found from t_b and t_e, the times taken for the front and rear end of zone II(a) to emerge (see fig. 4). Zone II(b), the unreacted ammonia zone, obviously occupies the same column length L'_1 as the reacted ammonia zone, i.e., zone II(a).

The usual pressure drop across a column resulting in a

gas speed variation along the column, can be represented by means of formulae developed by Keulemans[66]. His equation (10) in the symbols used here is given by

$$t_g = \frac{2 V_g \left\{\left(\frac{p_i}{p_o}\right)^3 - 1\right\}}{3 V'_t \left\{\left(\frac{p_i}{p_o}\right)^2 - 1\right\}} \quad \ldots\ldots\ldots\ldots\ldots\ldots\ldots (31)$$

Equation (31) can be written as

$$t_g = \frac{2 \cdot L \cdot a \cdot \left\{\left(\frac{p_i}{p_o}\right)^3 - 1\right\}}{3 \cdot V'_1 \cdot a \left\{\left(\frac{p_i}{p_o}\right)^2 - 1\right\}} = \frac{2 L \left\{\left(\frac{p_i}{p_o}\right)^3 - 1\right\}}{3 V'_1 \left\{\left(\frac{p_i}{p_o}\right)^2 - 1\right\}} \quad \ldots\ldots (32)$$

where V'_1 = linear gas flow-rate at column exit.

The time spent by an ammonia molecule in the gas phase is proportional to the number of moles in that phase, thus

$$t_g = \left(\frac{n_g}{n_g + n_l}\right) \cdot t_e \quad \ldots\ldots\ldots\ldots\ldots\ldots\ldots\ldots\ldots\ldots\ldots\ldots (33)$$

Equation (33) is based on the assumption that the complexing starts at the inlet of the column.

Similarly

$$t'_g = (t_e - t_b) \cdot \left(\frac{n_g}{n_g + n_l}\right) \quad \ldots\ldots\ldots\ldots\ldots\ldots\ldots\ldots\ldots\ldots (34)$$

$$\text{where } t'_g = \frac{2 L'_1 \left\{\left(\frac{p_L}{p_o}\right)^3 - 1\right\}}{3 V'_1 \left\{\left(\frac{p_L}{p_o}\right)^2 - 1\right\}} \quad \ldots\ldots\ldots\ldots\ldots\ldots\ldots (35)$$

and p_L = pressure of carrier gas at a distance L'_1 from the outlet.

Equations (33) and (34) give

$$\frac{t_g}{t_e} = \frac{t'_g}{t_e - t_b} \quad \ldots\ldots\ldots\ldots\ldots\ldots\ldots\ldots\ldots\ldots\ldots\ldots\ldots\ldots (36)$$

Inserting (32) and (35) in (36) results in

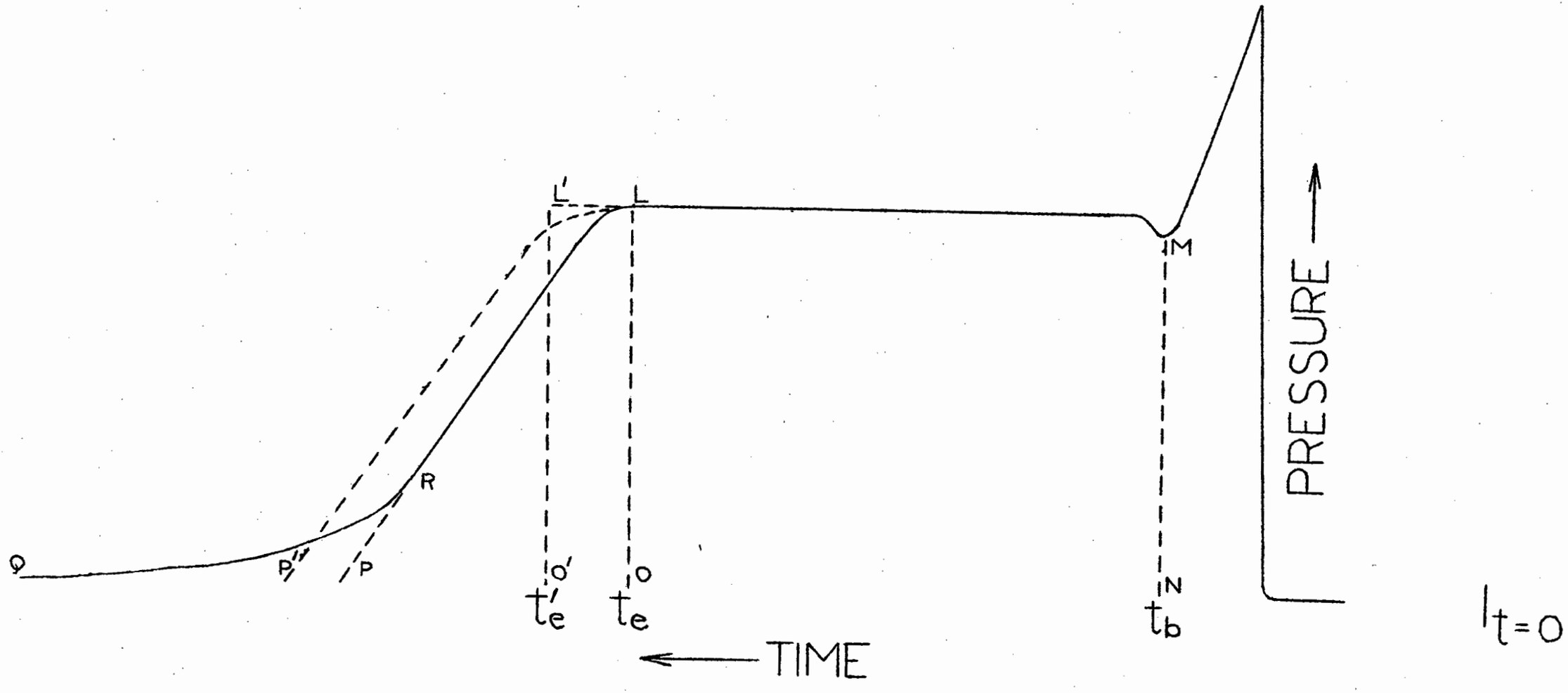

FIGURE 5. QUANTITATIVE TREATMENT OF A REAL CHROMATOGRAM.

$$\frac{L\left\{\left(\frac{p_i}{p_o}\right)^3 - 1\right\}}{\left\{\left(\frac{p_i}{p_o}\right)^2 - 1\right\} \cdot t_e} = \frac{L'_1\left\{\left(\frac{p_L}{p_o}\right)^3 - 1\right\}}{(t_e - t_b)\left\{\left(\frac{p_L}{p_o}\right)^2 - 1\right\}} \quad \ldots\ldots (37)$$

Keulemans equation (6) in the symbols used here is given by

$$\frac{x_1}{L} = \frac{\left(\frac{p_i}{p_o}\right)^2 - \left(\frac{p}{p_o}\right)^2}{\left(\frac{p_i}{p_o}\right)^2 - 1}$$

where x_1 = distance from upstream end of column to point where carrier pressure is p

$p = p_L$ when $x_1 = L - L'_1$

$$\therefore \frac{L - L'_1}{L} = 1 - \frac{L'_1}{L} = \frac{\left(\frac{p_i}{p_o}\right)^2 - \left(\frac{p_L}{p_o}\right)^2}{\left(\frac{p_i}{p_o}\right)^2 - 1}$$

whence $$\frac{L'_1}{L} = \frac{\left(\frac{p_L}{p_o}\right)^2 - 1}{\left(\frac{p_i}{p_o}\right)^2 - 1} \quad \ldots\ldots\ldots\ldots\ldots\ldots (38)$$

Inserting (38) in (37) results in

$$\frac{\left(\frac{p_i}{p_o}\right)^3 - 1}{t_e} = \frac{\left(\frac{p_L}{p_o}\right)^3 - 1}{t_e - t_b} \quad \ldots\ldots\ldots\ldots (39)$$

Rearranging (39) yields

$$\left(\frac{p_L}{p_o}\right)^3 = 1 + \frac{(t_e - t_b)\left\{\left(\frac{p_i}{p_o}\right)^3 - 1\right\}}{t_e} \quad \ldots\ldots\ldots (40)$$

Equations (38) and (40) can be used to find L'_1 from the measurable quantities, t_e, t_b, p_i, p_o and L, and were originally derived by du Plessis [85], but in a slightly different manner.

A real chromatogram is now treated as follows (see fig. 5): areas of zone II(a), LMNO, II(b), LOP and III, RPQ, are measured.

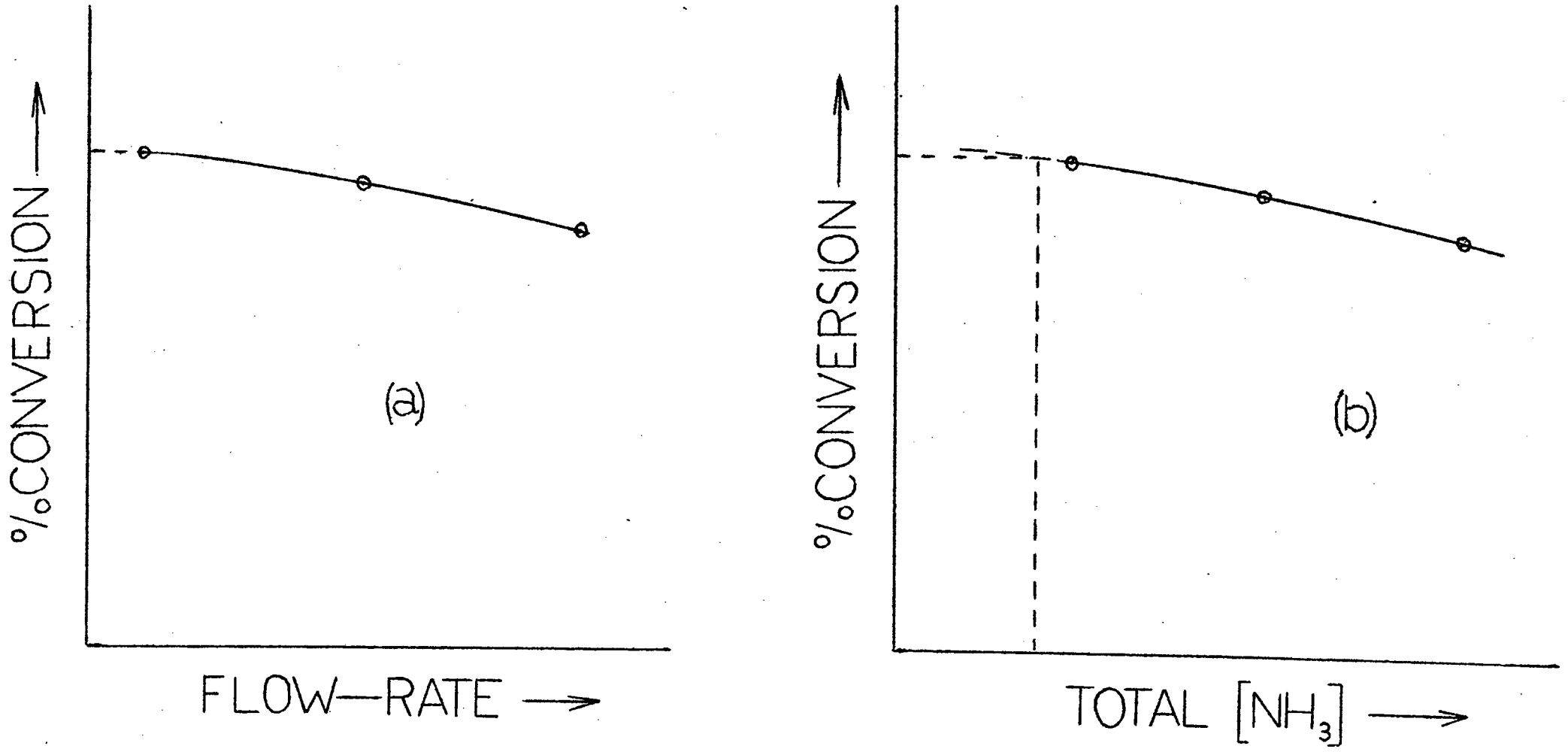

FIGURE 6. VARIATION OF CHROMATOGRAM MEASUREMENTS WITH FLOW—RATE.

The area of zone III is divided proportionately between the areas of II(a) and II(b), since the zone broadening causes affect both the reacted and unreacted ammonia, and hence the decayed tail will be derived from both. Thus the final area of zone II(a) is given by

$$A(II(a)) = A\ (LMNO) + \frac{A(LMNO)}{A(LMNP)} \cdot A(RPQ)$$

while $A(II(b)) = A\ (LOP) + \frac{A(LOP)}{A(LMNP)} \cdot A(RPQ)$

The reason for taking zone III into account is due to the assumption that complexing starts at the inlet of the column, and the formulae for deriving L'_1 are based on this assumption. Thus L'_1 is determined from t_b, t_e' and not from t_b, t_e. The rear end of zone II(b) now becomes P' not P. Equation (17) is used to determine the amount of ammonia in corrected zone II(a), L'MNO' and II(b), LOP'.

The amount of undissolved ammonia of zone II(a) can be calculated from the dissociation pressure, and the volume, $\frac{L'_1 V_g}{L}$ of the gas phase. This is subtracted from the ammonia eluted in zone II(a), giving the actual amount eluted from the liquid phase while a univariant state prevails.

Thus the reacted and unreacted amounts of ammonia in the liquid phase can be determined at a particular flow-rate. If chromatograms at different flow-rates are similarly treated, with the flow-rate as the only variable, extrapolation to zero flow-rate can be made, giving the equivalent static amounts of reacted and unreacted ammonia.

Two plots are necessary, as shown in fig. 6. The shapes of the curves are those found experimentally. The terms

"% conversion" and "total $\left[NH_3\right]$" in fig. 6 are defined as

$$\text{"\% conversion"} = \frac{\text{reacted ammonia in liquid phase} \times 100}{\text{reacted + unreacted ammonia in liquid phase}}$$

"total $\left[NH_3\right]$" = reacted + unreacted ammonia in liquid phase, per unit length of packing.

Plot (b) in fig. 6 is necessary, as the value of L'_1 is found to vary with flow-rate. This is most probably due to rate-effects (see 4.5.3., 4.6.3., 4.7.6. (p.87), 4.8.6., (p.95), and 4.8.7. (p.99)) as well as to the fact that with increasing flow-rate, the amount of complex formed decreases with a corresponding decrease in the value of L'_1. The extrapolated "% conversion" value of plot (a) is used in plot (b) to determine the "total $\left[NH_3\right]$" value at zero flow-rate.

All information required in ascertaining F (K) and hence y is now available.

2.5.4 Temperature dependence of the dissociation pressure and the equilibrium function

Ideally p_d is dependent only on temperature and is independent of such non-thermodynamic quantities as flow-rate, sample size and silver concentration.(in practice this is not so : see 4.5.7., 4.6.6., 4.7.6., and 4.8.6.). Thus a plot of log p_d against $^1/T$ should yield a straight line graph, whose slope is equal to $-\frac{\Delta H}{2.303\ R}$, where ΔH is the overall heat of reaction of complex II per mole of ammonia. The overall reaction is defined as

$$Ag\ X\ (NH_3)_x\ (s) + y\ NH_{3(g)} \rightleftharpoons Ag\ X\ (NH_3)_{(x+y)}\ (s) \quad \ldots\ldots\ \Delta H$$

and is made up of the following reactions:-

(a) $y\ NH_3\ (g) \rightleftharpoons y\ NH_{3(l)}$ $\ldots\ldots\ \Delta H_1$

(b) $Ag\ X\ (NH_3)_x(s) + y\ NH_{3(l)} \rightleftharpoons Ag\ X(NH_3)_{(x+y)}(s)$ ..... ΔH_2

Thus $y\Delta H = \Delta H_2 + y\Delta H_1$ ..... (41)

where ΔH_2 = heat of reaction of complex II per mole of silver

ΔH_1 = heat of solution per mole of ammonia in the solvent.

Equation (25) gives the relationship

$$F(K) = \frac{k_3}{k_4} \cdot \frac{C_I}{C_{II}}$$

If $\frac{C_I}{C_{II}}$ is not a function of temperature, the graph of log F (K) against $^1/T$ should give a straight line with a slope equal to $-\frac{\Delta H_2}{2.303R}$. ΔH_1 can be measured chromatographically (see 2.2).

Equation (41) can thus be used as a check on the correctness or otherwise of y as obtained from F (K). The heat of reaction of complex II per mole of silver or ammonia is thus also determinable.

2.6 Part played by the solvent in complex formation

The exact role played by the solvent in complex formation is unknown. In practice however the solvent influences the complexes profoundly (see section 4). Values of x and y, bond strengths, p_d values, and number of complexes (or plateaux) formed, all vary from one solvent to another. It thus seems most likely that the solvent is bonded in the crystal structures of the complexes.

2.7 Successive plateaux

The number of plateaux in a chromatogram indicate the number of complexes formed having a discernible dissociation pressure. The successive plateaux emerge in order of decreasing height.

The treatment of successive plateaux is more conveniently discussed in 4.8.7., where an example will be described.

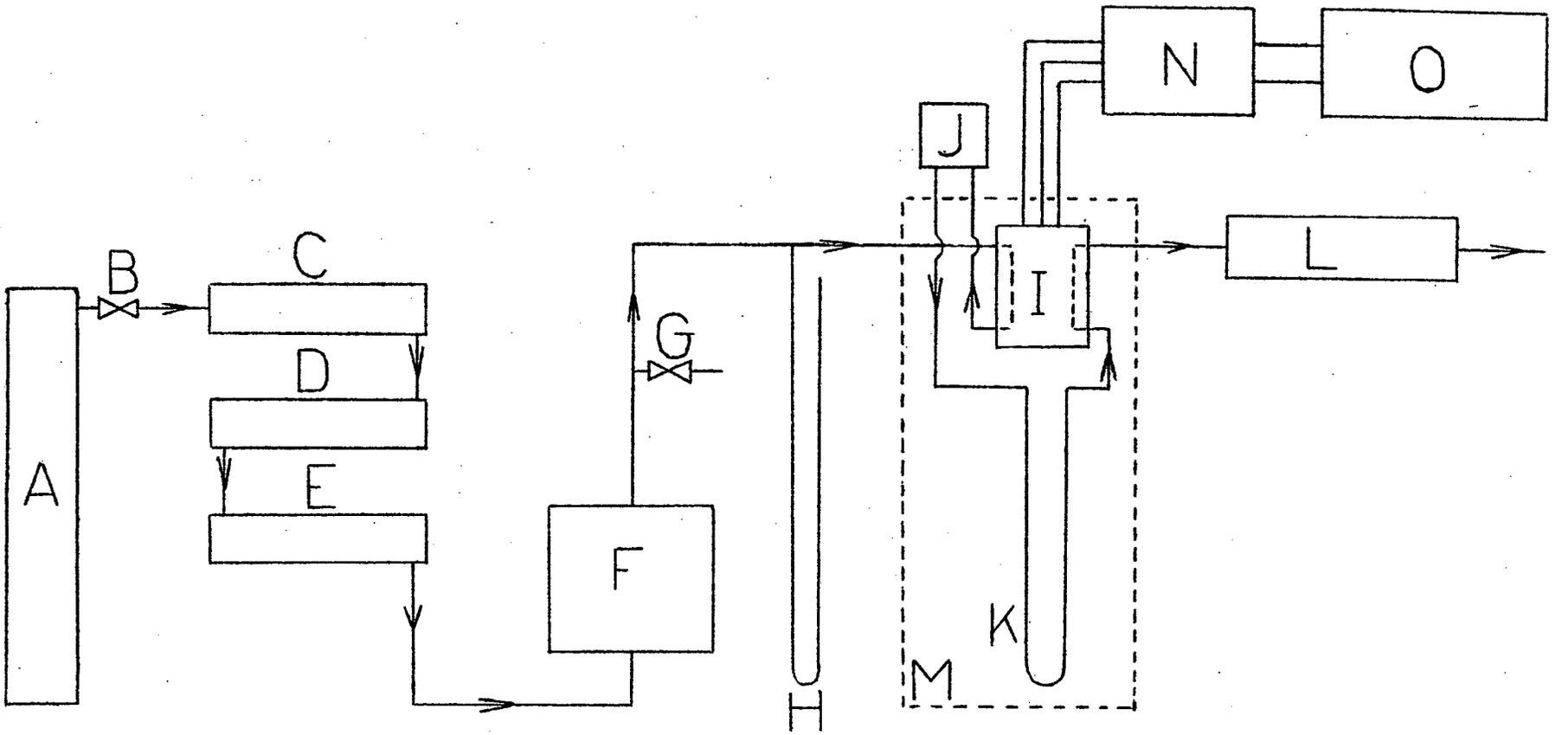

FIGURE 7. BLOCK DIAGRAM OF GAS-CHROMATOGRAPHIC APPARATUS. A, gas cylinder; B, two-stage regulator; C, flow-control; D, tube containing silica gel; E, tube containing phosphorus pentoxide; F, buffer vessel; G, tap to atmosphere; H, mercury manometer; I, katharometer; J, sample injector; K, column; L, flow-meter, M, air thermostat; N, bridge circuit; O, recorder.

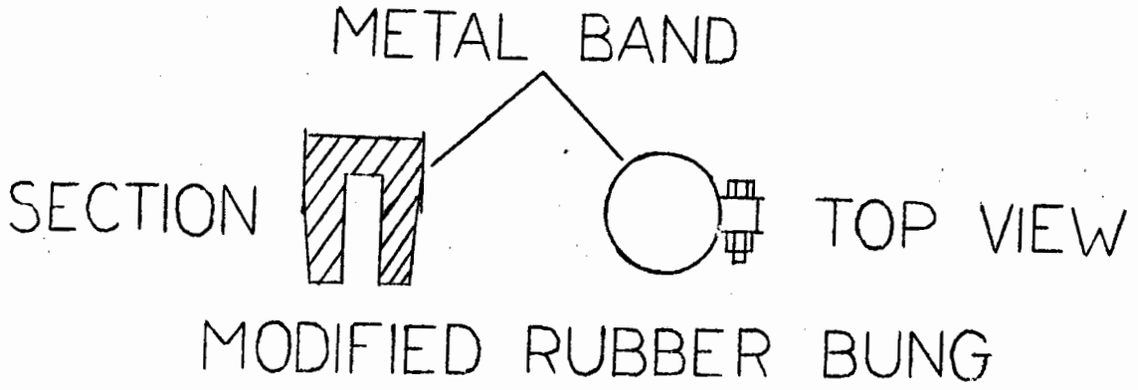

MODIFIED RUBBER BUNG

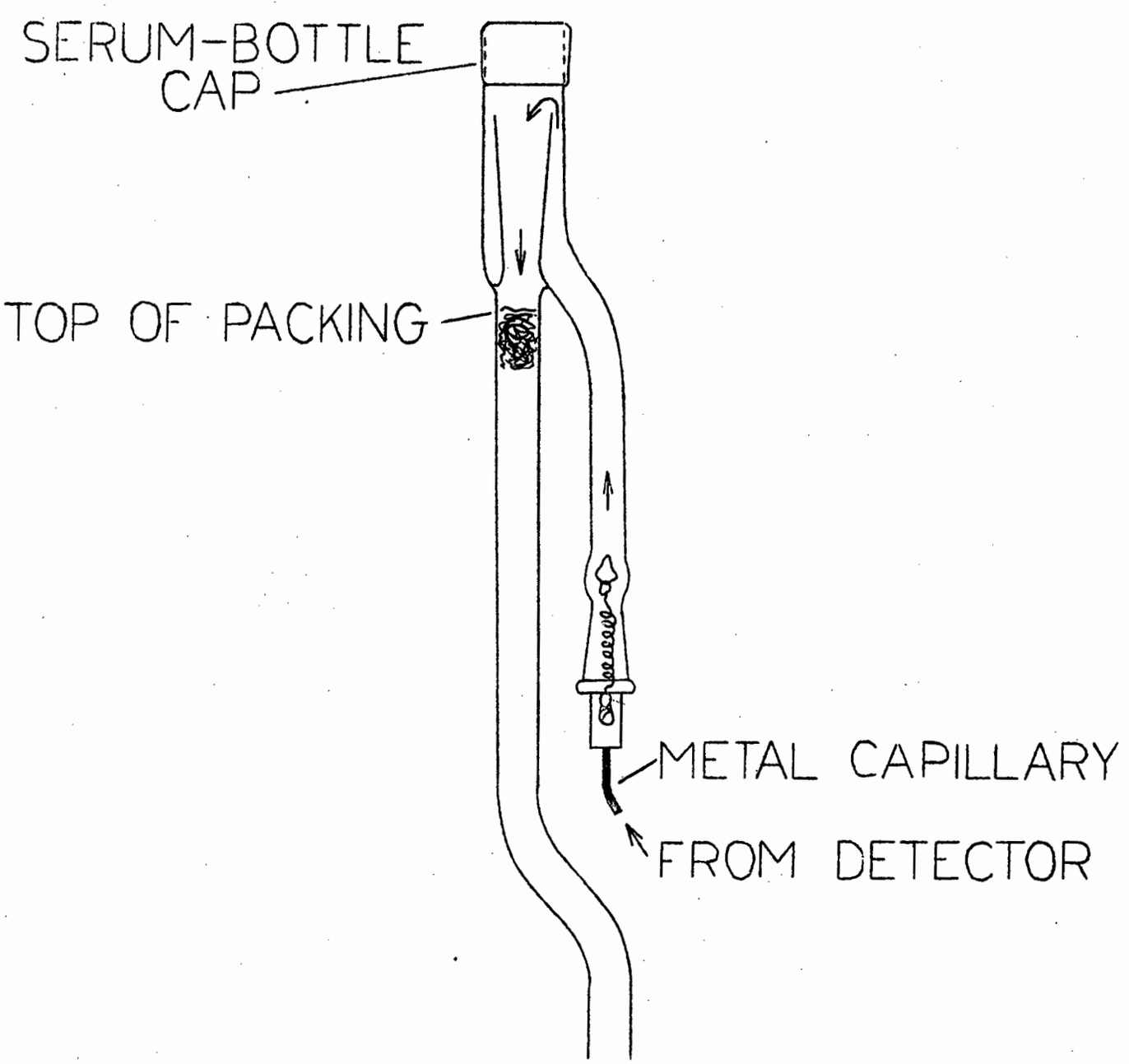

FIGURE 8. TOP OF COLUMN ADAPTED TO TAKE SERUM-BOTTLE CAP OR MODIFIED RUBBER BUNG. CARRIER GAS PATH INDICATED BY ARROWS.

SECTION 3

APPARATUS, MATERIALS AND EXPERIMENTAL PROCEDURES

3.1 General description of the apparatus

The gas chromatographic apparatus was of the conventional type, of which the air thermostat, katharometer, bridge circuit and some column tubes, were supplied by Messrs. Griffin and George Ltd. The rest of the apparatus was designed and built by du Plessis. Fig. 7 is a block diagram of the apparatus.

3.1.1 The column

The column consisted of a glass U - tube of 6.2 ± 0.2 mm. diameter, containing packing to the length of about 90 cm. The upstream end was adapted to take a serum bottle cap, or a modified rubber bung for sample injection by syringe (see fig. 8).

The column was packed by vibrating it against a slightly eccentric spindle of an electric motor, which enabled the packing to be channelled through a funnel, and compacted in the column. Columns so packed have been reported[65] to vary in linear packing density by about 5%. Each end of the U-tube was marked for easy determination of packing length.

The interstitial volume, V_g, of the column (important for determining the amount of undissolved ammonia of zone II(a)) was determined from the column dimensions, and the weights and densities of the packing constituents.

3.1.2 The air thermostat

The column was situated in an air thermostat which was found to be thermostatically effective from about 75°C upwards.

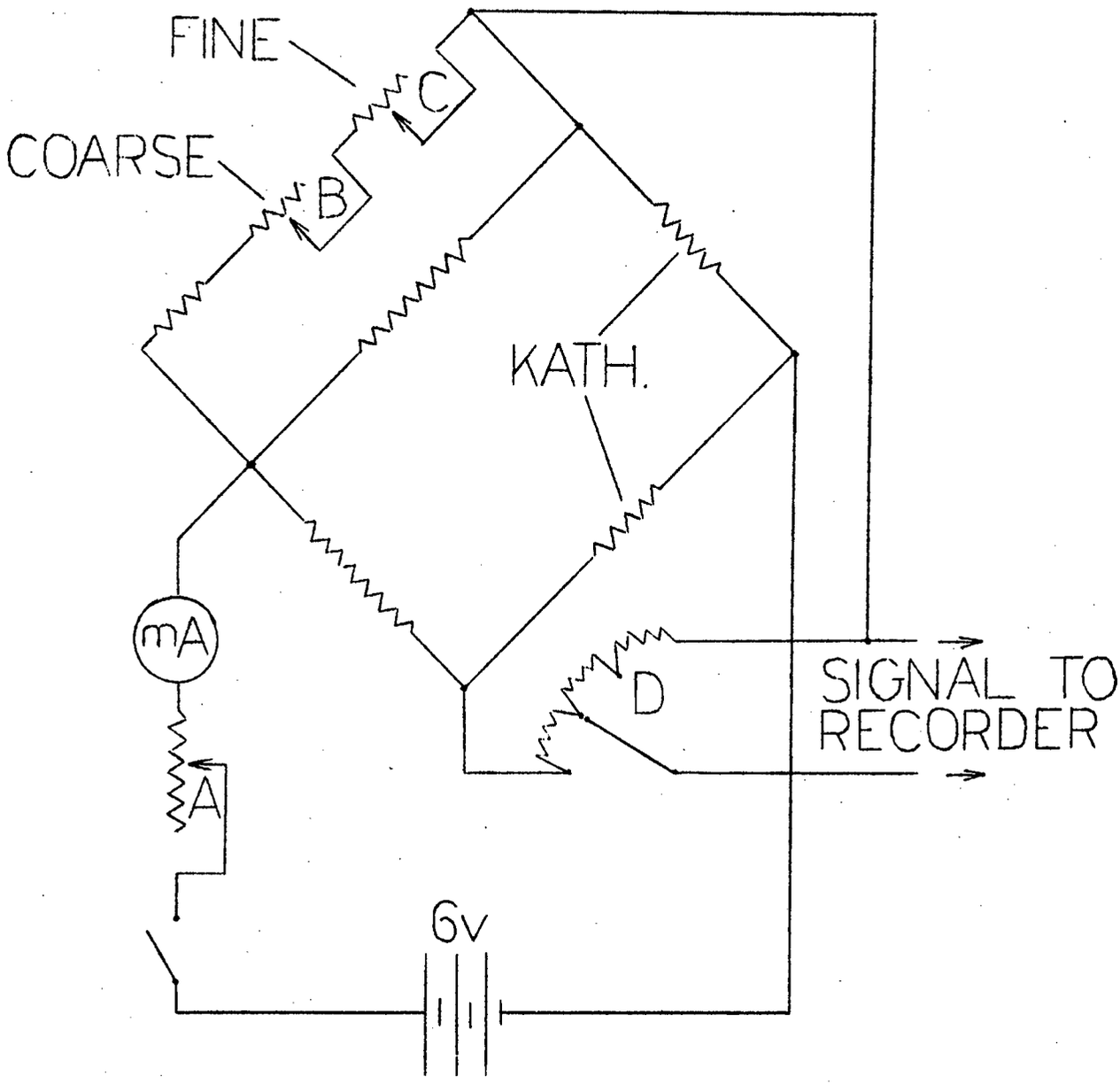

FIGURE 9. DETECTOR BRIDGE CIRCUIT. DIAGRAM IS FROM MANUFACTURER'S LITERATURE, WHICH DOES NOT GIVE THE RESISTANCES OF THE COMPONENTS.

In order to bring the oven into thermostatic operation at the temperature range required, i.e., room temperature to 36°C, a variable transformer was inserted in the heating current circuit of the oven.

The best temperature control was found by keeping the thermostatic switch open, and heating the oven with a low variac controlled heating current. The final temperature of the oven was reached, when the heat input equalled the heat losses to a near thermostatted room, whose temperature varied about 1°C in a day. By slight adjustment of the variac the temperature stability of the oven could be maintained to within 0.1°C. A thermocouple probe at 30°C showed a negligible spatial variation of temperature in the oven.

3.1.3 The detector and recorder

A metal-block katharometer mounted in the air oven, was used as a detector and had platinum filaments located in the carrier gas stream at either end of the chromatographic column.

Carrier gas flowed through a pre-heating loop in the thermostat to the first cell of the detector, then via the sample injector to the column, and thence to the second cell of the katharometer.

A Wheatstone bridge circuit which included the katharometer filaments in two of its balancing arms, as shown in fig. 9, had its off-balance signal fed to a recording potentiometer. Rheostat A regulated the bridge current, which was maintained at 150 mA. for all the work done, while B and C were used to adjust the base-line. The potential divider D, gave attenuations of

1, $^{1}/_{2}$ and $^{1}/_{4}$ the full output signal.

The recorder (Honeywell-Brown Model No. 153 x 12V - X - 6A8R) had a full-scale deflection of 3mV, a sensitivity of 17.1 x 10^{-2} mV per cm of chart, a response time of $5\frac{1}{2}$ sec. for full-scale travel, and chart speeds of 6, 7.2, 12, 20 and 24 inches per hr.

3.1.4 The carrier gas

The carrier gas, nitrogen, was obtained from a gas cylinder, and its flow-rate was controlled by a two-stage regulator, and a control device built by du Plessis, based on information given in the literature[68, 87]. A buffer vessel, F (fig. 7), a 4-litre bulb, smoothed out pressure oscillations due to operation of the flow-control. Flow-rates of 5 to 110 cm^3 min^{-1} were used, the lower flow-rate showing a drift of $\pm$ 1%, the upper flow-rate, a drift of $\pm$ $\frac{1}{2}$%.

The carrier gas was dried by passage over silica gel and phosphorus pentoxide. Stopcock G, was used to adjust the pressure at the column inlet, while manometer, H, measured the pressure drop across the column.

The flow-rate was measured by a soap-film meter, discharging to the atmosphere and claimed to have an accuracy much better than 1%[88, 89].

3.1.5 Injection by syringe

The syringes used had the following capacities and smallest graduations; cm^3: 1, 0.05; 5, 0.5; 10, 0.5; 20, 0.5.

The air in the small dead volume of the needle of the syringe was expelled by drawing in and syringing out a small quantity of ammonia. The sample of ammonia to be injected,

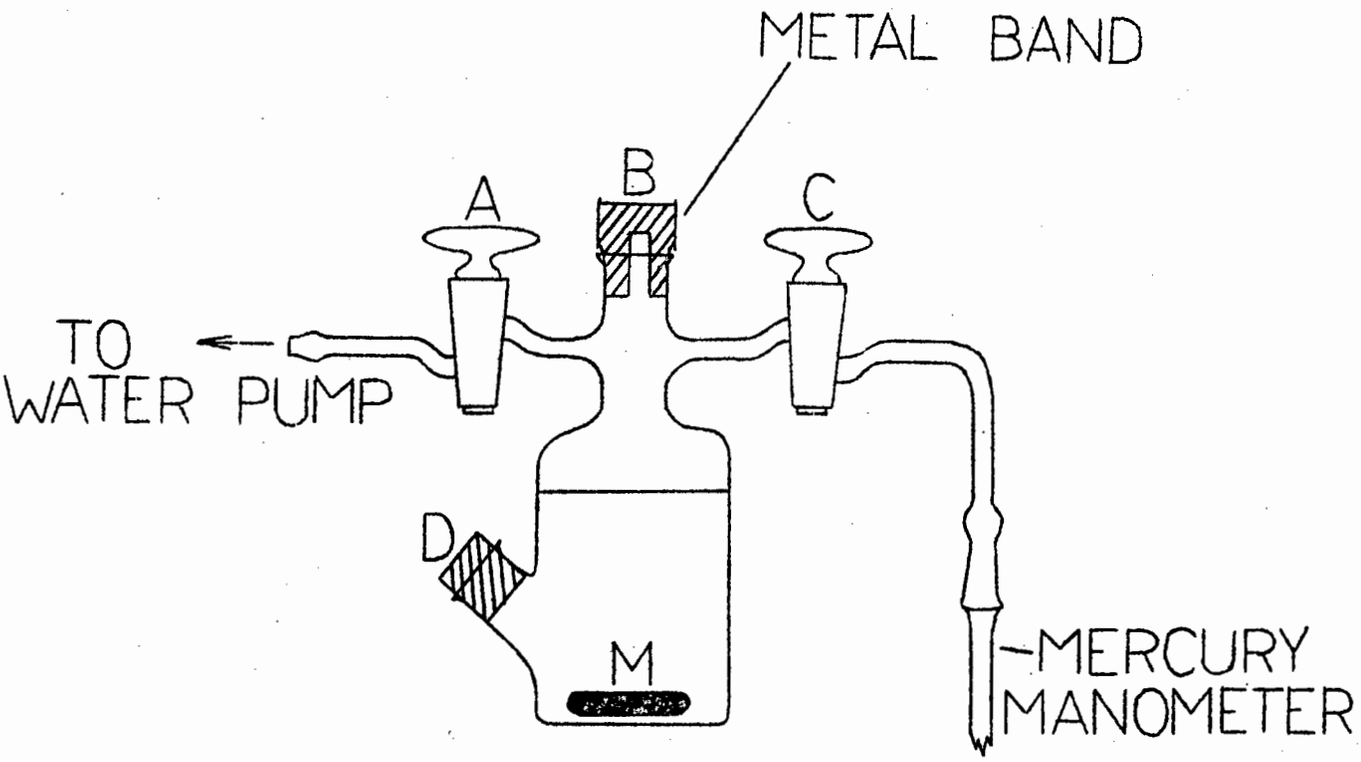

FIGURE 10. TENSIMETER.

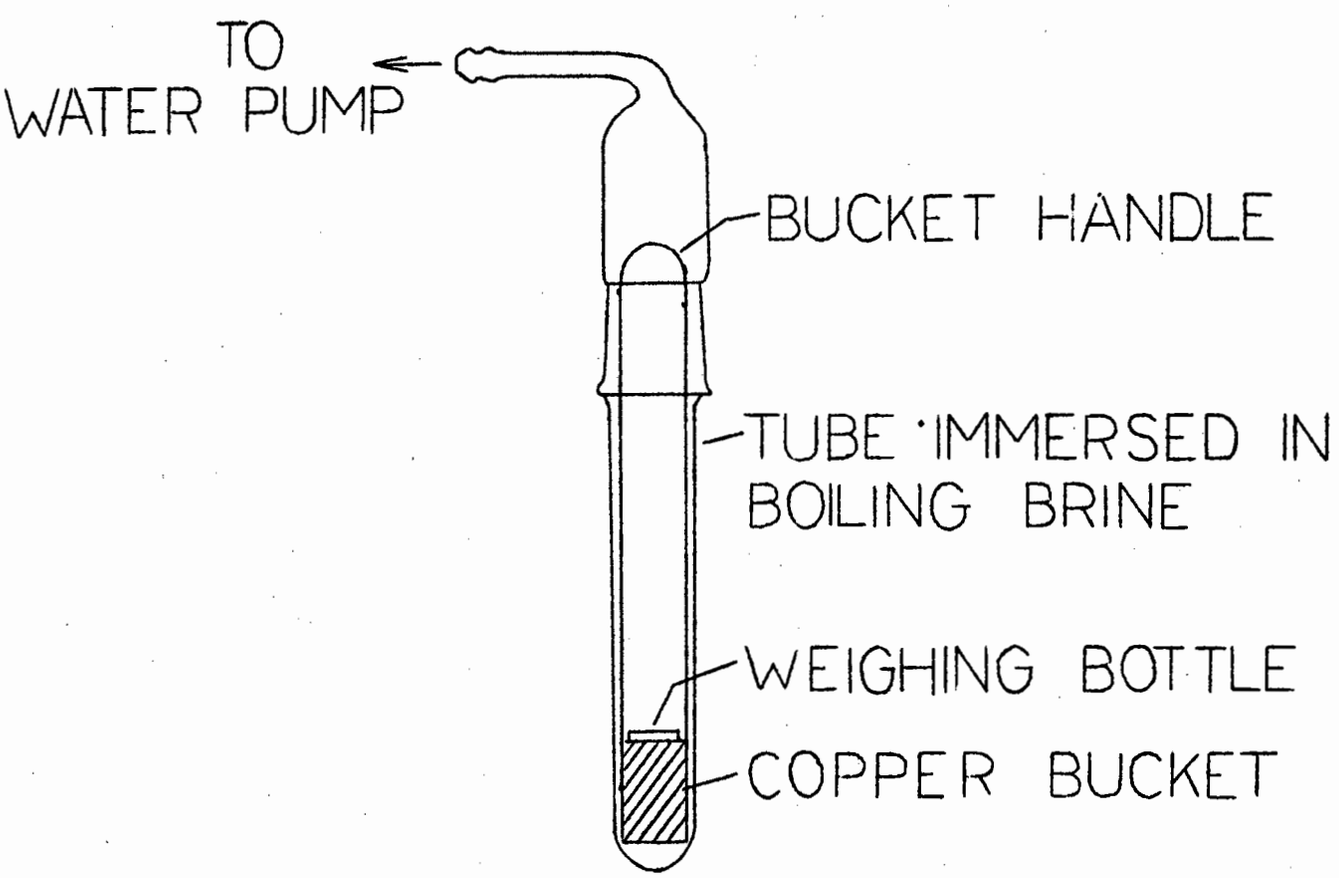

FIGURE 11. DEHYDRATING TUBE.

then occupied the syringe at room temperature and atmospheric pressure, which were noted. Injection of the sample was made through a serum bottle cap, or a modified rubber bung, when the column inlet pressure was more than 150 mm. above atmospheric pressure, as shown in fig. 8. The needle of the syringe was lubricated with silicone grease, when injecting through the bung, in order to facilitate its passage.

3.1.6 The tensimeter

The tensimeter shown in fig. 10 was used in a thermostatted room, and a thermometer was mounted alongside it. Its volume was found in relationship to the mercury level in the manometer by introducing measured volumes of water.

A known weight and volume of the complex forming solution was placed in the tensimeter which was partially evacuated and stopcock A closed. (The silver solution was shielded from light). The volume, pressure and temperature of the residual air was noted, and a known amount of ammonia was injected by syringe through bung B. In order to bring the gas and liquid phases into more intimate contact with each other, a magnetic stirrer, M, was used. It was allowed to stir the solution for about 15 hours, after which the pressure, volume, and temperature of the gases were again noted, (the manometer having come to a steady level) and used to calculate the amount of ammonia remaining in the gas phase, and by difference, the amount absorbed in the liquid phase.

Stopcock C, was then closed and the container was disconnected from the water-pump and the manometer, and weighed with its contents. A weighed syringe was used to withdraw some of the liquid phase from the container through bung D, which was

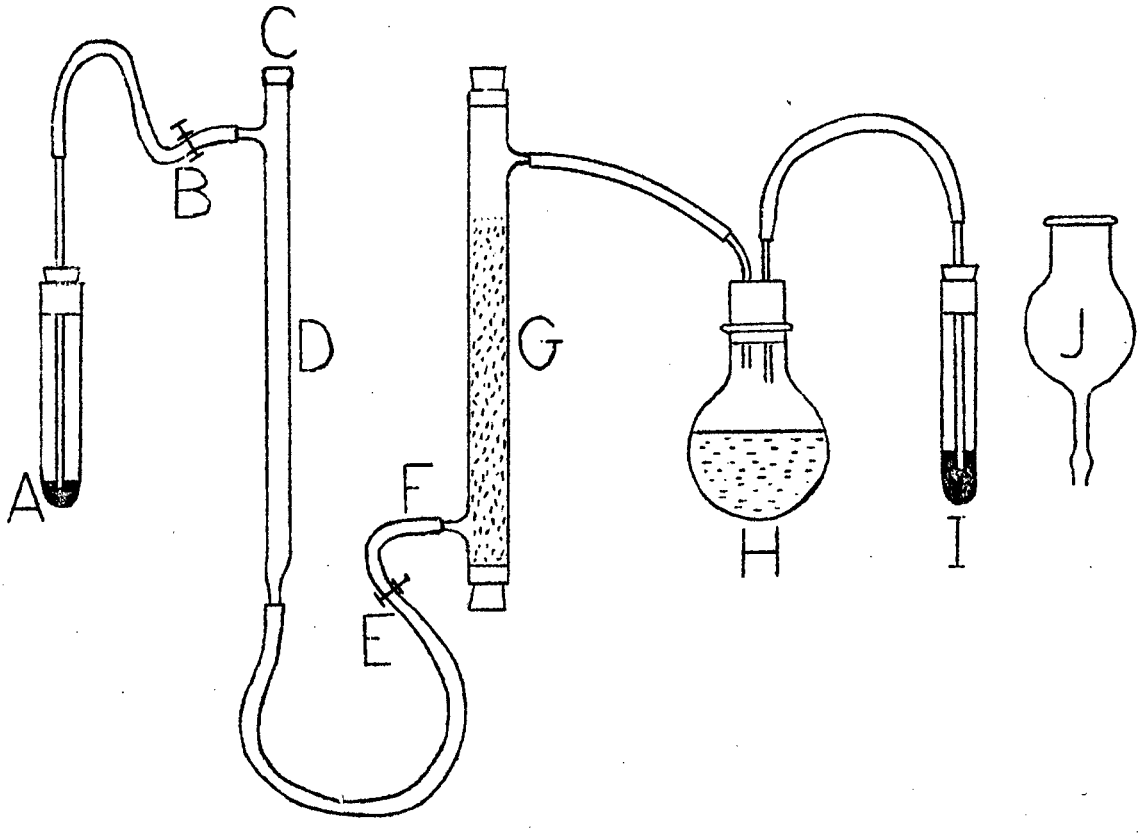

FIGURE 12. APPARATUS FOR THE PREPARATION AND STORAGE OF AMMONIA.

then syringed into a weighing bottle. The container was again weighed in order to determine how much liquid was withdrawn from it, while the syringe was also weighed, so that the small amount of liquid left in it, could be determined.

The weighing bottle plus its contents were weighed as were three similar control weighing bottles, containing the same liquid. These four weighing bottles were allowed to stand uncovered overnight in a cupboard. The purpose of this was to allow all the ammonia to be evaporated from the liquid in the experimental bottle, and to account for liquid evaporation, the control bottles were used. The following day all the bottles were weighed again.

From these weight measurements, the equilibrium function was computed (see 4.7.8).

3.2 The preparation of ammonia

Dry ammonia was prepared by warming a concentrated ammonia solution in flask H (fig. 12) and passing the ammonia expelled from solution over a drying agent (sodium hydroxide pellets) in tube G. The dried ammonia purged the apparatus of air and escaped to the atmosphere through mercury bubbler A. When the whole apparatus was considered filled with ammonia, screw-clips B and E were closed, and bubbler I, having a greater head of mercury than A, acted as a safety-valve for flask H. The rubber tubing was then detached at F, and fitted to bulb J, which was half-filled with mercury. Screw-clip E, was opened, which allowed the mercury to come into contact with the ammonia in tube D. The isolated ammonia in D was then manipulated with the mercury, so that syringes could be filled through the serum

bottle cap C. Gas chromatography showed that ammonia so prepared sometimes contained trace impurities.

3.3 The preparation of the packings

An approximate volume of the liquid phase was added to a known weight of solid support (fine glass beads, 0.1 mm diameter) and the exact amount of liquid phase added, was found by weight measurements.

Thorough coating of the beads with the liquid phase was achieved by mixing the two phases with a glass spatula.

3.3.1 Materials used

Table 3.3.1 gives the details about the materials used in the column packings. All solvents used were purified by distillation under reduced pressure. The variation of densities with temperature of the solvents was found either from International Critical Tables[90], or was determined by means of a pyknometer[91].

Table 3.3.1 Materials used for packings

Material	Manufacturer	Grade or Manufacturer's description	Specifications
Benzonitrile	British Drug Houses	Laboratory Reagent	-
	Riedel de Haën	-	-
Benzyl Cyanide	British Drug Houses	Laboratory Reagent	-
Fenchone	Eastman Kodak Co. N.Y.	Technical	-
Glass beads	English Glass Co.	"Ballotini" grade 15	0.1 mm diameter
Tetralin	British Drug Houses	Redistilled	-
ortho-Toluidine	British Drug Houses	Laboratory Reagent	-

Table 3.3.1 (continued)

Material	Manufacturer	Grade or Manufacturer's description	Specifications
meta-Toluidine	Eastman Kodak Co.	Practical	-
para-Toluidine	British Drug Houses	Laboratory Reagent	-
Silver Nitrate	May and Baker	Laboratory Chemical	$\leq$ 99.8%
	Hopkins and Williams	Analar	$\leq$ 99.9%

3.3.2 Drying of silver perchlorate

The silver perchlorate used was obtained from a sample of the salt prepared by du Plessis[92]. The sample was dried by transferring it in a weighing bottle without the lid to a copper bucket shown in fig. 11. The salt was subjected to about three hours of evacuation and warming (110°C). Analysis showed the salt to be anhydrous (theoretical Ag; 52.1%, found Ag; 52.0%, 52.0%, 52.2%). The bucket enabled the weighing bottle to be transferred rapidly to a dessicator.

SECTION 4

EXPERIMENTAL RESULTS

This section presents the experimental data obtained, and the interpretation of the results. The first sub-section explains the presentation of the data, while the second deals with the solid support. Each of the following sub-sections is devoted to a silver salt-solvent system, except for the last two sub-sections, which are concerned with ageing effects and the toluidine isomers.

4.1 The presentation of data

The following tables appear in some if not all of the sub-sections 4.3 to 4.8 and a few of the column headings in these tables are explained.

Tables showing characteristics of the packings

Column 1. Designation of the packing - S.P. for silver perchlorate, S.N. for silver nitrate, F for fenchone, T for tetralin, B for benzonitrile, B.C. for benzyl cyanide, and o - T., m - T., and p - T., for the ortho, meta and para-toluidines. Thus for example, S.P.F. would stand for silver perchlorate in fenchone.

Column 3. Ratio (s) of volume of fixed phase to mass of support.

Tables showing the influence of rate-effects on the chromatogram shapes

Column 1. Experiment number of chromatogram for easy reference.

Column 3. Flow-rate of carrier gas at atmospheric pressure and column temperature (i.e., flow-rate at column exit).

Column 4. Type of chromatogram shape as illustrated in fig. 19.

Columns 5, 6 and 7. Values of the dip phenomena D_1, D_2 and division of plateau height, D_3, as shown in fig. 19.

Tables listing the results and temperature dependence of the of the equilibrium function

Column 3. Molar ratio (R) of the total amount of ammonia at zero flow-rate (extrapolated value) in the liquid phase per unit length of column, to the equivalent amount of silver in the column.

Column 4. Percentage conversion of ammonia at zero flow-rate (extrapolated value, see fig. 6(a)).

Tables showing the variation of the equilibrium function with assumed y values

Column 2. Value of δ, the error involved in the assumed y value.

Columns 3 and 4. These headings denote the error factors involved in making incorrect y value assumptions, as indicated by equation (30).

Tables showing statistical analysis of dissociation pressure results

Column 2. Mean dissociation pressure value $\overline{p_d}$.

Column 3. Standard deviation about the mean value, σ.

Column 4. Coefficient of variation, $\frac{\sigma}{\overline{p_d}} \times 10^2$.

The drawings illustrating the chromatograms are of a semi-quantitative nature and the following very approximate scales were used for convenience for the different salt-solvent

systems.

Table 4.1.1 Scale factors used in the chromatogram illustrations

Salt-solvent system.	Vertical scale	Horizontal scale
S.P.F.	5 cm ≡ 68 x 10^{-3} atm	5 cm ≡ 8.6 min
S.P.T.	5 cm ≡ 59 x 10^{-3} atm	5 cm ≡ 10.2 min
S.N.B.	5 cm ≡ 134 x 10^{-3} atm	5 cm ≡ 5.0 min
S.N.B.C.	5 cm ≡ 126 x 10^{-3} atm	5 cm ≡ 13.1 min

Most of the calculations were done with a "Facit" (CA1-13) electrical calculating machine, while all the area measurements on the chromatograms were determined with an "Ott Compensating Polar Planimeter" which gave area measurement results reproducible to within 0.1 cm^2.

4.2 The solid support--treatment and results of tests on it

The glass beads ("ballotini", grade 15 - 0.1mm diameter) which were used both by du Plessis as solid support for his packings, and as solid support for the packings described in this thesis, resulted in columns of known interstitial volume. This quantity is important in determining the amount of undissolved ammonia of zone II(a).

Further advantages which have been reported[93] concerning the beads are (a) no stagnant interstices in the packing in which lateral diffusion in the gas phase can occur and (b) highest packing densities of different columns can be reproduced to within 5 per cent of each other.

The beads however, showed strong adsorptive properties for ammonia, and had to be treated in the following way, in order

to reduce their retentivity : they were boiled with a 30% solution of sodium hydroxide for about 5 minutes, and then washed with distilled water until no reaction to red litmus was observed. After drying in an oven at about 190°C for approximately 15 hours, the beads were sieved to remove larger cohering groups of beads, and thereafter stored in a dessicator until required.

Table 4.2.1 shows the reduction of affinity for ammonia by the glass beads after the alkali treatment.

Table 4.2.1 Results of tests on glass beads

Beads	Column length cm	Column temp. °C	Flow-rate $cm^3\ min^{-1}$	Sample µmole	V^o_R for peak max. cm^3
Untreated	93.7	19.1	35.6(2)	39	240
Untreated	93.7	19.1	35.6(2)	1 cm^3 air	17
Treated	92.3	19.5	8.2(4)	40	20
Treated	92.3	19.5	8.2(4)	1 cm^3 air	18

4.3 Silver nitrate in meta-toluidine

This system showed no absorption of ammonia, nor manifested plateau type chromatograms. This is due to the formation of a stable complex between the silver and m-toluidine[94], which prevents solid ammine complex formation.

4.3.1 Reasons for using silver nitrate in m-toluidine

The shape of the elution peak obtained from this salt-solvent system consisted of a sharp front followed by a trailing rear, which was a near straight line almost to the base-line (under-ideal type, see 2.2) for sample sizes up to

about 400 µmole. Larger sample sizes showed increasing curvature of the trailing rear, convex to the base-line. This resulted in the majority of peaks consisting of almost perfect triangles, whose areas could be measured to a high degree of accuracy, without a planimeter. du Plessis, who had no planimeter, used these peak areas to obtain the calibration constant C, by using equation (16).

The work described in this thesis required the value of C at a number of different temperatures, and when the experimental work was started, no planimeter was then available, hence the use of this salt-solvent system.

Once the planimeter was obtained, all the areas of the peaks leading to the evaluation of the calibration constant at different temperatures were remeasured with the planimeter. The final results of C are shown in table 4.3.2.

4.3.2 The packings

Table 4.3.1 gives information about the packings. The packings were initially white, turning slowly to a dark brown over a few weeks.

Table 4.3.1 Column packings of silver nitrate in m-toluidine

Packing	Column length cm.	$10^2 s$ (at 25°C) $cm^3\ gm^{-1}$	Silver conc. µmole cm^{-3} (at 25°C)
S.N. m - T(1)	91.2	2.33	364
S.N. m - T(2)	93.8	2.19	440

4.3.3 Numerical results of the calibration constant

Table 4.3.2 Silver nitrate in m-toluidine — numerical results of the calibration constant at different temperatures

Expt. no.	Flow-rate $cm^3\ min^{-1}$	Sample μmole	$10^3 C$ atm. cm^{-1}
	Column temperature, 21.0°C		
1	59.4(7)	81	2.21
2	59.4(7)	325	2.12
3	59.4(7)	207	2.07
4	59.4(8)	524	2.12
5	59.4(0)	652	2.13
6	59.4(9)	118	2.12
7	59.4(9)	291	2.15
8	59.4(2)	262	2.10
9	110.7(9)	820	2.21
10	110.8(4)	443	2.27
11	110.8(4)	442	2.28
12	111.0(1)	204	2.13
13	111.0(5)	385	2.16
14	111.0(1)	727	(2.01)
15	110.9(9)	768	2.16
16	110.9(9)	730	2.14
17	110.9(0)	732	2.26
18	110.9(0)	158	2.18
19	74.4(5)	41	(2.32)
20	74.5(0)	682	2.20
	Column temperature, 24.0°C		
21	51.8(3)	250	2.04
22	51.8(3)	356	2.08
23	51.7(9)	127	2.06
24	51.8(4)	204	2.15
25	51.8(2)	652	2.11
26	90.9(9)	485	2.22
27	91.0(0)	443	2.21
28	88.5(1)	82	2.22
29	88.5(1)	724	2.16
30	88.5(2)	825	2.20
31	63.2(1)	827	2.10
32	61.9(9)	763	2.10
33	62.3(3)	62	2.06
34	62.6(0)	64	2.09
35	60.5(9)	410	2.12
36	19.5(0)	411	2.17
37	17.8(2)	409	2.00
38	64.5(9)	526	2.04
39	64.5(9)	527	2.10
40	64.6(3)	563	2.03
41	64.6(3)	281	2.05

Table 4.3.2 (continued)

Expt. no.	Flow-rate $cm^3\ min^{-1}$	Sample µmole	10^3 C atm cm^{-1}
	Column temperature, 28.0°C		
42	60.4(1)	83	2.22
43	60.1(8)	164	1.91
44	59.9(0)	721	1.95
45	59.8(9)	615	1.95
46	59.8(9)	525	2.05
47	71.7(0)	417	1.92
48	71.7(0)	418	2.17
49	71.6(9)	418	2.00
50	71.6(9)	142	1.96
51	71.6(8)	143	1.96
52	71.6(7)	823	2.20
53	70.7(9)	824	1.93
54	96.4(3)	649	2.11
55	89.3(8)	652	2.08
56	101.5(1)	209	1.92
57	101.4(5)	208	2.04
58	101.5(0)	209	2.10
59	101.5(0)	104	2.13
60	16.9(2)	106	2.17
61	63.9(8)	247	1.95
	Column temperature, 32.0°C		
62	69.2(0)	206	(1.80)
63	68.2(6)	283	2.00
64	66.7(7)	284	1.91
65	66.0(2)	284	1.99
66	66.0(2)	385	1.97
67	66.0(2)	385	1.96
68	66.0(2)	644	1.86
69	97.6(4)	645	2.02
70	97.5(9)	645	1.89
71	97.5(4)	728	2.05
72	70.2(2)	728	1.89
73	74.0(9)	730	1.98
74	73.9(9)	82	2.00
75	73.2(5)	206	(2.12)
76	72.7(6)	206	1.91
77	72.6(2)	410	(1.78)
78	72.5(8)	411	2.09
79	60.8(6)	411	(2.22)
80	60.8(3)	568	2.06
81	60.1(2)	569	2.01

Table 4.3.2 (continued)

Expt. No.	Flow-rate $cm^3\ min^{-1}$	Sample μmole	$10^3.C$ atm. cm^{-1}
	Column temperature, 36.0°C		
82	66.8(9)	528	1.89
83	66.8(9)	614	1.80
84	66.8(9)	688	1.89
85	66.8(9)	127	1.85
86	63.0(1)	327	2.02
87	61.5(5)	411	2.01
88	78.0(3)	446	1.90
89	76.1(0)	81	1.89
90	76.0(4)	108	1.95
91	75.9(6)	742	1.89
92	75.9(6)	743	1.90
93	75.9(3)	819	1.89
94	75.9(3)	821	1.88
95	75.9(3)	823	1.90
96	75.3(7)	527	2.05
97	75.1(9)	615	1.92
98	75.0(8)	284	2.04
99	75.1(9)	329	2.05
100	75.1(9)	328	2.03

The bracketed values of the calibration constant indicate that they lie outside two standard deviations of the mean value.

The mean values of the calibration constants and their standard deviations are shown in table 4.3.3.

Table 4.3.3 Statistical analysis of the calibration constant results

Column temp. °C	$10^3.\bar{C}$ atm. cm^{-1}	$10^3.\sigma$ atm. cm^{-1}
21.0	2.17	0.07
24.0	2.11	0.06
28.0	2.04	0.10
32.0	1.98	0.07
36.0	1.93	0.07

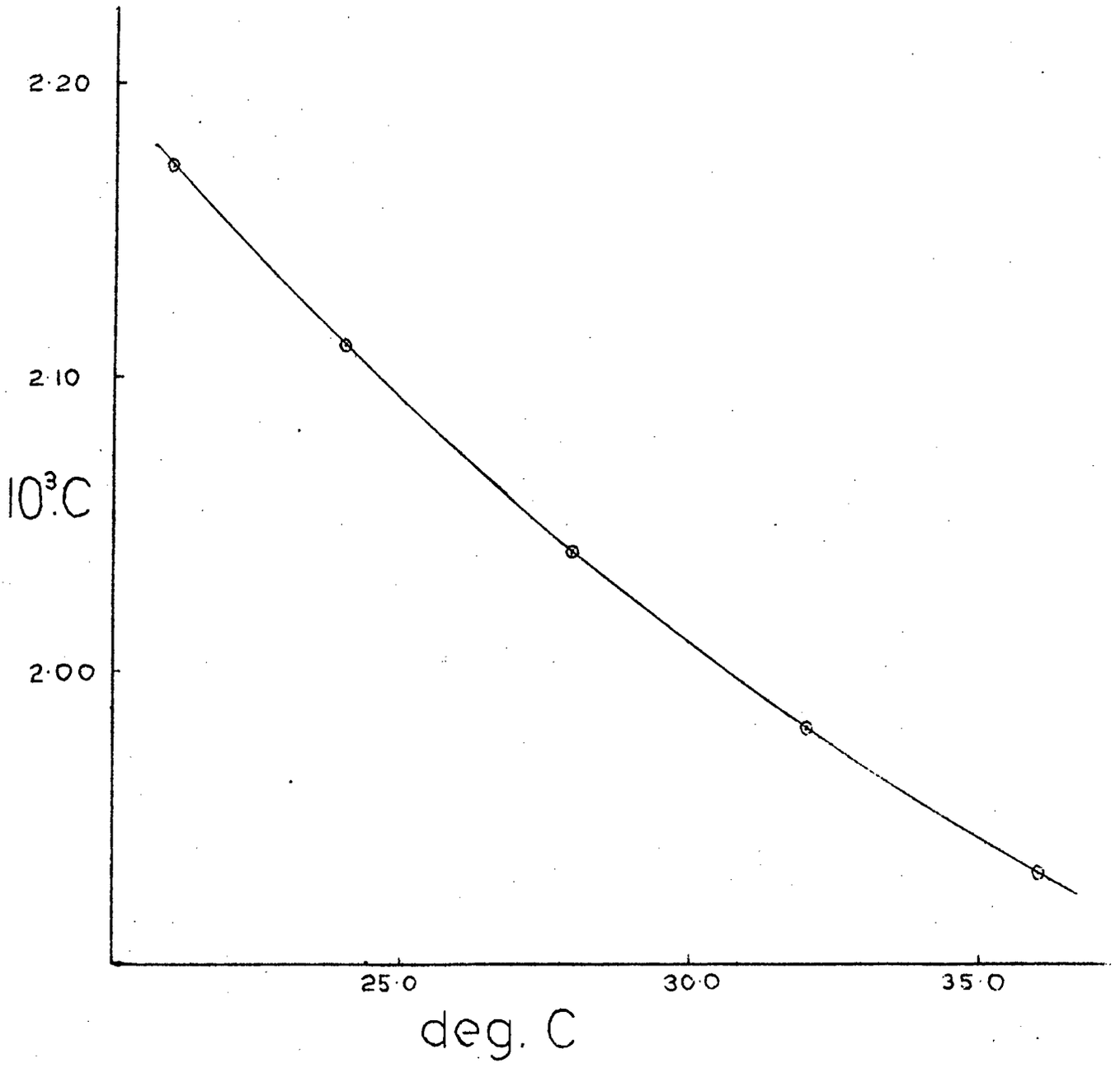

FIGURE 13. TEMPERATURE DEPENDENCE OF THE CALIBRATION CONSTANT.

The plot of the calibration constant as a function of temperature, shown in fig. 13 enabled values of C at temperatures other than those determined experimentally to be interpolated from the curve.

4.4 Syringe sample injection characteristics of the chromatograms

Sample injection by syringe was always marked on the chromatograms by a negative deflection of the recorder pen. As the sample size was increased, the pen returned more slowly to base-line, giving an increasingly large negative peak. This phenomenon was attributed to a surge of ammonia into the upstream cell of the katharometer, resulting in a negative signal to the recorder.

4.5 Silver perchlorate in fenchone

After the initial absorption of ammonia forming complex I, this system yielded a single plateau chromatogram, which under certain conditions manifested a variety of shapes, as a result of rate-effects.

4.5.1 The packings

Table 4.5.1 gives information about the column packings. The higher concentration packings turned greyish when the initial absorption took place, the intensity of the grey decreasing with decrease in silver concentration.

Table 4.5.1 Column packings of silver perchlorate in fenchone

Packing	Column length cm.	10^2s (at 25°C) cm^3 gm^{-1}	Silver conc. µmole cm^{-3} (at 25°C)
S.P.F.(1)	92.0	3.31	480
S.P.F.(2)	95.5	3.23	341
S.P.F.(3)	90.5	3.04	124

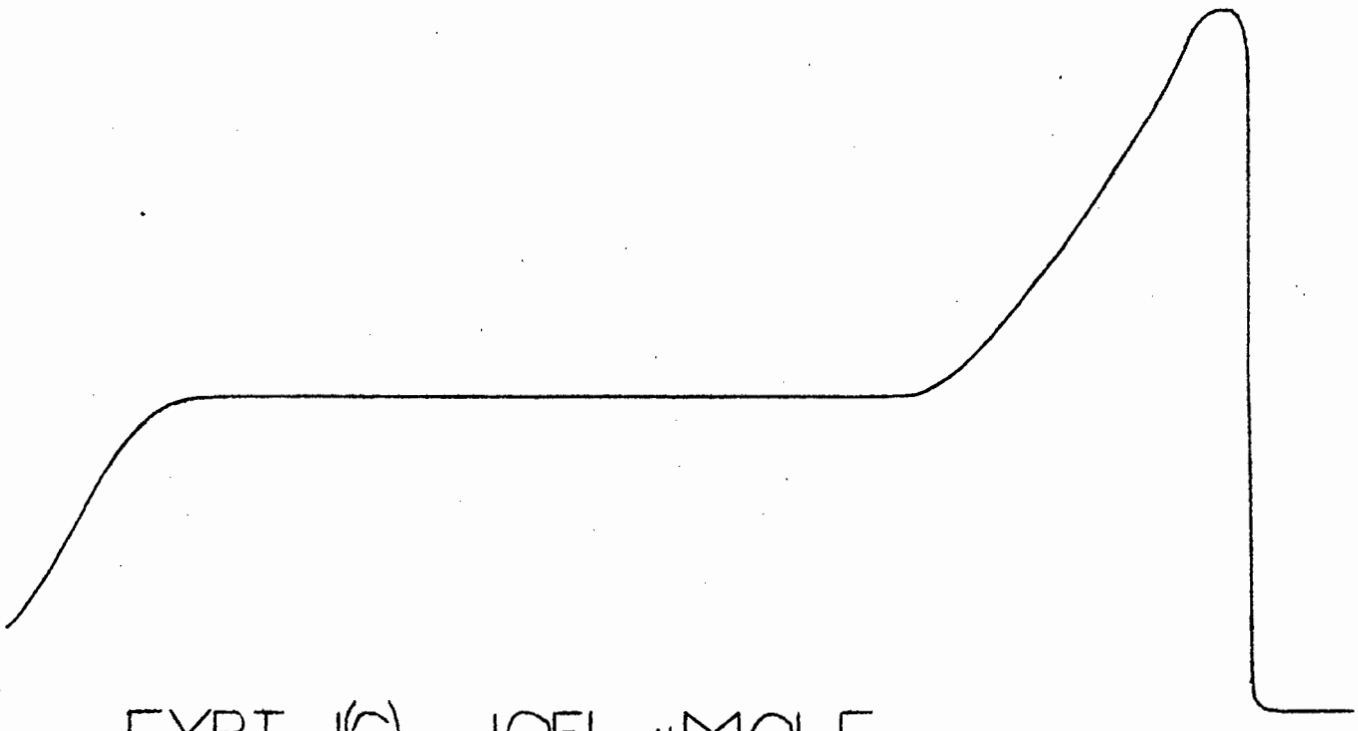

EXPT. 1(C). 1054 μMOLE.

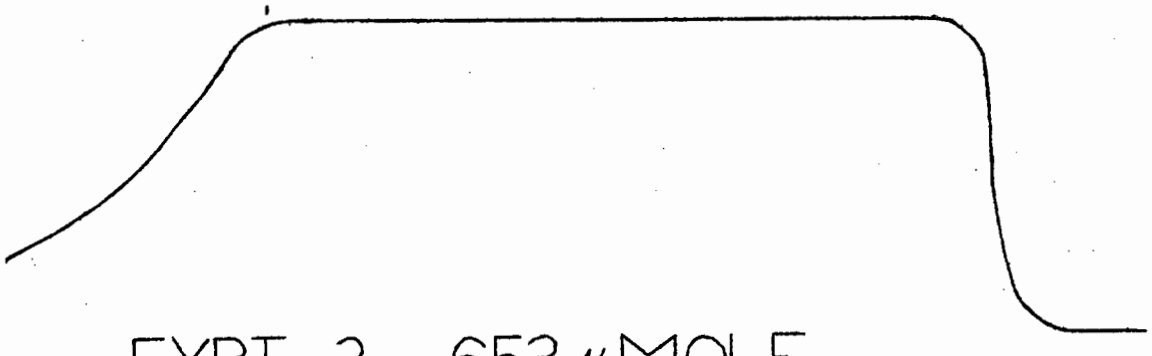

EXPT. 3 653 μMOLE.

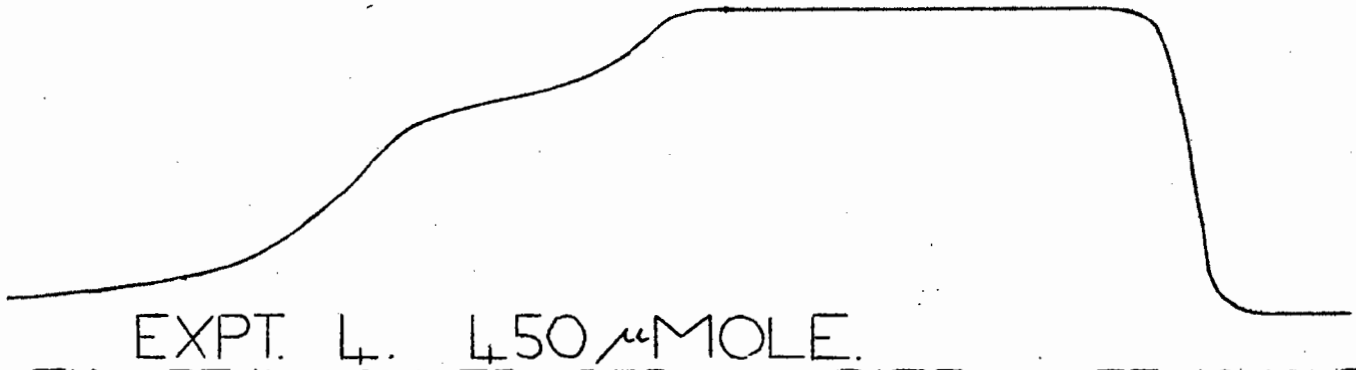

EXPT. 4. 450 μMOLE.

FIGURE 14. SILVER PERCHLORATE IN FENCHONE —EFFECT OF SAMPLE SIZE. PACKING S.P.F. (1). FLOW-RATE, 8·4 (1) $CM^3 MIN^{-1}$. COLUMN TEMPERATURE, 23·0°C.

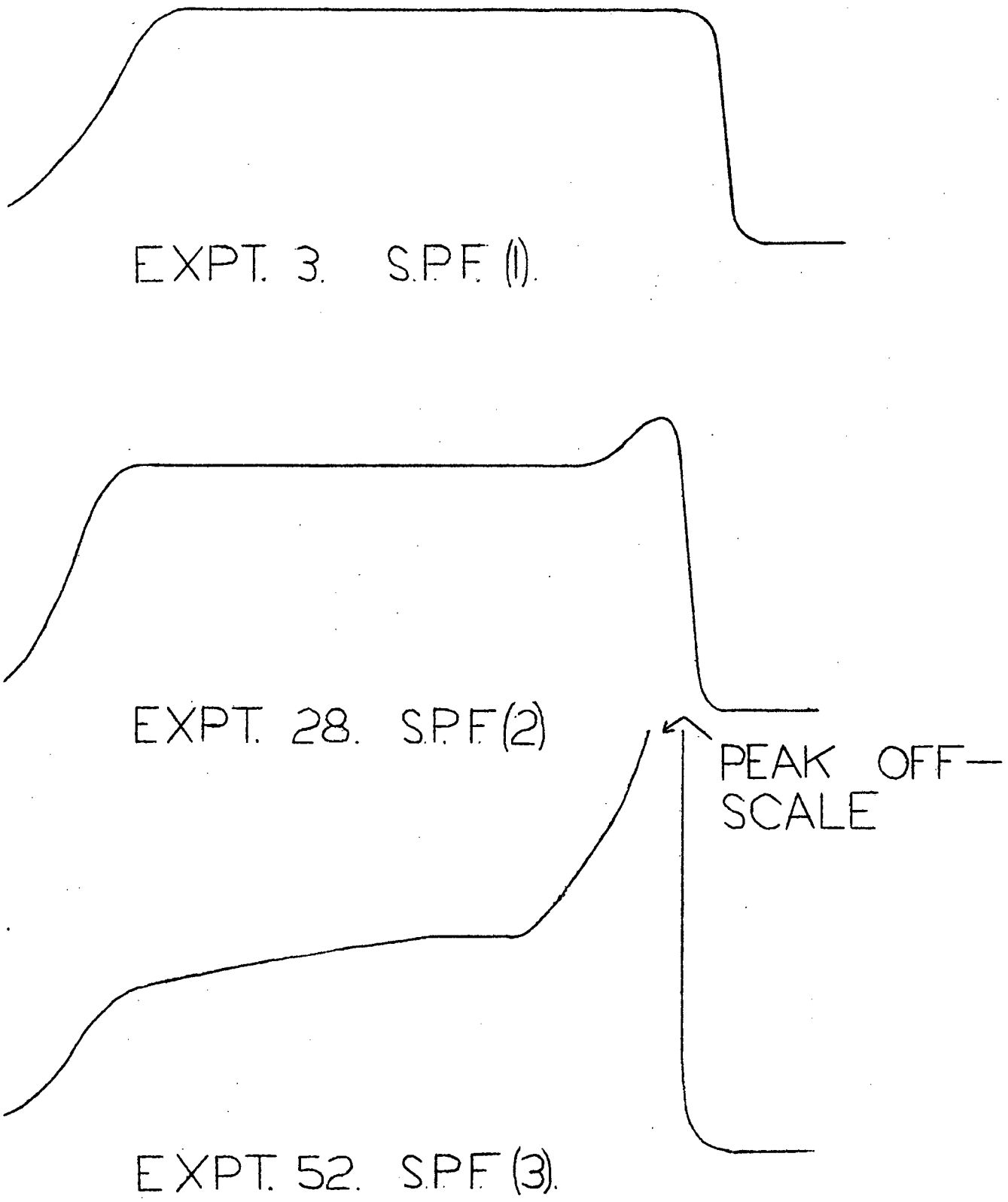

FIGURE 15. SILVER PERCHLORATE IN FENCHONE.—EFFECT OF SILVER CONCENTRATION. SAMPLE SIZE, (650-653) μMOLE, COLUMN LENGTH, (90-95) CM, FLOW-RATE, (6·6(1) 8·4(1)) CM^3 $MIN.^{-1}$, COLUMN TEMPERATURE, 23·0°C.

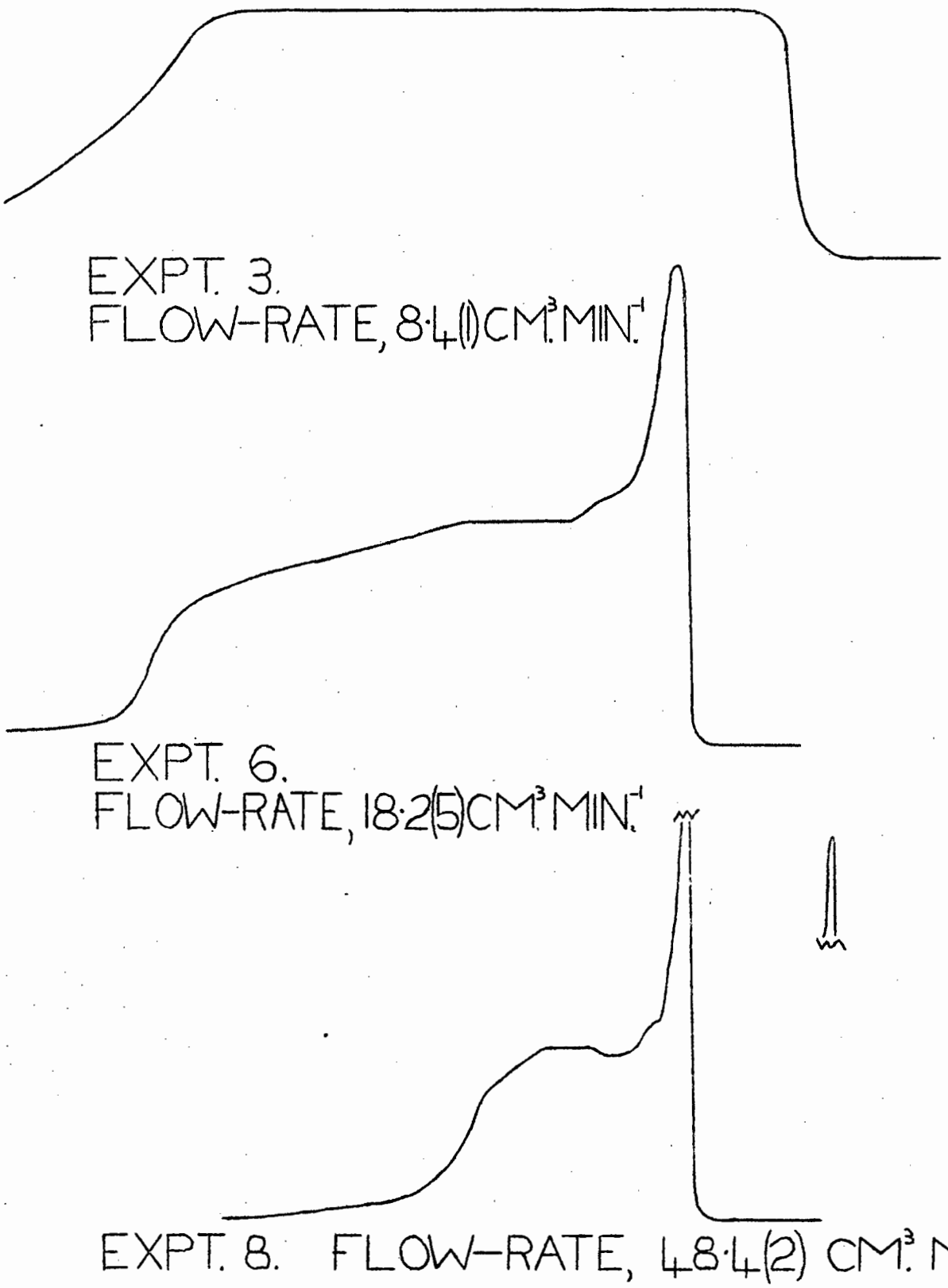

FIGURE 16. SILVER PERCHLORATE IN FENCHONE.—EFFECT OF FLOW-RATE. PACKING S.P.F.(1). SAMPLE SIZE, 653 μMOLE, COLUMN TEMPERATURE, 23·0°C.

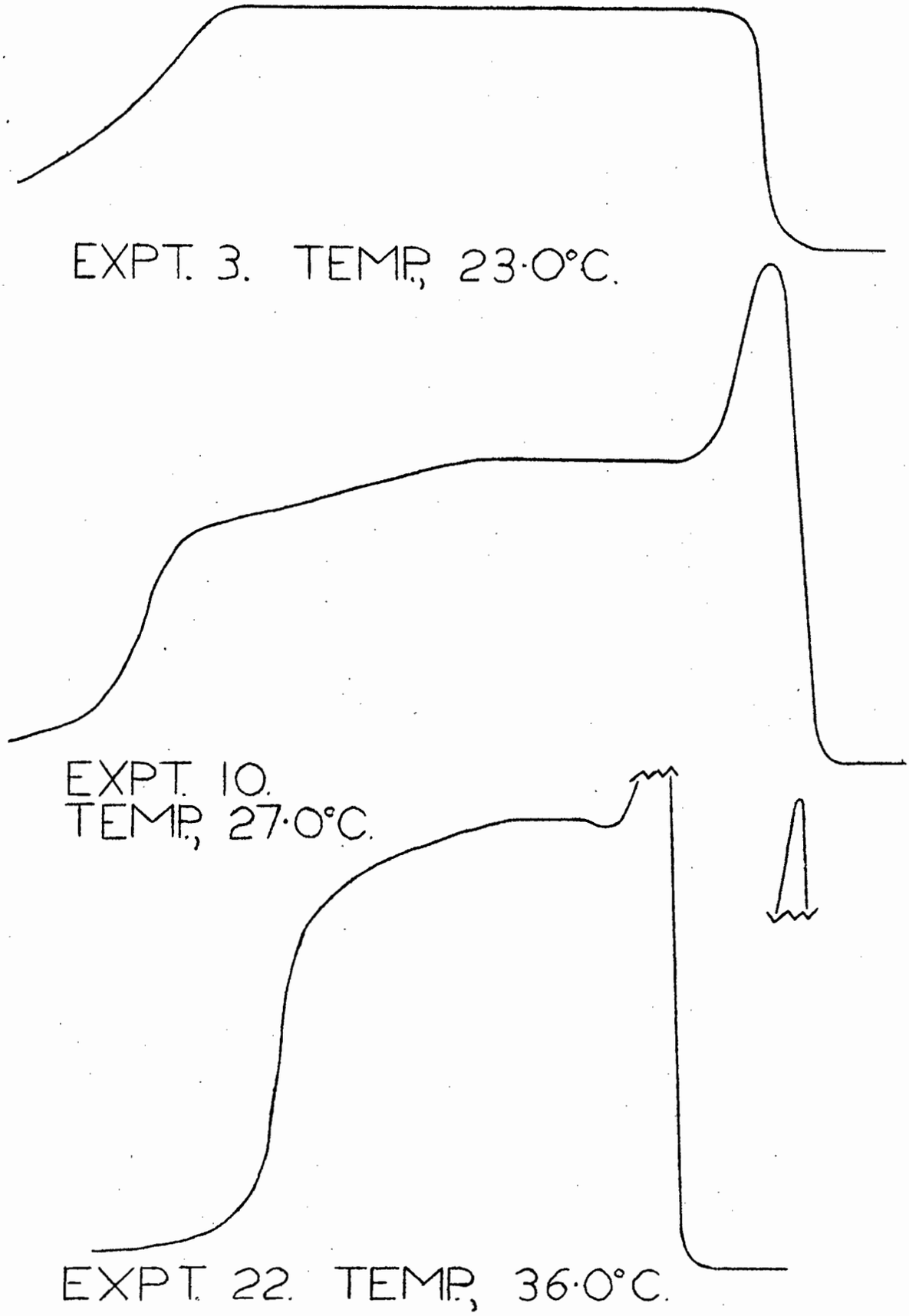

FIGURE 17. SILVER PERCHLORATE IN FENCHONE.—EFFECT OF COLUMN TEMPERATURE. PACKING S.P.F.(1). FLOW-RATE, (7·5(4)-8·4(1)) $CM^3.MIN^{-1}$, SAMPLE SIZE, (650-652) μMOLE.

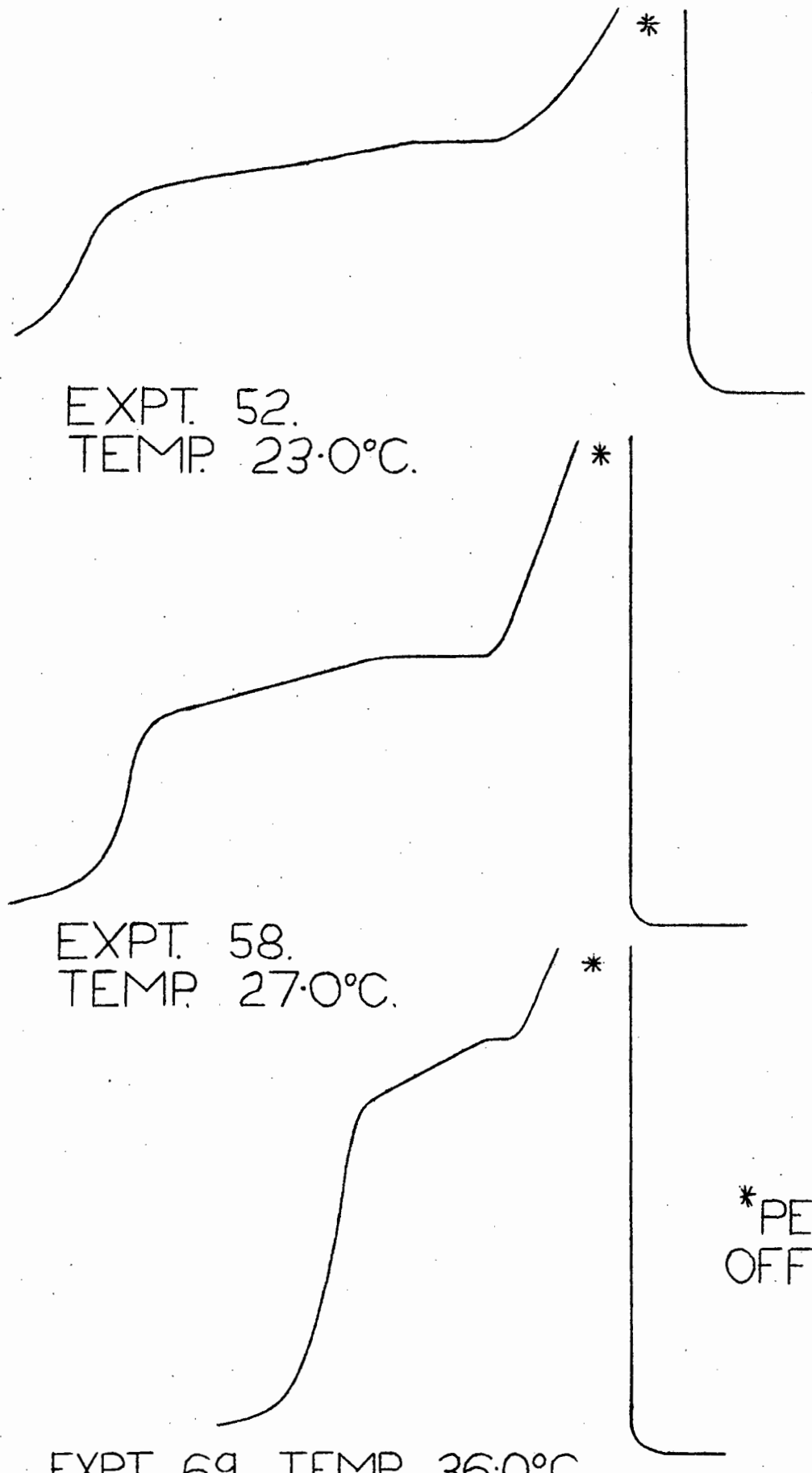

FIGURE 18. SILVER PERCHLORATE IN FENCHONE.—EFFECT OF COLUMN TEMPERATURE. PACKING S.P.F.(3). FLOW-RATE, (7·7(8)—9·8(1))CM^3 MIN^{-1}, SAMPLE SIZE, 652 μMOLE.

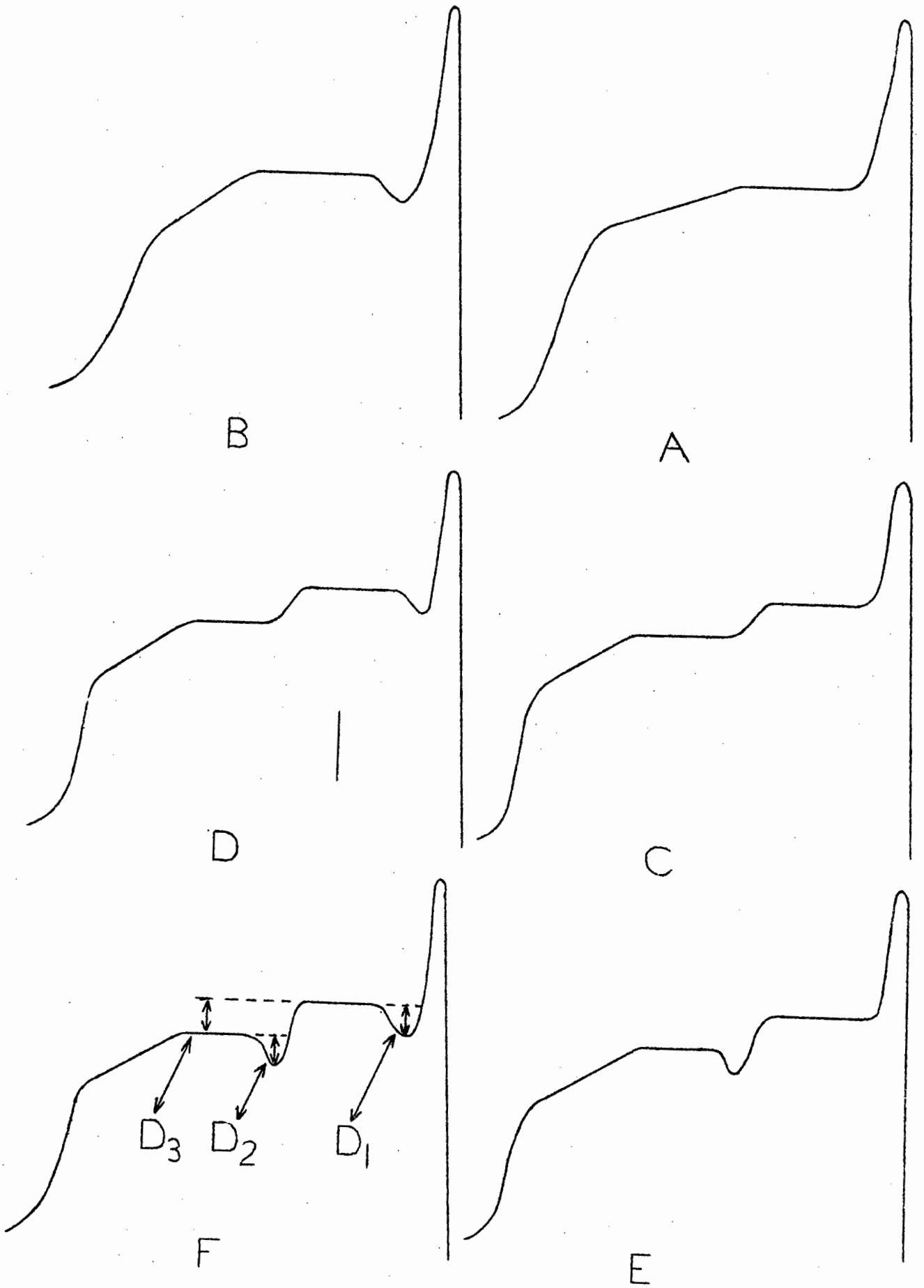

FIGURE 19. SILVER PERCHLORATE IN FENCHONE.—INFLUENCE OF RATE—EFFECTS ON PLATEAU PROFILE.

4.5.2 The initial absorption

The following initial absorptions (moles of ammonia per mole of silver perchlorate) were measured

Packing S.P.F.(1)	1.98
Packing S.P.F.(2)	2.20
Packing S.P.F.(3)	2.04

4.5.3 The chromatograms

Due to decomposition of complex I, as a result of the elution of ammonia at its dissociation pressure, a small amount of ammonia was injected before each quantitative injection, in order to ensure that all the silver was in the solid complex I form.

Figs. 14 to 18 show the effect of the column variables on the chromatograms. The relationship between the chromatograms, and the variation of the sample size, silver concentration and flow-rate is in accord with the explanation given in 1.4. The increase of the dissociation pressure of complex II with temperature indicates an exothermic process for the complex forming reaction. Thus raising the temperature inhibits the complexing reaction, and the rate of conversion of ammonia from zone I to zone II is accordingly decreased (figs. 17, 18).

Rate-controlling steps of the complexing process are now considered in order to explain certain anomalous features of the plateau profile shown in fig. 19.

For the complexing process occurring in the chromatographic column, any of the following steps may be rate-controlling :

(1) diffusion of the ammonia in the gas phase to the gas-liquid interface

(2) reaction at the gas-liquid interface (resistance to mass transfer of the ammonia from the gas phase to the liquid phase).

(3) diffusion of the ammonia in the organic solvent to the surface of solid complex I.

(4) reaction of the ammonia with complex I to form complex II.

(5) decomposition of solid complex II at its dissociation pressure.

(6) diffusion of the ammonia in the organic solvent to the gas-liquid interface.

(7) reaction at the gas-liquid interface (resistance to mass transfer of the ammonia from the liquid phase to the gas phase).

Step (1) cannot be considered rate-controlling, as the ammonia band permeates the packing and is hence in intimate contact with the liquid phase at all times.

Steps (2) and (3) cannot be rate-controlling otherwise the conversion rate of ammonia from zone I to zone II would be independent of silver concentration. This is not the case as can be seen from fig. 15.

Similarly steps (6) or (7) cannot be rate-controlling, otherwise the rate of efflux of ammonia from the liquid phase would be independent of the amount of complex II formed, which is not the case, as can be seen from figs. 14 and 15. The decay of the rear end of the plateaux of the smallest sample size in fig. 14, and the smallest silver concentration in fig. 15, indicates that the rate of efflux of ammonia from the liquid phase is insufficient to replenish the ammonia swept away by the carrier gas, for complex concentrations

below a certain value.

Consideration of equation (22) indicates that if step (4) was rate-controlling, the factor $k_4 S_{II} - k_3 S_I [NH_{3(l)}]^y$ would be very large, and the ammonia gas concentration would hence be easily maintained. However the appreciable amount of complex formed (figs. 14 to 18), and the values obtained of the equilibrium function (see table 4.5.3) do not suggest that step (4) is slow relative to step (5).

When the ammonia gas pressure is greater than the dissociation pressure, there is a net gain of ammonia in the liquid phase, which is used up in complex formation. However, under plateau conditions, when there is a net loss of ammonia from the liquid phase, step (4) is competing with step (7) for the ammonia in that phase. If step (7) is very fast (as it usually is) the amount of complex formed during the elution of the plateau region will be small. Consequently if the decomposition rate of the complex is slow, the ammonia liquid concentration level cannot be maintained, and the rate of step (7) decreases. The consequent decrease in the rate of replenishment of ammonia to the gas phase, results in the plateau decay.

Thus step (5), the decomposition rate of the complex, seems the most likely rate-controlling step.

The decomposition rate of the complex depends upon the amount of complex present, and variables which affect the amount of complex formed, cause decay of the plateau. Thus decreasing the sample size (fig. 14) and silver concentration (fig. 15) while increasing the temperature (figs. 17,18), leads to a decrease in the amount of complex formed, with consequent plateau decay. Furthermore, increasing the flow-rate, necessitates an increase

of the ammonia concentration in the liquid phase in order to maintain the plateau level, as indicated by equation (20). Thus at a particular concentration of the complex and a high enough flow-rate, the decomposition rate of the complex is too slow to maintain the requisite ammonia liquid phase concentration level, with consequent decay of the plateau (fig. 16).

Fig. 19 shows the plateau profiles obtained with the silver perchlorate - fenchone system as a result of the rate-effects. Fig. 19C type of chromatogram occurs at the higher flow-rates, and is explained in the following way : as the complex begins to decompose, its initial concentration range results in a high enough decomposition rate for the higher plateau level to be maintained. However, as it decomposes, its decomposition rate decreases, and eventually the ammonia concentration level in the liquid phase decreases to a new dynamic steady state value, with a corresponding drop in the plateau height. Finally the decomposition rate of the complex becomes so slow, that the ammonia liquid phase concentration level cannot be kept at any steady value, and hence the decay of the rear end of the plateau.

At lower flow-rates fig. 19A type of chromatogram occurs, as the removal of ammonia by carrier gas is much slower, and the decomposition of the complex is fast enough to maintain the higher plateau level, until eventual decay occurs.

The dips shown in figs. 19B, D, E and F are attributed to delayed decomposition of the complex. The drop in the ammonia liquid phase concentration level (due to the delayed complex decomposition) results in the dip. When the complex begins decomposing the ammonia liquid phase concentration level is

restored and the plateau level regained.

The depths of the dips D_1 and D_2, and the plateau height difference D_3 shown in fig. 19F are given in table 4.5.2.

Table 4.5.2 Silver perchlorate in fenchone - influence of rate-effects on the chromatogram shapes

Expt. No.	Column temp. °C	Flow-rate $cm^3 min^{-1}$	Chromatogram type (fig.19,A,B,C,D,E,F)	10^3 D_1 Atm.	10^3 D_2 Atm.	10^3 D_3 Atm.
Packing S.P.F.(1), 92.0 cm, 736 µmole of silver perchlorate, 8.00 µmole cm^{-1}. Sample size of ammonia, (650 - 653) µmole.						
5	23.0	18.2(5)	C	-	-	1.6
6	23.0	18.2(5)	C	-	-	2.4
7	23.0	48.4(2)	A	-	-	-
8	23.0	48.4(2)	E	-	0.7	2.6
9	27.0	7.5(4)	B	0.8	-	-
10	27.0	7.5(4)	A	-	-	-
11	27.0	22.0(8)	C	-	-	2.5
12	27.0	22.0(8)	E	-	1.2	2.0
13	27.0	44.4(4)	F	0.7	1.0	2.2
14	27.0	44.4(4)	D	1.8	-	2.8
15	32.0	8.0(5)	B	1.1	-	-
16	32.0	8.0(5)	B	1.0	-	-
17	32.0	22.7(2)	F	1.5	1.0	3.9
18	32.0	22.7(2)	D	2.1	-	4.0
19	32.0	42.3(9)	F	2.6	1.6	4.0
20	32.0	42.3(9)	D	3.2	-	6.4
21	36.0	8.1(4)	B	2.6	-	-
22	36.0	8.1(4)	B	1.6	-	-
23	36.0	24.5(9)	F	2.9	0.5	6.2
24	36.0	24.5(9)	D	2.9	-	7.2
25	36.0	42.6(1)	D	4.7	-	7.4
26	36.0	42.6(1)	D	5.5	-	8.6
Packing S.P.F.(2), 95.5 cm, 524 µmole of silver perchlorate, 5.49 µmole cm^{-1}. Sample size of ammonia, (650 - 653) µmole						
29	23.0	23.2(0)	A	-	-	-
30	23.0	23.2(0)	B	0.6	-	-
31	23.0	46.9(4)	B	2.2	-	-
32	23.0	46.9(4)	E	-	0.8	3.1

Table 4.5.2 (continued)

Expt. No.	Column temp. °C	Flow-rate $cm^3 min^{-1}$	Chromatogram type (fig.19,A,B,C,D,E,F)	$10^3 D_1$ Atm.	$10^3 D_2$ Atm.	$10^3 D_3$ Atm.
33	27.0	7.1(8)	B	2.8	-	-
34	27.0	7.1(8)	B	2.6	-	-
35	27.0	24.6(4)	B	2.3	-	-
36	27.0	24.6(4)	B	1.0	-	-
37	27.0	42.1(3)	B	2.9	-	-
38	27.0	42.1(3)	C	-	-	1.5
39	32.0	7.0(6)	B	0.9	-	-
40	32.0	7.0(6)	B	1.6	-	-
41	32.0	19.5(3)	E	-	0.4	1.8
42	32.0	19.5(3)	E	-	0.7	0.8
43	32.0	46.8(2)	F	0.7	0.5	3.7
44	32.0	46.8(2)	C	-	-	3.1
45	36.0	6.3(6)	B	1.5	-	-
46	36.0	6.3(6)	B	2.8	-	-
47	36.0	20.9(5)	F	1.7	0.7	3.9
48	36.0	20.9(5)	D	2.1	-	1.6
49	36.0	39.7(5)	F	3.0	0.4	5.1
50	36.0	39.7(5)	F	2.9	0.7	3.1
Packing S.P.F.(3)., 90.5 cm, 202 µmole of silver perchlorate 2.24 µmole cm^{-1}. Sample size of ammonia, (650 - 653) µmole						
51	23.0	8.1(3)	A	-	-	-
52	23.0	8.1(3)	A	-	-	-
53	23.0	24.7(5)	A	-	-	-
54	23.0	24.7(5)	A	-	-	-
55	23.0	42.8(3)	B	2.6	-	-
56	23.0	42.8(3)	B	2.8	-	-
57	27.0	7.7(8)	A	-	-	-
58	27.0	7.7(8)	A	-	-	-
59	27.0	25.2(4)	B	2.6	-	-
60	27.0	25.2(4)	B	3.4	-	-
61	27.0	45.4(2)	B	4.8	-	-
62	27.0	45.4(2)	B	4.8	-	-

Table 4.5.2 (continued)

Expt. No.	Column temp. °C	Flow-rate $cm^3 min^{-1}$	Chromatogram type (fig.19,A,B,C,D,E,F)	$10^3 D_1$ Atm.	$10^3 D_2$ Atm.	$10^3 D_3$ Atm.
63	32.0	7.9(7)	A	-	-	-
64	32.0	7.9(7)	A	-	-	-
65	32.0	23.9(9)	B	1.9	-	-
66	32.0	23.9(9)	B	1.6	-	-
67	32.0	42.0(2)	B	2.9	-	-
68	32.0	42.0(2)	B	3.0	-	-
69	36.0	9.8(1)	A	-	-	-
70	36.0	9.8(1)	A	-	-	-
71	36.0	26.1(3)	B	1.5	-	-
72	36.0	26.1(3)	B	2.5	-	-
73	36.0	51.1(8)	B	9.4	-	-
74	36.0	51.1(8)	B	9.3	-	-

There is no regular appearance of the dips, although there appears to be some trend of D_1 with flow-rate for packings S.P.F.(1) and (3) but not for (2).

The low silver concentration packing S.P.F.(3) shows no division of the plateau height at any flow-rate. This is attributed to the fact that the amount of complex formed is so small, and thus its decomposition rate is correspondingly so slow, that the undecayed portion of the plateau is the lowest possible dynamic steady state value that can be maintained before decay occurs. Values of the dissociation pressures in 4.5.7 tend to bear this out.

4.5.4 Treatment of decayed plateau type chromatograms

It was noticed that the slope of the rear end of the chromatograms, where decay took place, was almost constant (figs. 14 to 18). This fact was utilized in determining the division between zone II(a) and II(b) of the chromatograms.

The straight sloping portion of the rear end was extended

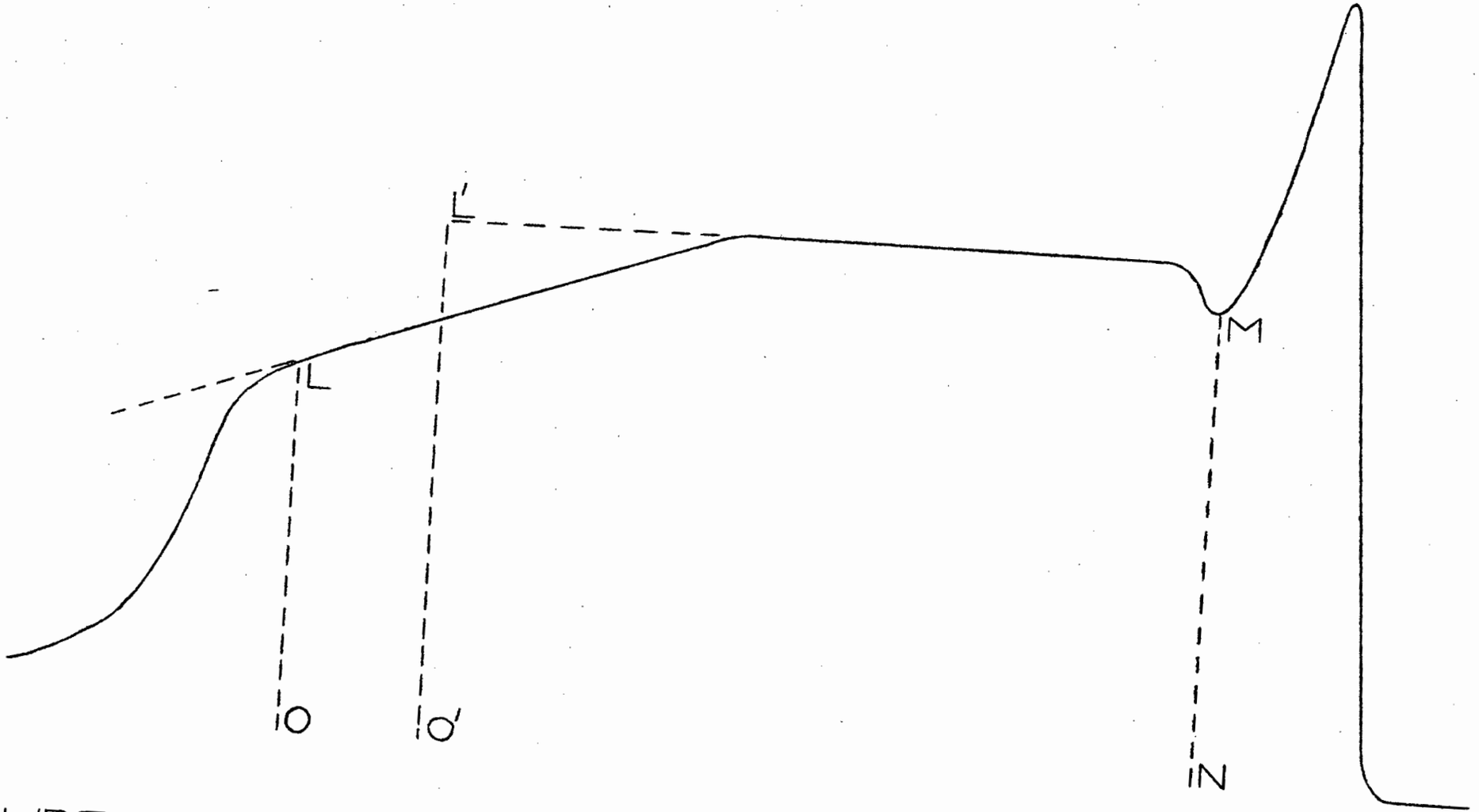

FIGURE 20. SILVER PERCHLORATE IN FENCHONE.
QUANTITATIVE TREATMENT OF DECAYED CHROMATOGRAMS

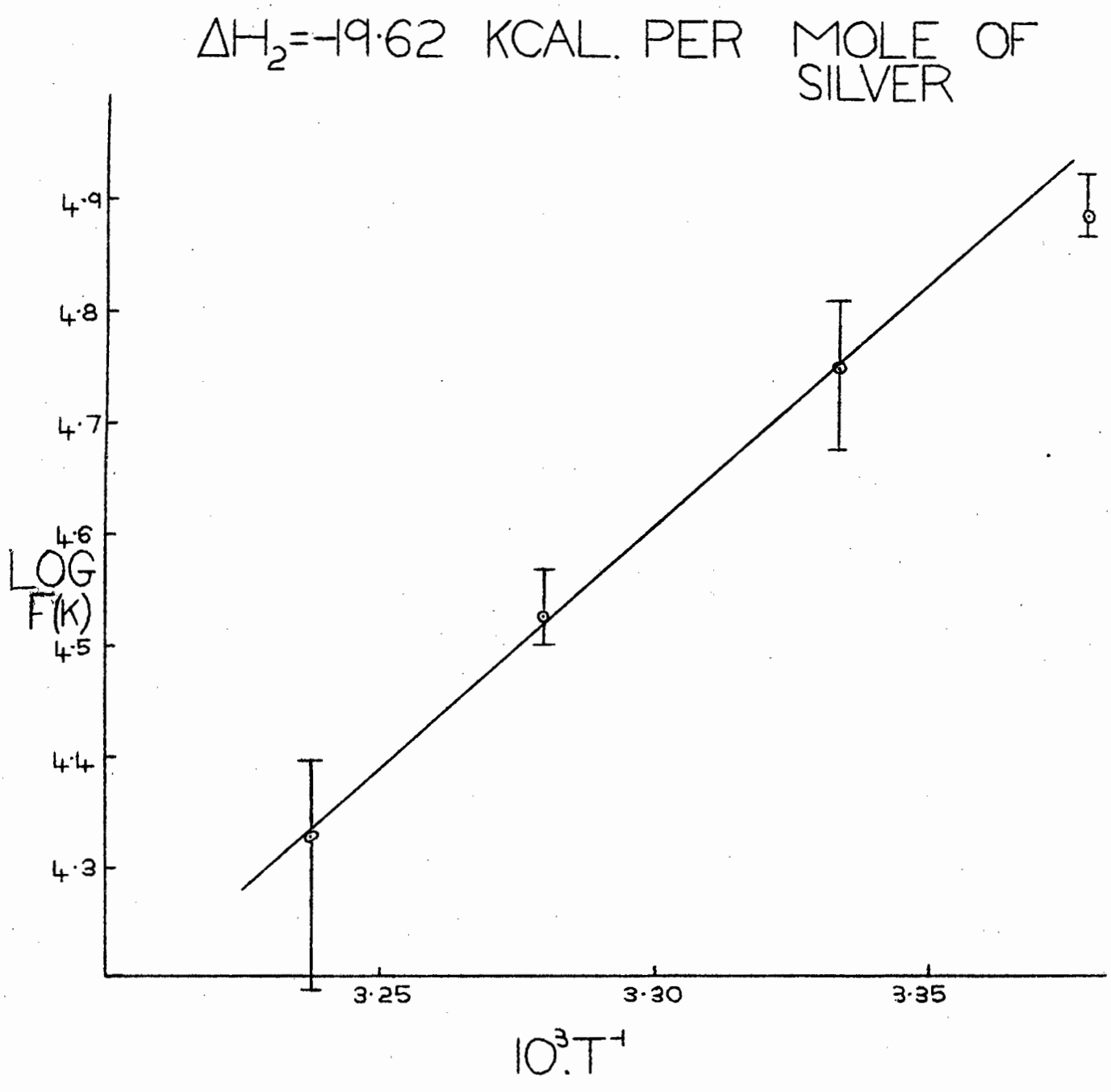

FIGURE 21. SILVER PERCHLORATE IN FENCHONE. EXPERIMENTAL PLOT OF THE TEMPERATURE DEPENDENCE OF THE EQUILIBRIUM FUNCTION.

as shown in fig. 20, and where divergence occurred between the extended straight dotted line and the curvature of the chromatogram, the rear end of zone II(a), LO, was located. The decayed zone II(a) i.e, MNOL was reconstructed to give the equivalent undecayed zone II(a), MNO'L'. The chromatogram was then quantitatively treated in an identical fashion to an undecayed chromatogram, as outlined in 2.5.1 (fig. 5).

The reconstruction of the decayed chromatograms was necessary as equation (40) is based on the assumption of a constant value of the gas-liquid distribution of ammonia, as indicated by the constant plateau height.

The reconstruction can be justified by the fact that the actual length of column occupied by zone II(a), as it begins to emerge from the column is independent of the decay. However the slow decomposition which causes the decay also causes an increase of the time interval between the emergence of the front and rear ends of zone II(a), and if the increased value of t_e is inserted in equation (40), a too large value of L'_1 would be obtained.

Chromatograms manifesting plateau height division as illustrated in fig. 19 were reconstructed by taking the highest plateau level as the correct one, while chromatograms showing continuous decay (see 4.6.3, fig. 28) were reconstructed by taking the highest plateau point as the correct plateau level.

4.5.5 The equilibrium function and its temperature dependence

Values of the equilibrium function are shown in table 4.5.3. Constancy of the values of F (K) was obtained for $y = 3$. The plot of log F (K) as a function of $^1/T$ (fig. 21)

gave a straight line from which the heat of reaction of the complex, ΔH_2, was computed.

The extrapolated values in columns 3 and 4 of table 4.5.3 were obtained from the type of curves shown in fig. 6. Three widely differing flow-rates were used to obtain the experimental points of these curves, each experimental point being the mean of two results.

These remarks apply to all the other systems studied.

Table 4.5.3 Silver perchlorate in fenchone - results, and temperature dependence of the equilibrium function

Packing S.P.F.	Column temp. °C	Molar ratio (R)	% conversion	10^{-4} F (K) litre^3 mole^{-3}
(1)	23.0	1.41	96.3(5)	8.2(4)
(2)	23.0	0.95	94.3(8)	7.0(2)
(3)	23.0	1.77	88.7(1)	7.2(4)
(1)	27.0	0.94	95.6(9)	6.4(0)
(2)	27.0	1.17	94.5(0)	5.5(7)
(3)	27.0	1.67	86.8(3)	4.6(7)
(1)	32.0	0.84	94.4(0)	3.2(0)
(2)	32.0	1.08	93.2(6)	3.1(4)
(3)	32.0	1.80	86.1(0)	3.6(7)
(1)	36.0	0.75	93.5(5)	2.5(0)
(2)	36.0	0.89	90.4(3)	1.5(4)
(3)	36.0	1.96	84.4(0)	2.3(4)

Each experimental point in fig. 21 is the mean of the equilibrium function results at each temperature, while the length of each vertical line about the experimental point indicates the range between the maximum and minimum values.

The assumption that the ratio of the geometrical constants (relating the surface areas of the complexes to their mole numbers)

is not a function of temperature (2.5.3) is not necessarily correct. However the trend which may have appeared in fig. 21 as a result of this possible temperature dependence is lost in the large scatter of the equilibrium function values.

The temperature plot of the equilibrium function for the S.N.B. system (fig.35) having a smaller scatter of F (K) values (see 4.7.4.), suggests that if the ratio of the geometrical constants is temperature dependent, it is to a small degree within the experimental scatter.

Several sources of error are present in the method of determining F(K) and give rise to a large variation of its values at a particular temperature. These errors may be listed as follows:

(a) the principal source of error is the uncertainty in location of the rear end of the reacted zone (zone II(a)) resulting in uncertainty in the experimental points of the extrapolation curves (fig. 6).

(b) the large difference between the viscosities of the carrier gas, nitrogen, and the sample gas, ammonia (viscosities at 18.0°C: N_2, 175 μpoise : NH_3, 106 μpoise) results in flow-rate variations as the ammonia band passes through the column. These flow-rate variations tend to become significant for large ammonia sample sizes, and high p_d values. This leads to uncertainties in the value of the measured flow-rate, as the soap-film flow-meter dissolves the ammonia and does not measure its contribution to the total flow-rate.

(c) the so called "surge" effect[89], resulting in an increase in the true flow-rate, due to the transfer of ammonia from the liquid to the gaseous phase at the end of the column, and

resulting in a chromatogram area smaller than that corresponding to the measured flow-rate. The utilization of this flow change has even been suggested as a possible method of peak detection.[95]

(d) the loss of liquid substrate due to evaporation by the carrier gas, results in uncertainty in the value of the ammonia concentration factor in the equilibrium function expression. This loss is offset to some extent by the fact that the packing towards the end of the column is replenished by solvent transferred from nearer the inlet[96], and the error is thus decreased, as the chromatograms are records of the ammonia distribution between the phases in the latter half of the column.

(e) the surge of ammonia into the upstream cell of the katharometer as a result of syringe injection (see 4.4) is not taken into account by the formulae developed for the determination of L'_1. Thus L'_1 and the quantities associated with it are error prone. Also, no account is taken of the small void volume between the packing and detector.

In the determination of y, the equilibrium function was found to vary in the manner predicted in 2.5.2, as shown in table 4.5.4. The blank spaces indicate where negative values were obtained.

Table 4.5.4 Silver perchlorate in fenchone - variation of F'(K) with assumed y values

Packing S.P.F.	δ	$\frac{(n_I y - \Delta)}{(n_I(y+\delta)-\Delta)}$	$\left[\frac{n_{NH_3} - \Delta}{V_f}\right]^{-\delta}$ litre$^{\delta}$ mole$^{-\delta}$	F'(K) (at 23.0°C) litre$^{y+\delta}$ mole$^{-(y+\delta)}$
(1)	-2	-	3.33×10^{-4}	-
(2)	-2	20.5	3.33×10^{-4}	4.78×10^{2}
(3)	-2	-	6.15×10^{-4}	-

Table 4.5.4 continued

Packing	ε	$\frac{(n_I\, y - \Delta)}{(n_I\,(y+\varepsilon)-\Delta)}$	$\left[\frac{n_{NH_3} - \Delta}{V_f}\right]^{-\varepsilon}$ litre$^{\varepsilon}$ mole$^{-\varepsilon}$	F'(K) (at 23.0°C) litre$^{y+\varepsilon}$ mole$^{-(y+\varepsilon)}$
(1)	-1	2.00	18.26×10^{-3}	2.99×10^{3}
(2)	-1	1.91	18.25×10^{-3}	2.44×10^{3}
(3)	-1	3.34	24.79×10^{-3}	6.00×10^{3}
(1)	0	1	1	8.24×10^{4}
(2)	0	1	1	7.02×10^{4}
(3)	0	1	1	7.24×10^{4}
(1)	+1	0.67	54.8	3.01×10^{6}
(2)	+1	0.68	54.8	2.61×10^{6}
(3)	+1	0.59	40.0	1.72×10^{6}
(1)	+2	0.50	3.0×10^{3}	12.34×10^{7}
(2)	+2	0.51	3.0×10^{3}	10.82×10^{7}
(3)	+2	0.42	1.6×10^{3}	1.88×10^{7}

There is one exception to the trend for $\varepsilon = -1$, due to the wide experimental scatter of the equilibrium function. However the much wider scatter of values of F'(K) for $y = 2$ than for $y = 3$, together with the expected trend obtained for $y = 2$ at other temperatures, as shown in table 4.5.5, resulted in the adoption of $y = 3$ as the true stoichiometric value.

Table 4.5.5 Silver perchlorate in fenchone-trend of F'(K) with silver concentration for $y = 2$

Packing S.P.F.	Column temp. °C	10^{-3}.F'(K) litre^{2} mole^{-2}
(1)	27.0	2.30
(2)	27.0	2.57
(3)	27.0	3.59

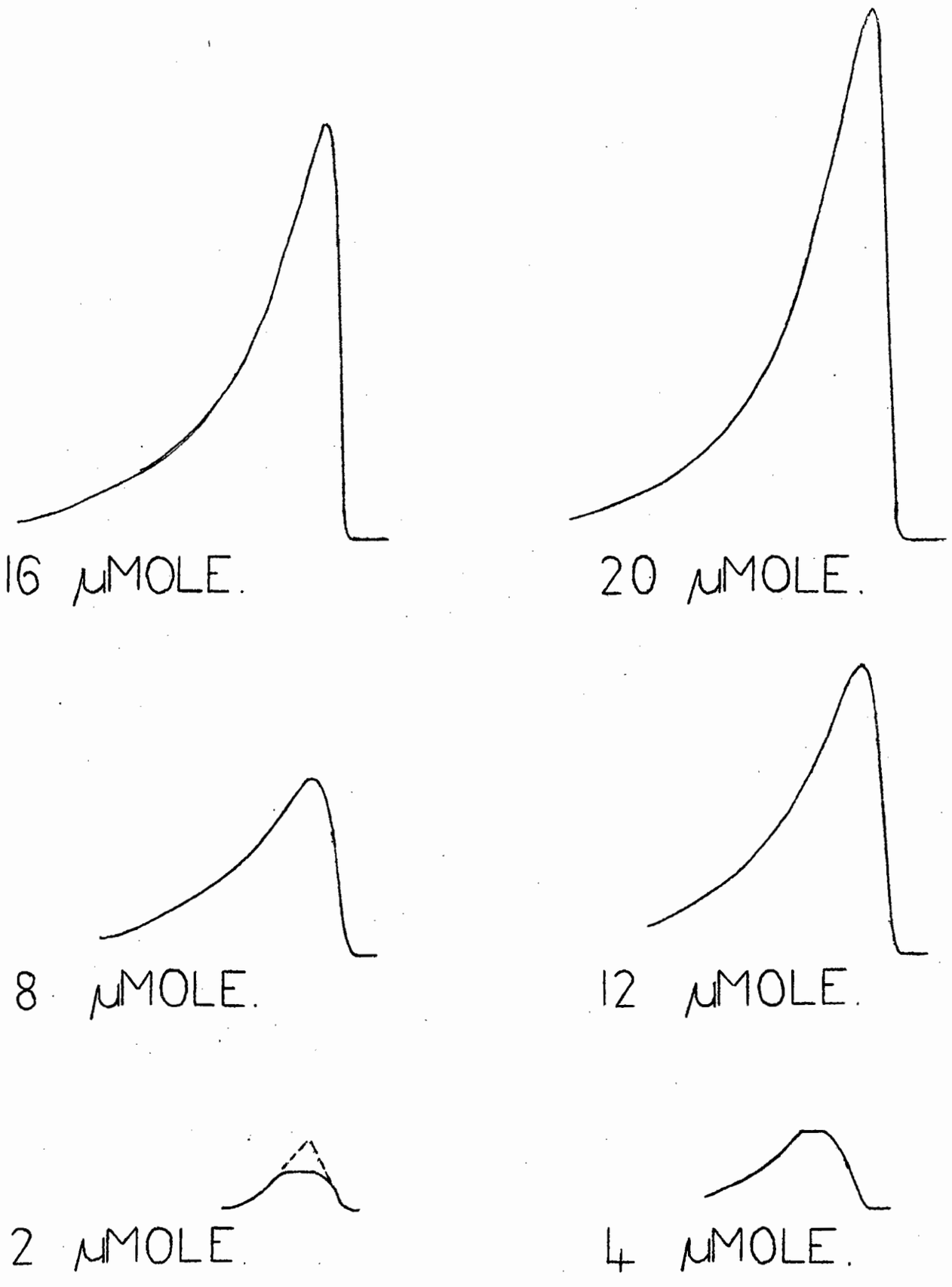

FIGURE 22. PURE FENCHONE SUBSTRATE. VARIATION OF PEAK ASSYMMETRY WITH AMMONIA SAMPLE SIZE.

Table 4.5.5 continued

Packing S.P.F.	Column Temp. °C	$10^{-3}.F'(K)$ litre^2 mole^{-2}
(1)	32.0	1.30
(2)	32.0	1.59
(3)	32.0	3.66
(1)	36.0	1.02
(2)	36.0	(0.81)
(3)	36.0	3.42

4.5.6 Heat of solution of ammonia in fenchone

The heat of solution of ammonia in fenchone was determined on a column of approximately 90cm length, containing pure fenchone as the liquid substrate.

The partition coefficient was determined from equation (13). $V^{o}_{R}{}'$ was found from the difference in retention volumes of the peak maxima of the ammonia and air peaks.

The non-ideality of ammonia in fenchone was taken into account by using extremely small sample size of ammonia ($\sim$ 2 µmole) which resulted in peaks being only slightly skew, of the "under-ideal" type (see 2.2). The variation of peak shape with sample size is shown in fig. 22.

Each value of the partition coefficient in table 4.5.6 is the mean of three results.

These remarks apply to all systems where the heat of solution of ammonia in the organic solvent was determined.

Table 4.5.6 Variation of the partition coefficient with temperature

Column temp. °C	t_r min.	t_g min.	$t_r - t_g = t_f$ min.	V^o_R' cm^3	V_f cm^3	K
23.4	5.8(6)	2.0(5)	3.8(1)	34.3(4)	1.55(1)	22.1(4)
31.1	4.3(1)	1.5(8)	2.7(3)	32.7(5)	1.56(0)	20.9(9)
36.1	4.2(5)	1.5(8)	2.6(7)	31.8(5)	1.56(6)	20.3(4)

The heat of solution ΔH_1, of ammonia in fenchone was found to be - 1.22 Kcal per mole of ammonia.

4.5.7 Dissociation pressures, and their temperature dependence

The values of the dissociation pressures shown in table 4.5.7 were obtained from the highest plateau levels of the chromatograms.

Table 4.5.7 Silver perchlorate in fenchone - effect of the column variables on the dissociation pressure

Expt. no.	Column temp. °C	Flow-rate $cm^3\ min^{-1}$	$10^3 . p_d$ atm.
Packing S.P.F.(1), 92.0cm, 736 µmole of silver perchlorate, 8.00 µmole cm^{-1}. Sample size of ammonia, (650-653)µmole			
3	23.0	8.4(1)	58.9(3)
4	23.0	8.4(1)	61.0(6)
5	23.0	18.2(5)	56.2(1)
6	23.0	18.2(5)	56.2(0)
7	23.0	48.4(2)	51.8(6)
8	23.0	48.4(2)	53.3(1)
9	27.0	7.5(4)	70.7(0)
10	27.0	7.5(4)	70.7(3)
11	27.0	22.0(8)	67.5(2)
12	27.0	22.0(8)	67.5(2)
13	27.0	44.4(4)	63.0(0)
14	27.0	44.4(4)	64.5(6)

Table 4.5.7 continued

Expt. no.	Column temp. °C	Flow-rate $cm^3\ min^{-1}$	$10^3 \cdot p_d$ atm.
15	32.0	8.0(5)	87.7(5)
16	32.0	8.0(5)	86.7(2)
17	32.0	22.7(2)	85.5(3)
18	32.0	22.7(2)	85.5(4)
19	32.0	42.3(9)	81.7(3)
20	32.0	42.3(9)	81.7(3)
21	36.0	8.1(4)	101.8(3)
22	36.0	8.1(4)	102.4(4)
23	36.0	24.5(9)	101.9(0)
24	36.0	24.5(9)	102.2(1)
25	36.0	42.6(1)	97.4(3)
26	36.0	42.6(1)	98.0(4)
Packing S.P.F.(2), 95.5cm, 524 µmole of silver perchlorate, 5.49 µmole cm^{-1}. Sample size of ammonia, (650-653)µmole.			
27	23.0	6.6(1)	57.6(3)
28	23.0	6.6(1)	57.6(5)
29	23.0	23.2(0)	54.6(7)
30	23.0	23.2(0)	54.6(7)
31	23.0	46.9(4)	52.5(4)
32	23.0	46.9(4)	52.0(3)
33	27.0	7.1(8)	70.8(1)
34	27.0	7.1(8)	71.7(1)
35	27.0	24.6(4)	65.4(6)
36	27.0	24.6(4)	65.9(6)
37	27.0	42.1(3)	63.8(2)
38	27.0	42.1(3)	65.1(3)
39	32.0	7.0(6)	87.6(7)
40	32.0	7.0(6)	87.7(5)
41	32.0	19.5(3)	84.9(8)
42	32.0	19.5(3)	83.5(6)
43	32.0	46.8(2)	78.1(7)
44	32.0	46.8(2)	77.4(6)
45	36.0	6.3(6)	101.6(7)
46	36.0	6.3(6)	102.8(3)
47	36.0	20.9(5)	98.8(2)
48	36.0	20.9(5)	98.0(4)
49	36.0	39.7(5)	94.7(2)
50	36.0	39.7(5)	94.0(3)
Packing S.P.F.(3), 90.5 cm, 202 µmole of silver perchlorate, 2.24 µmole cm^{-1}. Sample size of ammonia, (650-653)µmole.			
51	23.0	8.1(3)	50.8(3)
52	23.0	8.1(3)	50.2(4)

Table 4.5.7 continued

Expt. no.	Column temp. °C	Flow-rate $cm^3\ min^{-1}$	$10^3 . p_d$ atm.
53	23.0	24.7(5)	47.7(7)
54	23.0	24.7(5)	48.2(9)
55	23.0	42.8(3)	47.0(9)
56	23.0	42.8(3)	48.2(9)
57	27.0	7.7(8)	61.1(9)
58	27.0	7.7(8)	61.6(8)
59	27.0	25.2(4)	57.3(2)
60	27.0	25.2(4)	58.8(8)
61	27.0	45.4(2)	57.5(7)
62	27.0	45.4(2)	59.2(1)
63	32.0	7.9(7)	76.9(8)
64	32.0	7.9(7)	77.3(8)
65	32.0	23.9(9)	72.9(4)
66	32.0	23.9(9)	73.4(2)
67	32.0	42.0(2)	69.7(8)
68	32.0	42.0(2)	70.0(9)
69	36.0	9.8(1)	91.1(0)
70	36.0	9.8(1)	91.8(0)
71	36.0	26.1(3)	87.5(4)
72	36.0	26.1(3)	87.3(9)
73	36.0	51.1(8)	88.9(3)
74	36.0	51.1(8)	90.1(7)

The drop in value of the dissociation pressure with decreasing silver concentration and increasing flow-rate, is in accord with the discussion of the rate-effects, given in 4.3.3.

The dependence of the dissociation pressure on the rate-effects is reflected in the large standard deviations and coefficients of variation shown in table 4.5.8.

Table 4.5.8 Silver perchlorate in fenchone - statistical reflection of the rate dependence of the dissociation pressures

Column temp. °C	$10^3 . \overline{p_d}$ atm.	$10^3 . \sigma$ atm.	$10^2 . \frac{\sigma}{\overline{p_d}}$
23.0	52.9(7)	4.2(6)	8.0(4)
27.0	64.2(4)	4.5(6)	7.1(0)
32.0	80.5(1)	6.1(6)	7.6(5)
36.0	96.4(2)	5.6(0)	5.8(1)

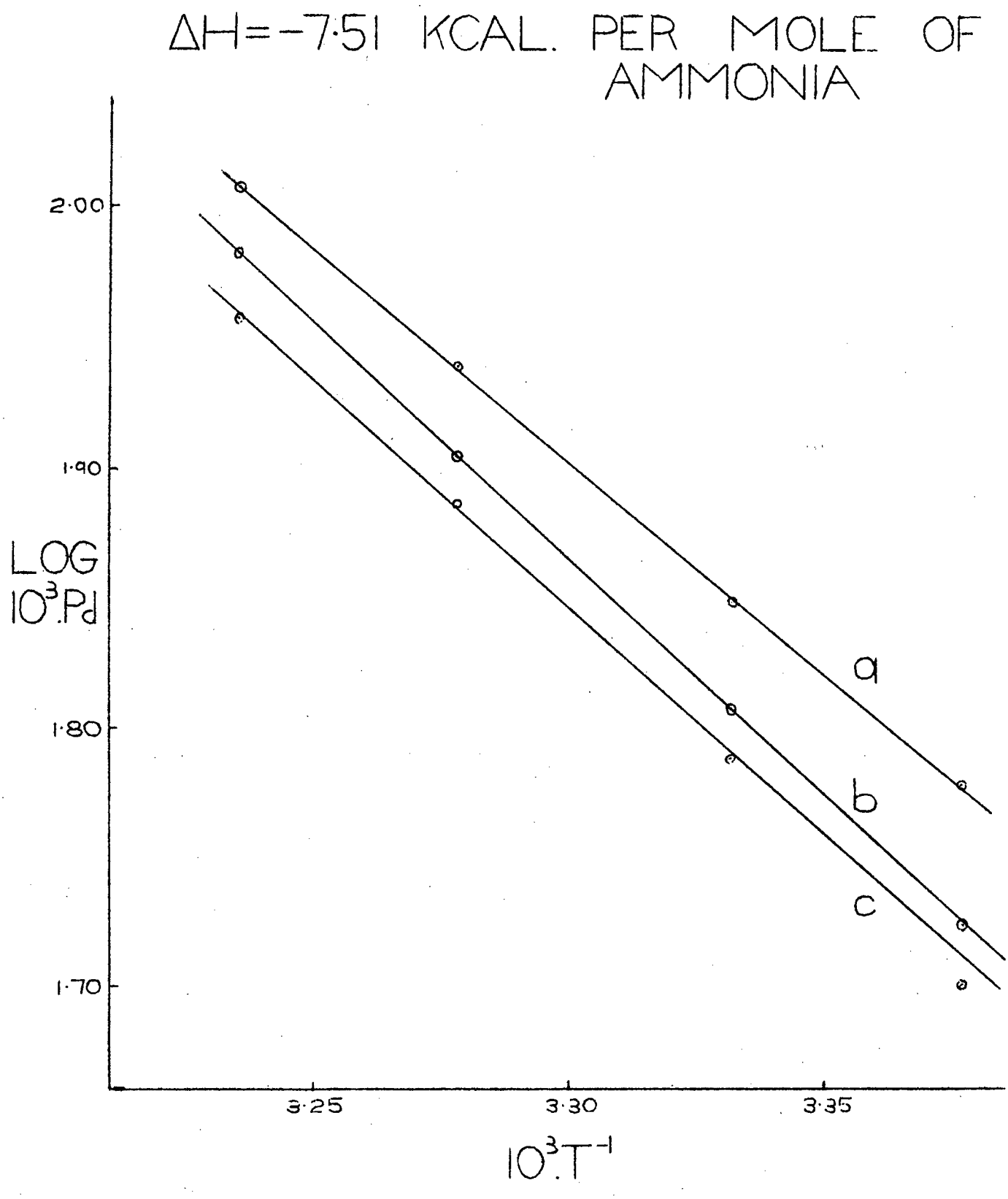

FIGURE 23. SILVER PERCHLORATE IN FENCHONE—EFFECT OF COLUMN TEMPERATURE ON THE DISSOCIATION PRESSURE.

In order to obtain the overall heat of reaction ΔH, plots of the temperature dependence of the dissociation pressures were made, as shown in fig. 23. Graph (a) is the plot of the dissociation pressure for packing S.P.F.(1) at the lowest flow-rates, (c) is the plot for S.P.F.(3) at the lowest flow-rates, while (b) is the plot for the mean values of the dissociation pressure shown in table 4.5.8.

As can be seen, there is only a small variation in the slope of the three graphs, indicating that the rate factors do not influence the slopes to any marked extent.

The plot for S.P.F.(2) was not made, as its graph would almost coincide with the graph of S.P.F.(1), as can be seen from the values in table 4.5.7. This coincidence of the p_d values of packings S.P.F.(1) and S.P.F.(2) at the lowest flow-rates, suggests that above a certain silver concentration, and for small enough flow-rates, the values of the dissociation pressures obtained, are very close to the true thermodynamic values. This fact, coupled with the small variation of the slopes of the graphs, led to the adoption of the value of the slope of graph (a) in calculating ΔH.

Comparison of the overall heat of reaction with the heats of the stages (eqn. (41) of 2.5.4) leads to:

$$y\,\Delta H/\text{Kcal. (mole silver)}^{-1} = 3.(-7.51) = -22.53$$

$$\Delta H_2 + y\Delta H_1/\text{Kcal. (mole silver)}^{-1} = -19.62 + 3.(-1.22) = -23.28$$

The agreement is perhaps fortuitous considering the large experimental scatter of the equilibrium function values.

4.5.8 Stoichiometric interpretation

The values of the initial absorption (4.5.2) of

ammonia to form solid complex I, and the value of y obtained for complex II, suggest the occurrence of the following reactions in the liquid phase

$$AgClO_{4(l)} + 2NH_{3(l)} \rightleftharpoons AgClO_4(NH_3)_{2(s)}$$

$$AgClO_4(NH_3)_{2(s)} + 3NH_{3(l)} \rightleftharpoons AgClO_4(NH_3)_{5(s)}$$

The solvent has been omitted from these equations, because there is as yet no clear understanding of its exact role.

4.6 Silver perchlorate in tetralin

This system showed initial absorption of ammonia, after which single plateau chromatograms were obtained showing rate-effects.

4.6.1 The packings

New packings (before injection of ammonia) which were greyish in colour, turned white on the formation of complex I. The details of the packings are given in table 4.6.1.

Table 4.6.1 Column packings of silver perchlorate in tetralin

Packing	Column length cm	$10^2 \cdot s$ (at 25°C) $cm^3\ gm^{-1}$	Silver conc. $\mu mole\ cm^{-3}$ (at 25°C)
S.P.T.(1)	92.3	3.24	449
S.P.T.(2)	95.1	2.96	254
S.P.T.(3)	91.3	3.17	92.5

4.6.2 The initial absorption

The following initial absorptions (moles of ammonia per mole of silver perchlorate) were measured

Packing S.P.T.(1)	1.97
Packing S.P.T.(2)	2.09
Packing S.P.T.(3)	1.95

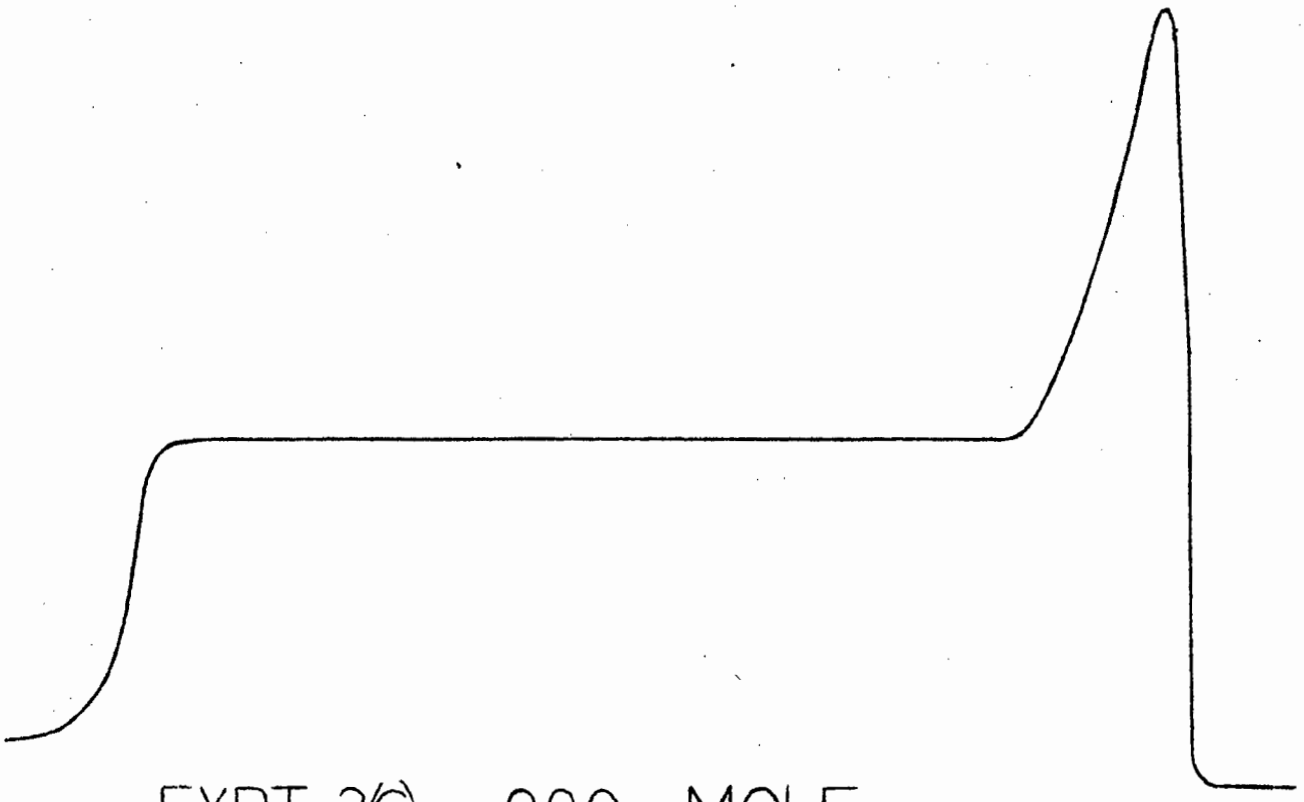

EXPT. 2(C) 980 μMOLE.

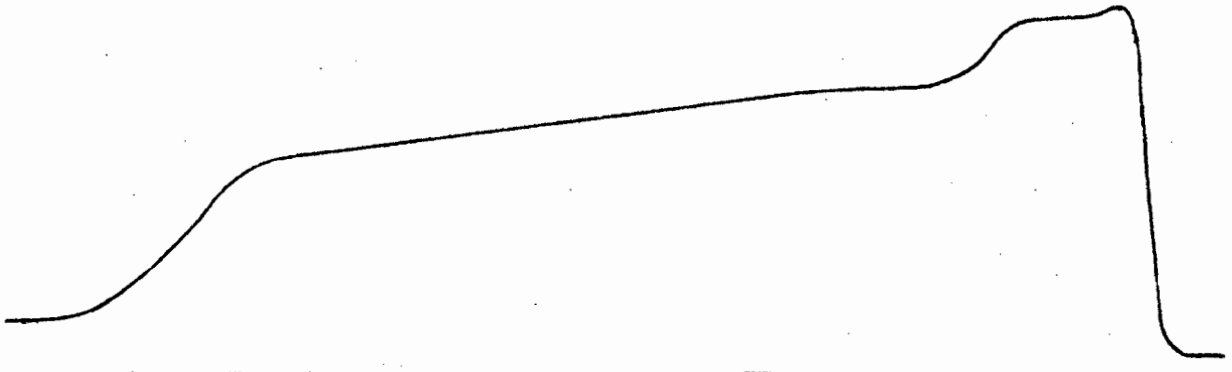

EXPT. 3 613 μMOLE.

FIGURE 24. SILVER PERCHLORATE IN TETRALIN—EFFECT OF SAMPLE SIZE. PACKING S.P.T.(1). FLOW-RATE, 9·7(3) $CM.^3$ $MIN.^{-1}$, COLUMN TEMPERATURE, 23·0°C.

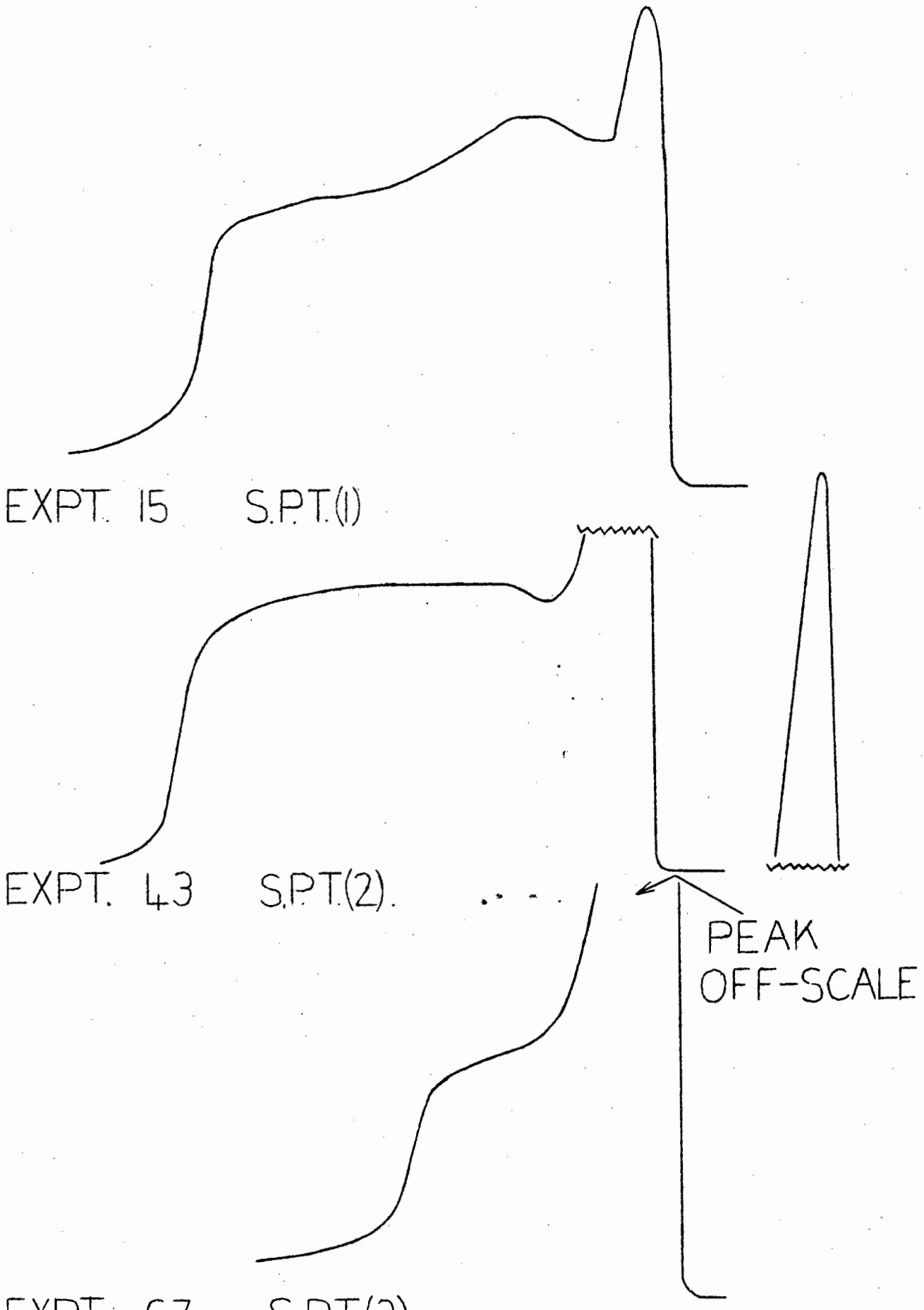

FIGURE 25. SILVER PERCHLORATE IN TETRALIN—EFFECT OF SILVER CONCENTRATION. SAMPLE SIZE, (610–614) μMOLE, COLUMN LENGTH, (91–95) CM., FLOW-RATE, (7·3(7)–7·8(0)) CM^3. MIN., COLUMN TEMPERATURE, 32·0°C

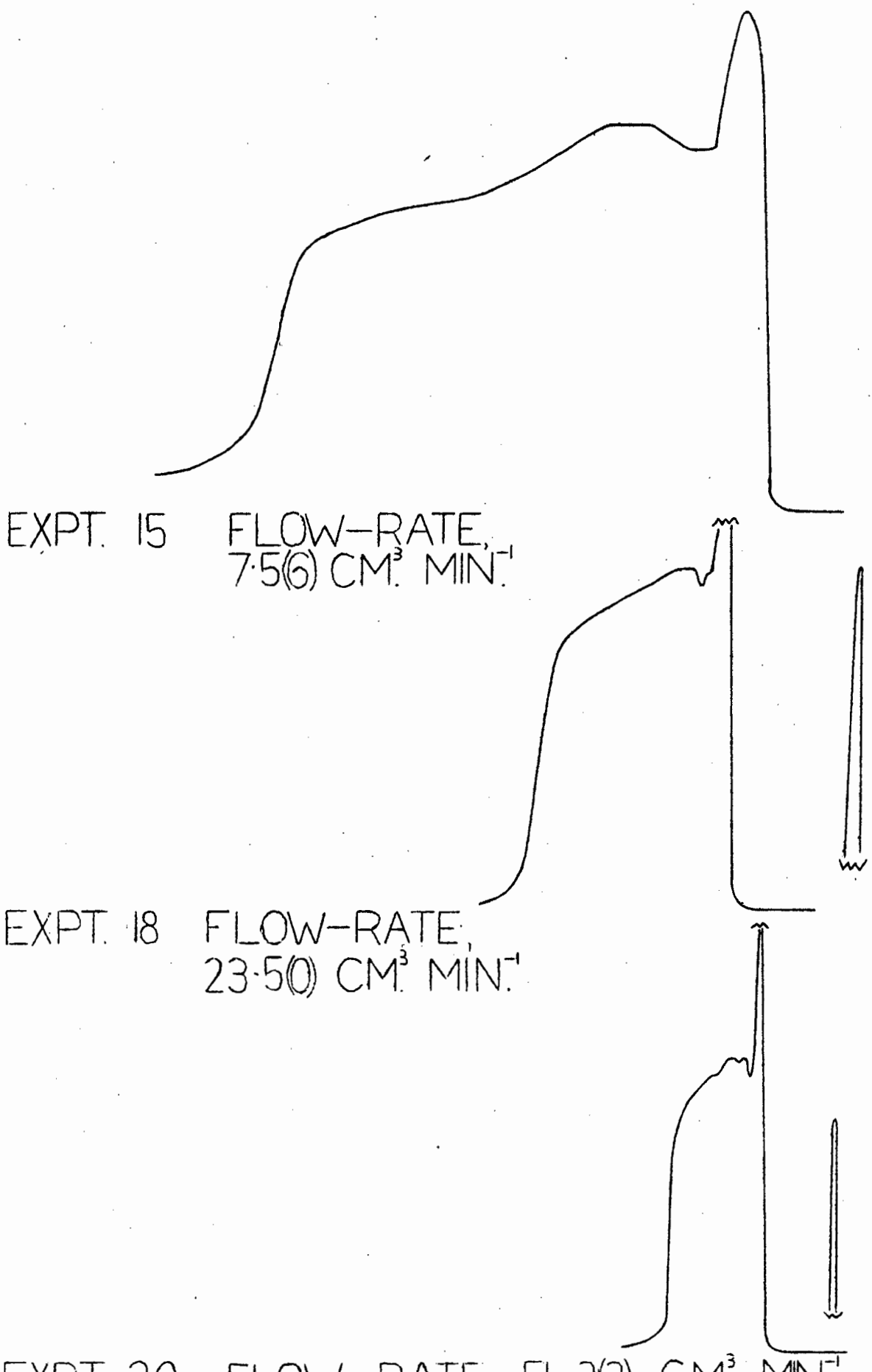

FIGURE 26. SILVER PERCHLORATE IN TETRALIN—EFFECT OF FLOW-RATE. PACKING S.P.T.(1). SAMPLE SIZE, 613 μMOLE. COLUMN TEMPERATURE, 32·0°C.

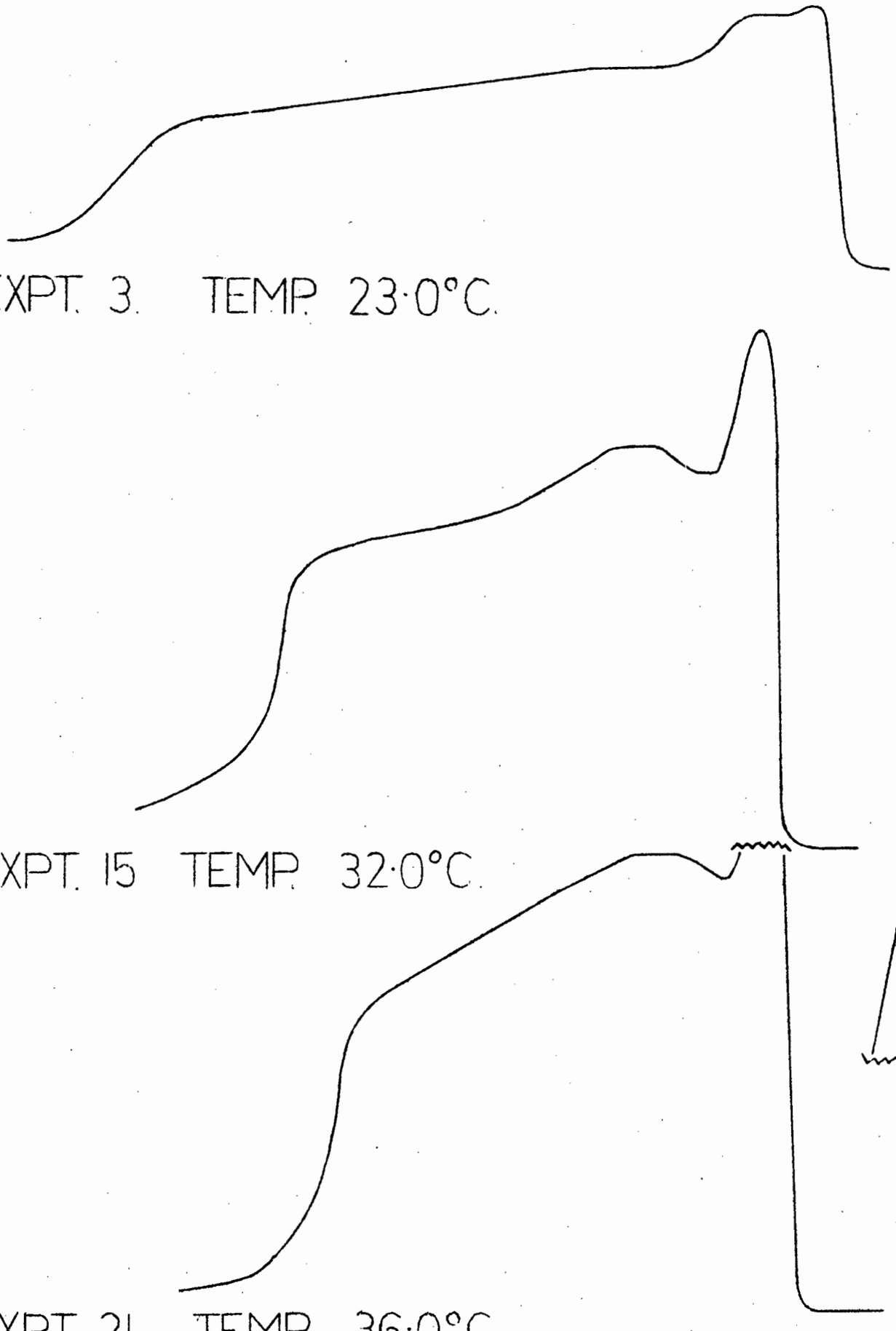

FIGURE 27. SILVER PERCHLORATE IN TETRALIN—EFFECT OF COLUMN TEMPERATURE. PACKING S.P.T.(I). FLOW-RATE, (7·5(6)–9·7(3)) CM^3 MIN^{-1}, SAMPLE SIZE, (612–615) μMOLE.

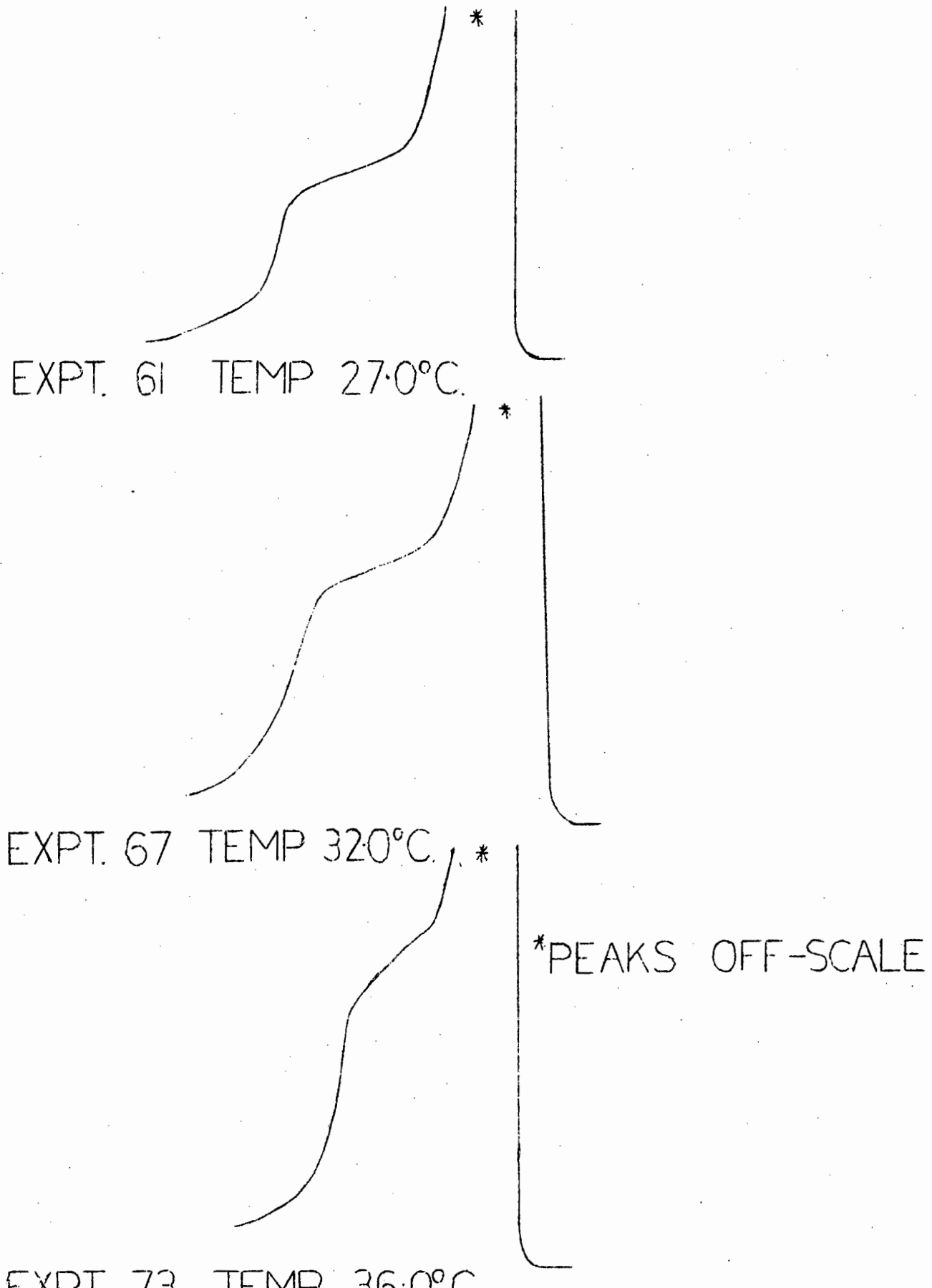

FIGURE 28. SILVER PERCHLORATE IN TETRALIN — EFFECT OF COLUMN TEMPERATURE. PACKING S.P.T.(3) FLOW-RATE, (7·8(0)–10·5(6)) $CM^3 MIN^{-1}$, SAMPLE SIZE, (610–613) μMOLE.

4.6.3 The chromatograms

The chromatograms for the tetralin system shown in figs. 24 to 28 are extremely similar to those obtained for the fenchone system.

The decay of the chromatograms can be attributed to the slow decomposition rate of complex II in an identical fashion to that outlined for the fenchone system. The plateau profiles obtained as a result of the rate-effects are of the same type as illustrated in fig. 19 and are listed in table 4.6.2.

Table 4.6.2 Silver perchlorate in tetralin - influence of rate-effects on the chromatogram shapes

Expt. No.	Column temp. °C	Flow-rate $cm^3\ min^{-1}$	Chromatogram type fig.19,A,B,C, D,E,F.	$10^3 \cdot D_1$ atm.	$10^3 \cdot D_2$ atm.	$10^3 \cdot D_3$ atm.
Packing S.P.T.(1), 92.3 cm, 673 µmole of silver perchlorate, 7.29 µmole cm^{-1}. Sample size of ammonia, (610-615) µmole.						
5	23.0	24.3(9)	A	-	-	-
6	23.0	24.3(9)	C	-	-	2.8
7	23.0	45.8(8)	A	-	-	-
8	23.0	45.8(8)	B	0.9	-	-
9	27.0	9.3(8)	B	2.1	-	-
10	27.0	9.3(8)	B	1.9	-	-
11	27.0	25.7(8)	A	-	-	-
12	27.0	25.7(8)	D	1.0	-	0.9
13	27.0	50.3(9)	A	-	-	-
14	27.0	50.3(9)	A	-	-	-
15	32.0	7.5(6)	B	4.8	-	-
16	32.0	7.5(6)	B	4.7	-	-
17	32.0	23.5(0)	B	2.0	-	-
18	32.0	23.5(0)	D	4.5	-	3.0
19	32.0	54.3(3)	D	4.0	-	3.7
20	32.0	54.3(3)	D	3.1	-	2.7
21	36.0	8.0(7)	B	3.9	-	-
22	36.0	8.0(7)	B	3.9	-	-
23	36.0	23.0(8)	B	4.5	-	-
24	36.0	23.0(8)	B	5.3	-	-
25	36.0	46.4(4)	F	4.9	1.0	2.5
26	36.0	46.4(4)	F	4.4	2.3	1.3

Table 4.6.2 continued

Expt. No.	Column temp. °C	Flow-rate $cm^3\ min^{-1}$	Chromatogram type fig.19,A,B,C, D,E,F.	$10^3.D_1$ atm.	$10^3.D_2$ atm.	$10^3.D_3$ atm.
Packing S.P.T.(2), 95.1 cm, 356 µmole of silver perchlorate, 3.74 µmole cm^{-1}. Sample size of ammonia, (610-615) µmole.						
30	23.0	6.8(0)	A	-	-	-
31	23.0	6.8(0)	A	-	-	-
32	23.0	19.6(9)	B	3.0	-	-
33	23.0	19.6(9)	B	1.8	-	-
34	23.0	44.7(9)	B	3.9	-	-
35	23.0	44.7(9)	B	3.6	-	-
36	27.0	7.1(0)	A	-	-	-
37	27.0	7.1(0)	A	-	-	-
38	27.0	18.7(3)	B	3.5	-	-
39	27.0	18.7(3)	B	3.5	-	-
40	27.0	43.5(7)	B	4.8	-	-
41	27.0	43.5(7)	B	4.0	-	-
42	32.0	7.3(7)	B	2.5	-	-
43	32.0	7.3(7)	B	2.9	-	-
44	32.0	18.9(9)	B	4.0	-	-
45	32.0	18.9(9)	B	3.1	-	-
46	32.0	40.9(9)	B	5.6	-	-
47	32.0	40.9(9)	B	1.7	-	-
48	36.0	6.8(4)	B	1.4	-	-
49	36.0	6.8(4)	B	2.2	-	-
50	36.0	23.2(6)	B	3.5	-	-
51	36.0	23.2(6)	B	4.6	-	-
52	36.0	45.9(0)	B	3.7	-	-
53	36.0	45.9(0)	B	2.7	-	-
Packing S.P.T.(3), 91.3 cm, 155 µmole of silver perchlorate, 1.70 µmole cm^{-1}. Sample size of ammonia, (610-615) µmole.						
55	23.0	9.9(3)	A	-	-	-
56	23.0	9.9(3)	A	-	-	-
57	23.0	29.6(0)	decayed	-	-	-
58	23.0	29.6(0)	decayed	-	-	-
59	23.0	49.2(1)	A	-	-	-
60	23.0	49.2(1)	A	-	-	-
61	27.0	10.5(6)	decayed	-	-	-
62	27.0	10.5(6)	decayed	-	-	-
63	27.0	30.5(5)	A	-	-	-
64	27.0	30.5(5)	A	-	-	-
65	27.0	55.4(7)	A	-	-	-
66	27.0	55.4(7)	A	-	-	-

Table 4.6.2 continued

Expt. No.	Column temp. ^{o}C	Flow-rate $cm^3\ min^{-1}$	Chromatogram type fig.19,A,B,C, D,E,F.	$10^3.D_1$ atm.	$10^3.D_2$ atm.	$10^3.D_3$ atm.
67	32.0	7.8(0)	decayed	-	-	-
68	32.0	7.8(0)	decayed	-	-	-
69	32.0	27.4(3)	A	-	-	-
70	32.0	27.4(3)	A	-	-	-
71	32.0	57.7(3)	A	-	-	-
72	32.0	57.7(3)	A	-	-	-
73	36.0	9.4(8)	decayed	-	-	-
74	36.0	9.4(8)	decayed	-	-	-
75	36.0	28.2(9)	A	-	-	-
76	36.0	28.2(9)	A	-	-	-
77	36.0	56.8(4)	A	-	-	-
78	36.0	56.8(4)	A	-	-	-

Lower silver concentration packings S.P.T.(2) and S.P.T.(3), show no division of plateau levels, indicating that the constant plateau heights are the highest dynamic steady state levels that can be maintained before decay occurs.

Chromatogram types marked "decayed" in the second column of table 4.6.2, are of the type shown in fig. 28, and are obtained only from packing S.P.T. (3), because of its low silver concentration content (the decomposition rate of the complex being so slow, due to the small amount of complex formed, that no steady state level can be maintained at all).

Although chromatograms of type A are usually obtained at higher flow-rates from packing S.P.T.(3), the heights of the steady state levels of these chromatograms are usually located near the rear end of the continuous decayed plateau chromatograms that occur at the lower flow-rates. This was inferred from the values of the dissociation pressure for packing S.P.T.(3) (see 4.6.6).

Chromatograms numbered 9,10,15 and 16 in table 4.6.2 are of the type shown in figs 25 to 27 (Expt.15). Although

listed as type B, they are really a modified form of types B and D. The division of the plateau level causes a decrease in the slope of the decayed rear end, but as the decomposition rate of the complex is not fast enough to maintain a constant lower plateau level, continuous decay occurs.

The quantitative treatment of the decayed chromatograms of the tetralin system, is the same as that adopted for the fenchone system.

4.6.4 Temperature dependence of the equilibrium function

The scatter in the values of the equilibrium function shown in table 4.6.3 can again be ascribed to the errors involved, principally the uncertainty in the location of the rear end of zone II(a).

For y = 2 constant equilibrium function values were obtained. Fig. 29 shows the temperature plot of F(K), the length of each vertical line about the experimental points, indicating the range between the maximum and minimum values.

Table 4.6.3 Silver perchlorate in tetralin - results, and temperature dependence of the equilibrium function

Packing S.P.T.	Column temp. °C	Molar ratio (R)	% conversion	10^{-3} F(K) litre^2 mole^{-2}
(1)	23.0	1.06	94.7(7)	1.6(3)
(2)	23.0	1.38	90.4(2)	1.4(7)
(3)	23.0	1.66	77.4(0)	1.4(9)
(1)	27.0	0.92	93.8(0)	1.1(6)
(2)	27.0	1.25	89.1(0)	1.0(5)
(3)	27.0	2.02	74.8(0)	1.3(2)

Table 4.6.3 continued

Packing S.P.T.	Column temp. °C	Molar ratio (R)	% conversion	10^{-3} F(K) litre^2 mole^{-2}
(1)	32.0	0.86	93.0(0)	0.9(2)
(2)	32.0	1.18	89.1(5)	1.0(6)
(3)	32.0	2.24	68.7(0)	0.8(1)
(1)	36.0	0.81	92.4(0)	0.7(9)
(2)	36.0	1.28	86.6(0)	0.6(7)
(3)	36.0	2.11	70.0(0)	0.8(3)

The equilibrium function values were found to vary with assumed y values in the manner predicted in 2.5.2 and shown in table 4.6.4.

Table 4.6.4 Silver perchlorate in tetralin - variation of F'(K) with assumed y values

Packing S.P.T.	ε	$\left(\frac{n_I\, y - \Delta}{n_I\,(y+\varepsilon) - \Delta}\right)$	$\left[\frac{\bar{n}_{NH_3} - \Delta}{V_f}\right]^{-\varepsilon}$ litre$^{\varepsilon}$ mole$^{-\varepsilon}$	F'(K) (at 23.0°C) litre$^{y+\varepsilon}$ mole$^{-(y+\varepsilon)}$
(1)	-1	-	23.2×10^{-3}	-
(2)	-1	-	33.6×10^{-3}	-
(3)	-1	-	35.0×10^{-3}	-
(1)	0	1	1	1.63×10^{3}
(2)	0	1	1	1.47×10^{3}
(3)	0	1	1	1.49×10^{3}
(1)	+1	0.50	43.1	4.01×10^{4}
(2)	+1	0.43	29.7	1.87×10^{4}
(3)	+1	0.41	28.6	1.76×10^{4}
(1)	+2	0.33	18.6×10^{2}	11.52×10^{5}
(2)	+2	0.27	8.8×10^{2}	3.55×10^{5}
(3)	+2	0.26	8.2×10^{2}	3.18×10^{5}

4.6.5 Heat of solution of ammonia in tetralin

The heat of solution of ammonia in tetralin was determined chromatographically. Table 4.6.5 shows the variation of the partition coefficient with temperature.

Table 4.6.5 Variation of the partition coefficient with temperature

Column temp. °C	t_r min.	t_g min.	$t_r - t_g = t_f$ min.	$V^o_R{}'$ cm^3	V_f cm^3	K
21.2	2.5(4)	0.5(4)	2.0(0)	76.4(2)	1.93(1)	39.5(8)
29.1	2.4(4)	0.5(7)	1.8(7)	68.6(5)	1.94(2)	35.3(5)
36.2	2.2(8)	0.5(6)	1.7(2)	61.8(4)	1.95(3)	31.6(6)

From the temperature plot, ΔH_1 was found to be - 2.69 Kcal per mole of ammonia.

4.6.6 Dissociation pressures and their temperature dependence

Values of the dissociation pressures listed in table 4.6.6 were obtained from the highest plateau levels of the chromatograms. Where continuous decay of the plateau occurred, as found in some of the chromatograms obtained from packing S.P.T.(3), the initial height of the plateau was taken in computing the dissociation pressure.

Table 4.6.6 Silver perchlorate in tetralin - effect of the column variables on the dissociation pressure

Expt. no.	Column temp. °C	Flow-rate $cm^3\ min^{-1}$	$10^3 \cdot p_d$ atm.
Packing S.P.T.(1), 92.3 cm, 673 µmole of silver perchlorate, 7.29 µmole cm^{-1}. Sample size of ammonia, (610-615) µmole.			
3	23.0	9.7(3)	54.1(6)
4	23.0	9.7(3)	54.0(2)
5	23.0	24.3(9)	53.8(2)
6	23.0	24.3(9)	52.5(4)
7	23.0	45.8(8)	49.5(6)
8	23.0	45.8(8)	49.2(2)
9	27.0	9.3(8)	65.4(6)
10	27.0	9.3(8)	65.8(3)
11	27.0	25.7(8)	60.0(4)
12	27.0	25.7(8)	61.1(0)
13	27.0	50.3(9)	57.5(7)
14	27.0	50.3(9)	58.2(3)

Table 4.6.6 continued

Expt. no.	Column temp. °C	Flow-rate $cm^3\ min^{-1}$	$10^3 \cdot p_d$ atm.
15	32.0	7.5(6)	83.0(0)
16	32.0	7.5(6)	83.0(1)
17	32.0	23.5(0)	76.1(9)
18	32.0	23.5(0)	77.3(0)
19	32.0	54.3(3)	72.3(9)
20	32.0	54.3(3)	70.8(0)
21	36.0	8.0(7)	98.6(0)
22	36.0	8.0(7)	97.9(7)
23	36.0	23.0(8)	90.8(6)
24	36.0	23.0(8)	88.5(5)
25	36.0	46.4(4)	85.3(8)
26	36.0	46.4(4)	84.0(7)
Packing S.P.T.(2), 95.1 cm, 356 µmole of silver perchlorate, 3.74 µmole cm^{-1}. Sample size of ammonia, (610-615) µmole.			
30	23.0	6.8(0)	47.0(1)
31	23.0	6.8(0)	47.0(9)
32	23.0	19.6(9)	43.5(2)
33	23.0	19.6(9)	42.8(4)
34	23.0	44.7(9)	41.3(0)
35	23.0	44.7(9)	41.3(0)
36	27.0	7.1(0)	55.6(1)
37	27.0	7.1(0)	55.8(4)
38	27.0	18.7(3)	52.4(2)
39	27.0	18.7(3)	52.6(3)
40	27.0	43.5(7)	51.1(5)
41	27.0	43.5(7)	51.3(2)
42	32.0	7.3(7)	69.3(1)
43	32.0	7.3(7)	68.1(1)
44	32.0	18.9(9)	68.7(5)
45	32.0	18.9(9)	69.0(6)
46	32.0	40.9(9)	65.3(4)
47	32.0	40.9(9)	65.3(4)
48	36.0	6.8(4)	87.7(9)
49	36.0	6.8(4)	87.7(8)
50	36.0	23.2(6)	80.9(8)
51	36.0	23.2(6)	80.4(4)
52	36.0	45.9(0)	77.6(6)
53	36.0	45.9(0)	78.3(6)
Packing S.P.T.(3), 91.3 cm, 155 µmole of silver perchlorate, 1.70 µmole cm^{-1}. Sample size of ammonia, (610-615) µmole.			
55	23.0	9.9(3)	36.8(4)
56	23.0	9.9(3)	36.7(9)
57	23.0	29.6(0)	36.0(5)
58	23.0	29.6(0)	36.9(6)
59	23.0	49.2(1)	35.2(2)
60	23.0	49.2(1)	35.4(7)

Table 4.6.6 continued

Expt. no.	Column temp. °C	Flow-rate $cm^3\ min^{-1}$	$10^3 \cdot p_d$ atm.
61	27.0	10.5(6)	47.5(6)
62	27.0	10.5(6)	47.4(5)
63	27.0	30.5(5)	45.5(0)
64	27.0	30.5(5)	45.9(7)
65	27.0	55.4(7)	44.2(0)
66	27.0	55.4(7)	44.2(5)
67	32.0	7.8(0)	62.0(4)
68	32.0	7.8(0)	61.0(6)
69	32.0	27.4(3)	59.6(9)
70	32.0	27.4(3)	59.7(2)
71	32.0	57.7(3)	56.3(1)
72	32.0	57.7(3)	56.9(4)
73	36.0	9.4(8)	75.9(4)
74	36.0	9.4(8)	76.9(7)
75	36.0	28.2(9)	71.3(8)
76	36.0	28.2(9)	71.3(3)
77	36.0	56.8(4)	69.5(2)
78	36.0	56.8(4)	69.4(8)

The dependence of the dissociation pressures on silver concentration and flow-rate, is in accord with the rate-effects shown by the chromatograms (figs. 24 - 28), and the large standard deviations and coefficients of variation shown in table 4.6.7.

Table 4.6.7 Silver perchlorate in tetralin - statistical reflection of the rate dependence of the dissociation pressures.

Column temp. °C	$10^3 \cdot \overline{p_d}$ atm.	$10^3 \cdot \sigma$ atm.	$\frac{10^2 \cdot \sigma}{\overline{p_d}}$
23.0	44.2(1)	6.8(6)	15.52
27.0	53.4(5)	6.9(5)	13.00
32.0	68.0(2)	8.1(5)	11.98
36.0	81.7(4)	8.8(0)	10.77

The decrease in the coefficients of variation with rising temperature, both for the tetralin and fenchone systems (table 4.5.8) may possibly be explained as follows: as the

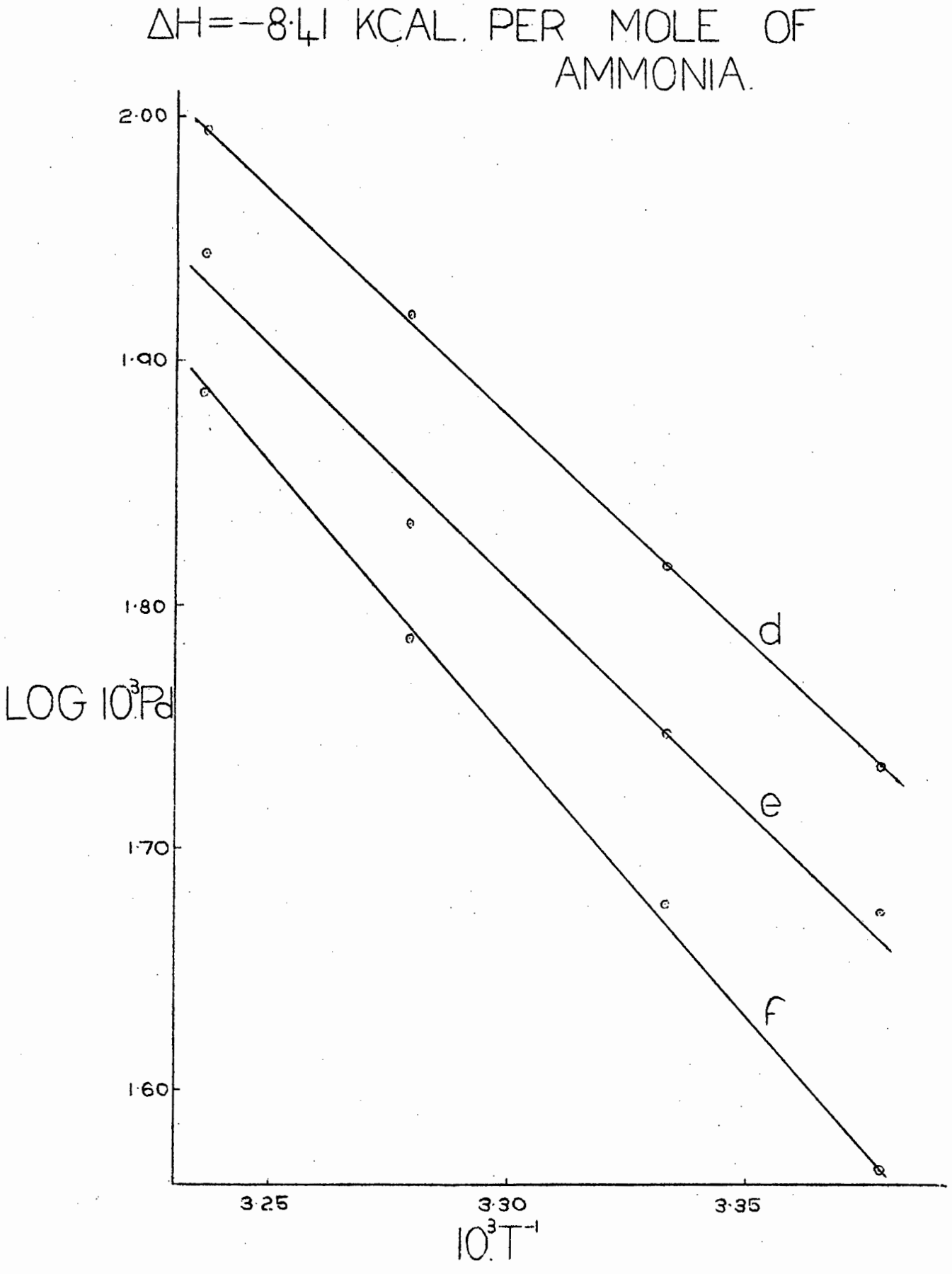

FIGURE 30. SILVER PERCHLORATE IN TETRALIN. TEMPERATURE PLOTS OF THE DISSOCIATION PRESSURES.

dissociation pressure increases with rising temperature, the concentration of ammonia in the gas phase to be maintained is increased, thus necessitating a larger rate of efflux of ammonia from the liquid phase. The rate constants of the reactions leading to the efflux of ammonia k_2, and for the complex decomposition k_4, increase with temperature, but this is offset to some extent by the fact that the amount of complex formed decreases. However, it is suggested, that the result of these effects gives a net efflux of ammonia from the liquid phase which is faster, and hence more favourable relative to the maintenance of the increased ammonia gas concentration, with a consequent decrease in the rate-effects on the plateau height as indicated by the smaller coefficients of variation.

Fig. 30 shows the temperature plots of the dissociation pressures for the three columns at the lowest flow-rates.

The very small experimental scatter of points for the high silver concentration plot (i.e., graph (d) - packing S.P.T.(1)) was assumed to indicate that the dissociation pressure values were very near the true thermodynamic values, and the slope of plot (d) was used to calculate the overall heat of reaction.

Graphs (e) and (f) for packing S.P.T.(2) and S.P.T.(3) showed a scatter of points unlike the fenchone system. However the similarity in slopes of graphs(e) and (d) suggests that for low enough flow-rates, and high enough silver concentrations, the slope is nearly independent of the rate-effects, which is in agreement with the findings for the fenchone system (4.5.7, fig. 23). Furthermore, all of the points on graph (f) (except for the lowest temperature one) were taken from chromatograms showing continous decay (fig. 28). This led to uncertainty

in the dissociation pressure values, which rather than the rate-effects might have influenced the slope of graph (f).

Comparison of the overall heat of reaction with the heats of the stages (eqn. (41) of 2.5.4) leads to :

$$y\Delta H/\text{Kcal.(mole silver)}^{-1} = 2.(-8.41) = -16.82$$

$$\Delta H_2 + y\Delta H_1/\text{Kcal.(mole silver)}^{-1} = -11.97 + 2.(-2.69) = -17.35$$

The agreement is again surprisingly good, considering the large variation in the values of the equilibrium function.

4.6.7 Stoichiometric interpretation

The experimental evidence indicates the following complexing reactions in the liquid phase

$$AgClO_{4(l)} + 2NH_{3(l)} \rightleftharpoons AgClO_4(NH_3)_{2(s)}$$

$$AgClO_4(NH_3)_{2(s)} + 2NH_{3(l)} \rightleftharpoons AgClO_4(NH_3)_{4(s)}$$

4.7 Silver nitrate in benzonitrile

This system showed the usual initial absorption of ammonia. Thereafter, single plateau chromatograms were obtained which showed no visible rate-effects such as plateau decay or plateau height division.

4.7.1 The packings

New packings turned dark grey and showed no colour change on addition of ammonia. Details of the packings are given in table 4.7.1

Table 4.7.1 Column packings of silver nitrate in benzonitrile

Packing	Column length cm	10^2.s(at 25°C) $cm^3\ gm^{-1}$	Silver conc. $\mu mole\ cm^{-3}$ (at 25°C)
S.N.B.(1)	92.6	2.71	495

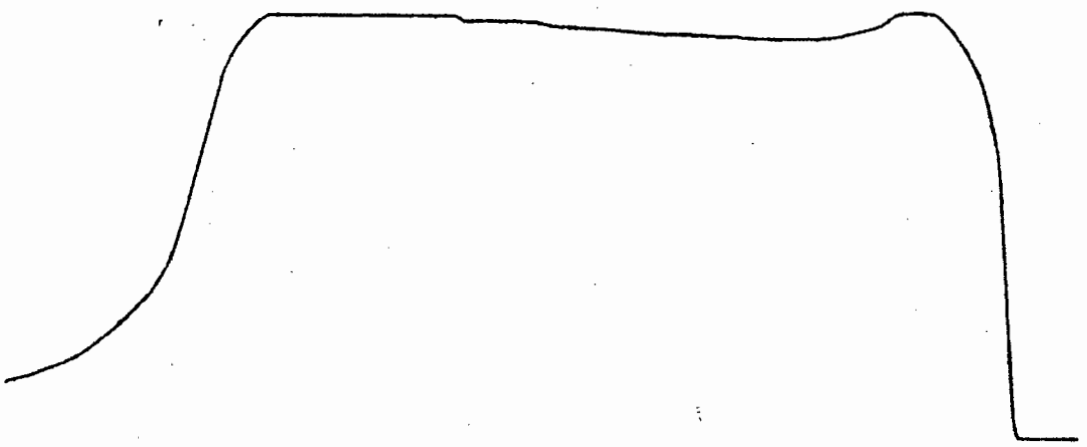

EXPT. 128. 828 μMOLE

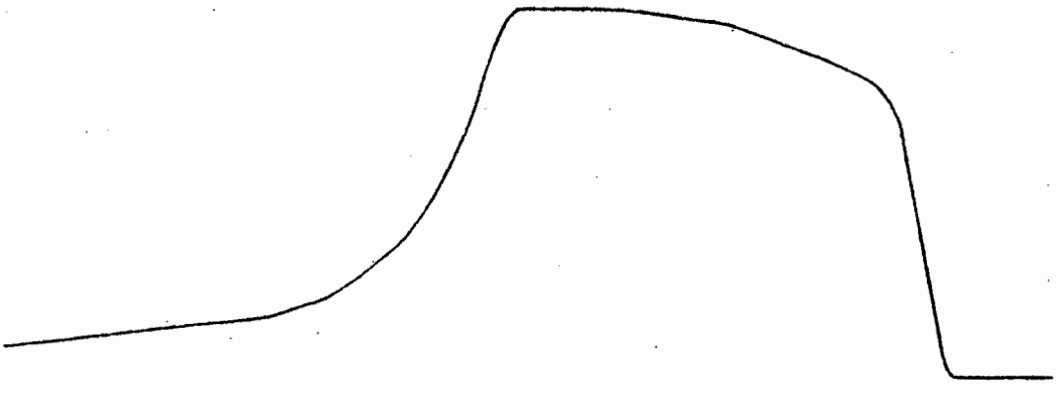

EXPT 14. 416 μMOLE.

FIGURE 31. SILVER NITRATE IN BENZONITRILE—EFFECT OF SAMPLE SIZE. PACKING S.N.B.(1)., FLOW-RATE, (5·8(2)–7·2(6)) $CM.^3$ $MIN.^{-1}$, COLUMN TEMPERATURE, 28·0°C.

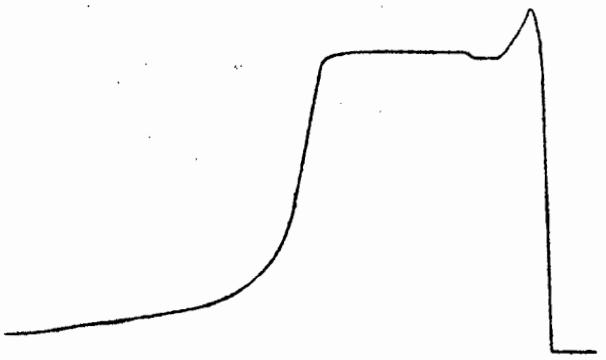

EXPT. 4. S.N.B.(1).

EXPT. 67. S.N.B.(3).

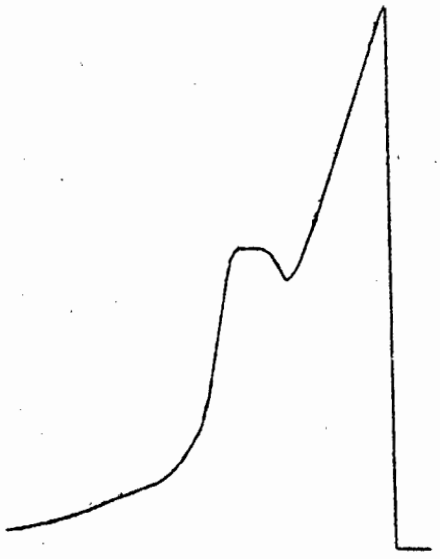

EXPT. 98. S.N.B.(4)

FIGURE 32. SILVER NITRATE IN BENZONITRILE—EFFECT OF SILVER CONCENTRATION. SAMPLE SIZE, (4·13–4·17) μMOLE, COLUMN LENGTH, 92·5 CM., FLOW-RATE, (20·6(1)–23·5(5)) CM^3 MIN^{-1}, COLUMN TEMPERATURE, 21·0°C.

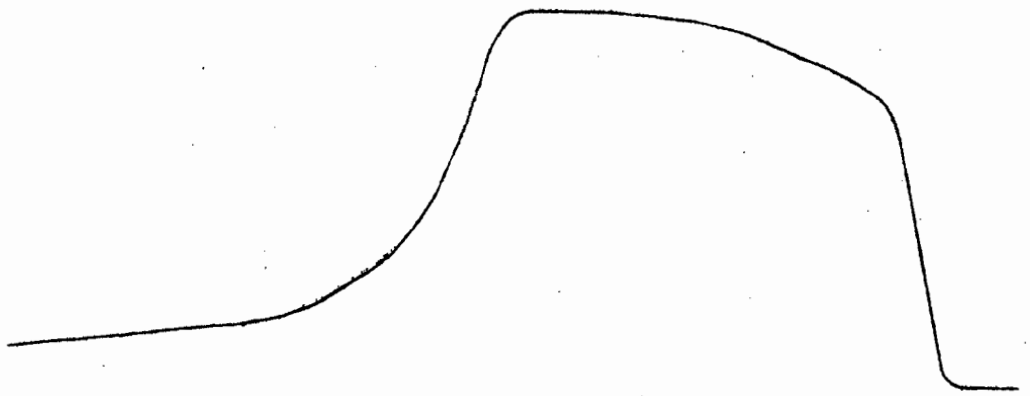

EXPT. 14. FLOW–RATE, 5·8(2) CM^3 MIN^{-1}

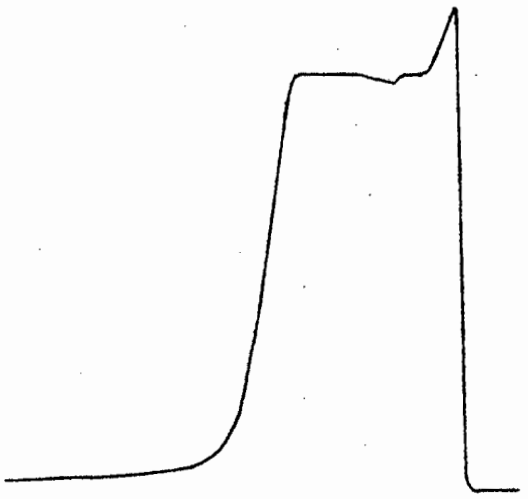

EXPT. 16. FLOW–RATE, 22·6(1) CM^3 MIN^{-1}

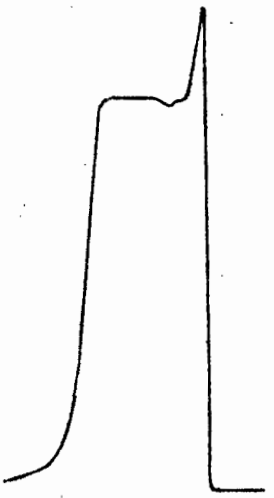

EXPT. 18. FLOW–RATE, 39·2(2) CM^3 MIN^{-1}

FIGURE 33. SILVER NITRATE IN BENZONITRILE—EFFECT OF FLOW–RATE. PACKING S.N.B.(1). SAMPLE SIZE, (4·15–4·18) μMOLE, COLUMN TEMPERATURE, 28·0°C.

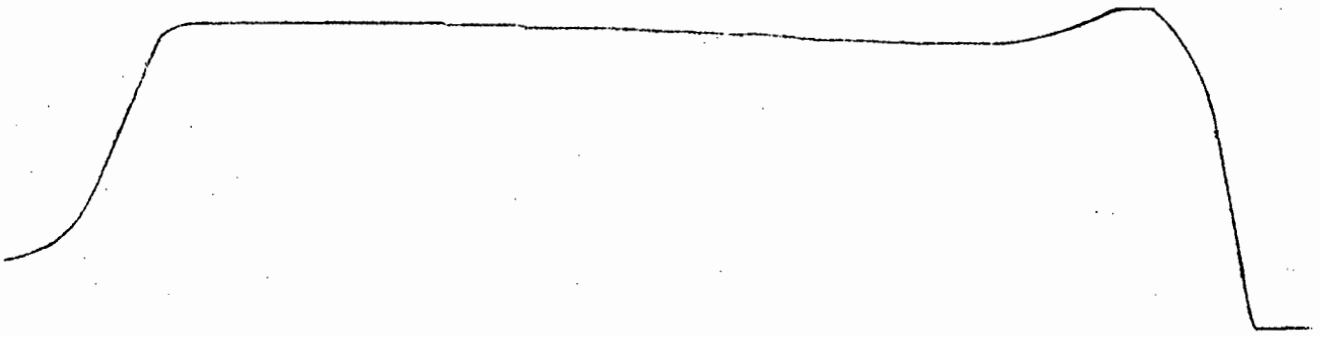

EXPT. 126 TEMP. 21·0°C.

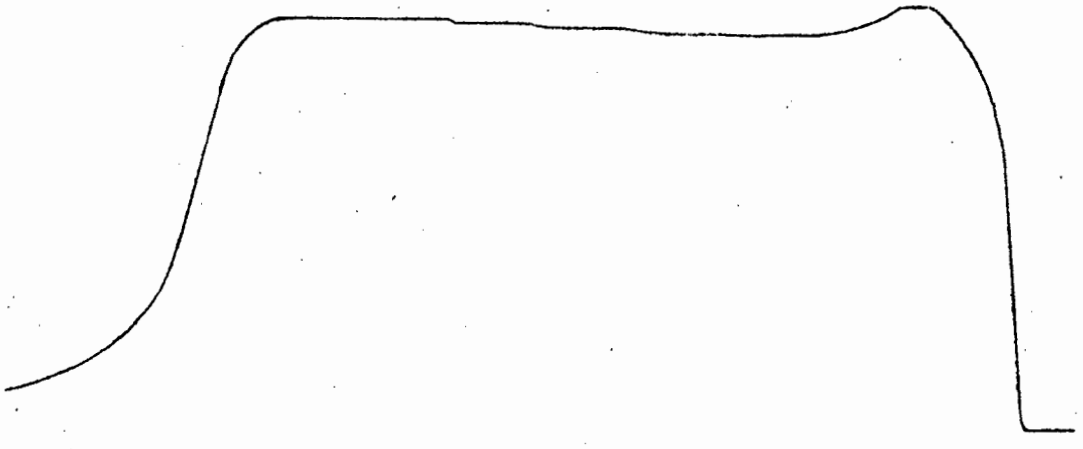

EXPT. 128. TEMP. 28·0°C.

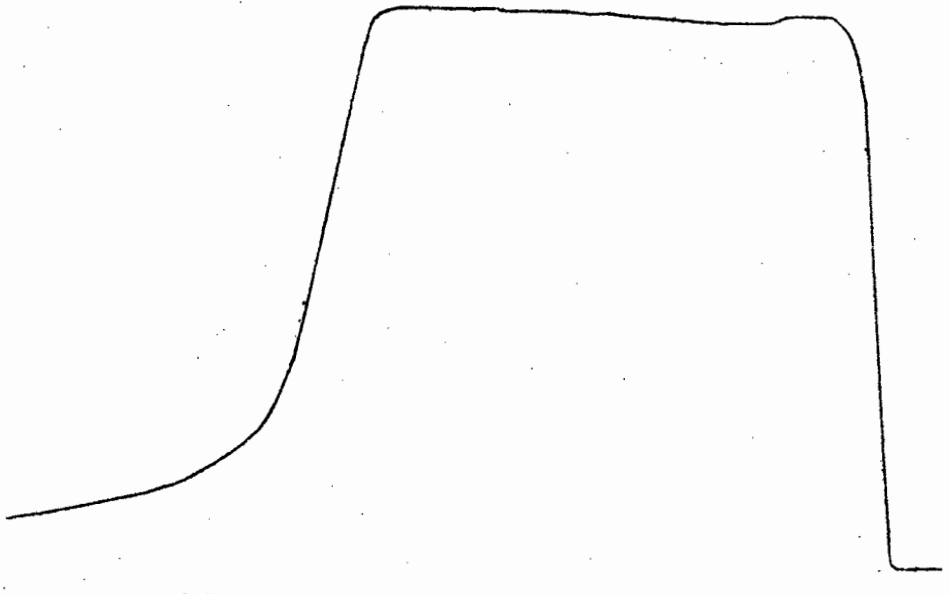

EXPT. 130. TEMP. 36·0°C.

FIGURE 34. SILVER NITRATE IN BENZONITRILE.—EFFECT OF COLUMN TEMPERATURE. PACKING S.N.B.(1). FLOW-RATE, (6·7(8)–7·3(4)) CM^3. MIN^{-1}. SAMPLE SIZE, (826–829) μMOLE.

Table 4.7.1 continued

Packing	Column length cm	10^2.s (at 25°C) $cm^3\ gm^{-1}$	Silver conc. $\mu mole\ cm^{-3}$ (at 25°C)
S.N.B.(2)	92.4	2.74	415
S.N.B.(3)	92.6	2.77	226
S.N.B.(4)	92.5	2.95	77.4
S.N.B.(5)	92.2	2.94	91.3

4.7.2 The initial absorption

The following values of the initial absorption (moles of ammonia per mole of silver nitrate) were found

Packing S.N.B.(1)	1.54
Packing S.N.B.(2)	1.58
Packing S.N.B.(3)	1.45
Packing S.N.B.(4)	1.55
Packing S.N.B.(5)	1.45

4.7.3 The chromatograms

The chromatograms obtained for this system showed no decay or division of plateau height as can be seen from figs. 31 to 34. There is however the usual dip D_1, due to delayed complex decomposition. This results in chromatograms of type B (fig. 19) but without the decayed rear end. The values of D_1 are listed for convenience with the dissociation pressure values, given in table 4.7.5.

By analogous reasoning to that given in 4.5.3, concerning the possible rate-controllings steps that can occur in the column, it can be deduced that the decomposition rate of complex II is fast enough to maintain the required liquid phase ammonia concentration, which results in sufficiently fast efflux of ammonia from the liquid phase, and thus gives a constant plateau height throughout zone II(a).

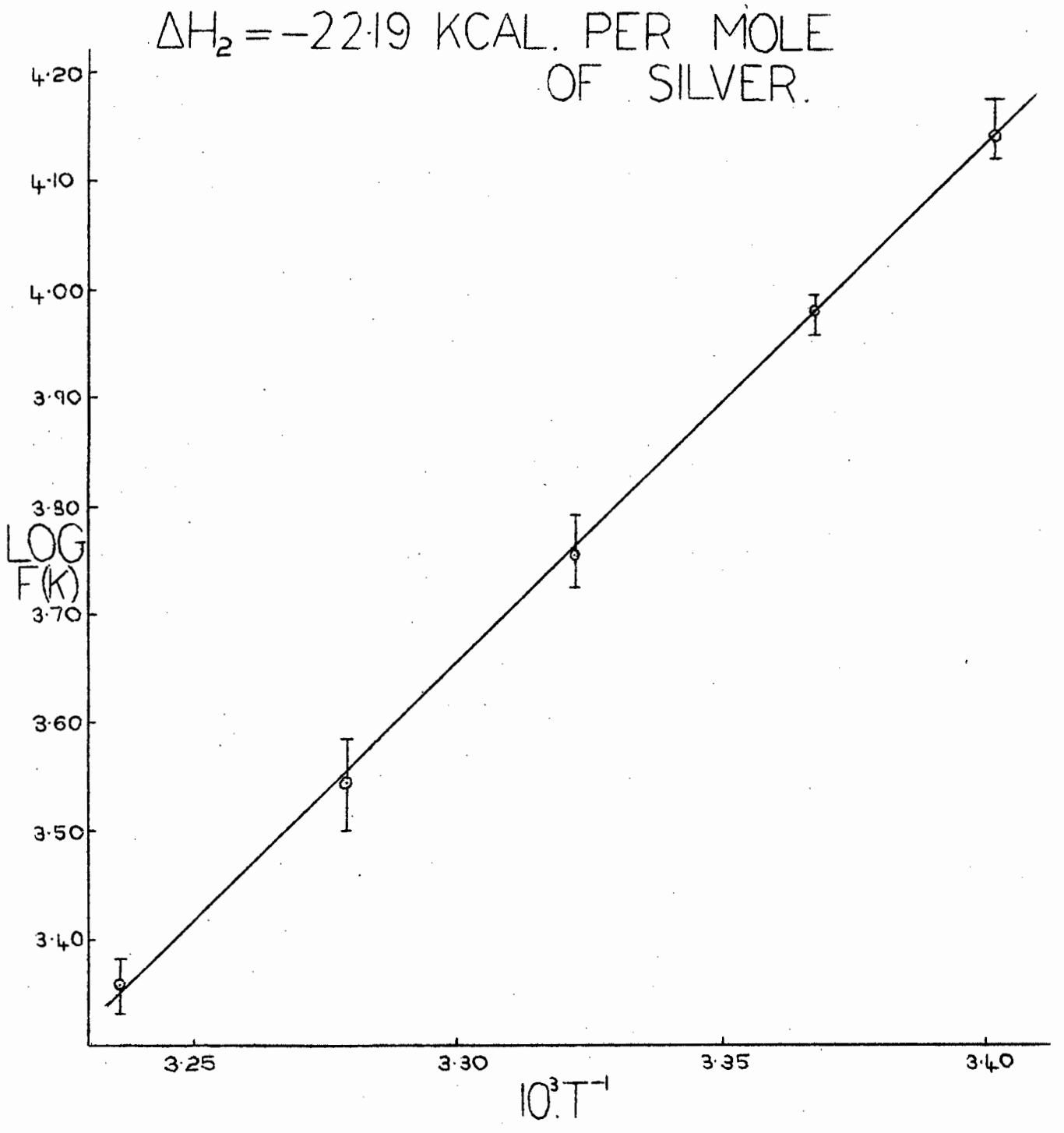

FIGURE 35. SILVER NITRATE IN BENZONITRILE. TEMPERATURE PLOT OF THE EQUILIBRIUM FUNCTION.

The undecayed chromatograms of this system were quantitatively treated as outlined in 2.5.1, fig. 5.

The shape of the chromatogram illustrated in figs. 31 and 33 (Expt. 14) is not due to rate-effects and is explained in 4.7.6. Chromatograms such as these could be quantitatively treated, since the rear end was undecayed, and the division between zone II(a) and II(b) fairly well defined.

4.7.4 Temperature dependence of the equilibrium function

Constant values of the equilibrium function were found for y = 4. The values are listed in table 4.7.2. There is a smaller scatter of values for this system than for the previous two, this being due to the more accurate location of the rear end of zone II(a), since there is no decay of the chromatograms.

The temperature dependence of the equilibrium function is shown in fig. 35 and gave a linear plot from which the heat of reaction of the complex, ΔH_2, was found. The length of the vertical lines about each point on the graph, again indicates the range of values about the mean.

Table 4.7.2. Silver nitrate in benzonitrile - results and temperature dependence of the equilibrium function

Packing S.N.B.	Column temp. °C	Molar ratio (R)	% conversion	10^{-3} F(K) litre^4 mole^{-4}
(1)	21.0	0.83	84.8(8)	14.3(2)
(2)	21.0	0.96	83.7(2)	13.3(9)
(3)	21.0	1.63	79.7(1)	15.1(5)
(4)	21.0	4.20	65.2(9)	13.5(5)
(1)	24.0	0.78	82.5(9)	9.3(5)
(2)	24.0	0.91	81.7(2)	10.1(2)
(3)	24.0	1.44	75.4(3)	9.1(9)
(4)	24.0	4.28	63.5(0)	10.1(0)

Table 4.7.2 continued

Packing S.N.B.	Column temp. ^{o}C	Molar ratio (R)	% conversion	10^{-3} F(K) $litre^{4}\ mole^{-4}$
(1)	28.0	0.71	79.3(2)	5.8(9)
(2)	28.0	0.83	78.0(6)	5.9(2)
(3)	28.0	1.39	71.5(7)	5.2(9)
(5)	28.0	3.52	62.7(3)	6.1(5)
(1)	32.0	0.71	75.9(5)	3.1(7)
(2)	32.0	0.88	76.2(1)	3.6(7)
(3)	32.0	1.50	69.8(4)	3.3(4)
(5)	32.0	3.74	60.0(8)	3.8(7)
(1)	36.0	0.55	68.8(9)	2.1(4)
(2)	36.0	0.79	71.8(2)	2.3(6)
(3)	36.0	1.36	65.6(1)	2.4(0)
(5)	36.0	3.70	55.5(0)	2.1(9)

Packing S.N.B.(4) was replaced by S.N.B.(5) as it was found that after a period of about two months (during which time no experimental work was carried out on S.N.B.(4)), the packing failed to give plateau type chromatograms. This was attributed to ageing effects (see 4.9).

The variation of F'(K) with assumed y values is in accord with the theoretical predictions given in 2.5.2 and is shown in table 4.7.3

Table 4.7.3 Silver nitrate in benzonitrile - variation of F'(K) with assumed y values

Packing S.N.B.	ε	$\left(\frac{n_I y - \Delta}{n_I(y+\varepsilon) - \Delta}\right)$	$\left[\frac{n_{NH_3} - \Delta}{V_f}\right]^{-\varepsilon}$ $litre^{\varepsilon}\ mole^{-\varepsilon}$	F'(K) (at 21.0°C) $litre^{y+\varepsilon}\ mole^{-(y+\varepsilon)}$
(1)	-3	1.10	2.38×10^{-4}	37.8
(2)	-3	1.62	2.85×10^{-4}	62.4
(3)	-3	-	4.24×10^{-4}	-
(4)	-3	-	14.28×10^{-4}	-
(1)	-2	2.54	3.84×10^{-3}	1.40×10^{2}
(2)	-2	2.67	4.33×10^{-3}	1.55×10^{2}
(3)	-2	3.87	5.65×10^{-3}	3.31×10^{2}
(4)	-2	-	12.69×10^{-3}	-

Table 4.7.3 continued

Packing S.N.B.	δ	$\left(\frac{n_I y - \Delta}{n_I(y+\delta) - \Delta}\right)^{-\delta}$	$\left(\frac{n_{NH_3} - \Delta}{V_f}\right)^{-\delta}$ litre $^{\delta}$ mole$^{-\delta}$	F'(K) (at 21.0°C) litre$^{y+\delta}$ mole$^{-(y+\delta)}$
(1)	-1	1.44	6.21×10^{-2}	1.27×10^{3}
(2)	-1	1.46	6.58×10^{-2}	1.29×10^{3}
(3)	-1	1.59	7.52×10^{-2}	1.81×10^{3}
(4)	-1	4.89	11.26×10^{-2}	7.46×10^{3}
(1)	0	1	1	1.43×10^{4}
(2)	0	1	1	1.34×10^{4}
(3)	0	1	1	1.51×10^{4}
(4)	0	1	1	1.35×10^{4}
(1)	+1	0.77	16.10	17.71×10^{4}
(2)	+1	0.76	15.20	15.55×10^{4}
(3)	+1	0.73	13.30	14.71×10^{4}
(4)	+1	0.56	8.88	6.70×10^{4}
(1)	+2	0.62	260.4	23.15×10^{5}
(2)	+2	0.62	230.9	19.08×10^{5}
(3)	+2	0.57	177.0	15.40×10^{5}
(4)	+2	0.39	78.8	4.12×10^{5}

4.7.5 Heat of solution of ammonia in benzonitrile

The heat of solution of ammonia in benzonitrile was determined in the usual way, the variation of the partition coefficient with temperature being shown in table 4.7.4.

Table 4.7.4 Variation of the partition coefficient with temperature

Column temp. °C	t_r min.	t_g min.	$t_r - t_g = t_f$ min.	V_R^o, cm^3	V_f cm^3	K
24.9	3.4(3)	1.6(8)	1.7(5)	32.9(0)	1.24(5)	26.4(3)
28.0	2.7(7)	1.3(9)	1.3(8)	31.7(7)	1.24(8)	25.4(6)
32.0	2.9(4)	1.4(5)	1.4(9)	33.5(6)	1.25(2)	(26.8(0))
36.0	2.4(1)	1.3(2)	1.0(9)	29.6(4)	1.25(6)	23.6(0)

The heat of solution of ammonia in benzonitrile was found to be - 1.81 Kcal per mole of ammonia.

4.7.6. Dissociation pressures and their temperature dependence

Table 4.7.5. lists the values of the dissociation pressures

as well as the dip D_1, due to delayed decomposition of the complex.

Table 4.7.5 Silver nitrate in benzonitrile - effect of experimental conditions on the dissociation pressures

Expt. no.	Column temp. ^oC	Flow-rate $cm^3\ min^{-1}$	$10^3.D_1$ atm.	$10^3.p_d$ atm.
Packing S.N.B.(1), 92.6 cm, 650 µmole of silver nitrate, 7.02 µmole cm^{-1}. Sample size of ammonia, (412 -418) µmole				
2	21.0	6.9(3)	-	89.7(5)
3	21.0	6.9(3)	-	90.2(1)
4	21.0	23.5(5)	1.7	102.2(7)
5	21.0	23.5(5)	1.6	101.6(4)
6	21.0	38.2(4)	1.6	99.4(9)
7	21.0	38.2(4)	1.8	100.2(5)
8	24.0	7.4(2)	-	102.9(2)
9	24.0	7.4(2)	-	103.4(1)
10	24.0	23.7(2)	1.9	116.3(9)
11	24.0	23.7(2)	1.8	117.1(5)
12	24.0	41.4(3)	1.4	110.9(0)
13	24.0	41.4(3)	1.9	109.8(9)
14	28.0	5.8(2)	-	119.3(0)
15	28.0	5.8(2)	-	119.8(6)
16	28.0	22.6(1)	1.0	133.1(7)
17	28.0	22.6(1)	0.4	133.2(5)
18	28.0	39.2(2)	1.0	128.0(3)
19	28.0	39.2(2)	0.9	129.0(9)
20	32.0	5.7(0)	-	144.5(4)
21	32.0	5.7(0)	-	144.4(8)
22	32.0	22.3(7)	1.4	152.7(0)
23	32.0	22.3(7)	1.5	150.8(8)
24	32.0	42.2(0)	1.3	148.7(4)
25	32.0	42.2(0)	1.0	149.0(5)
26	36.0	6.0(7)	-	167.7(6)
27	36.0	6.0(7)	-	167.2(2)
28	36.0	21.9(5)	1.2	172.7(7)
29	36.0	21.9(5)	1.7	174.3(2)
30	36.0	40.3(4)	2.2	168.3(0)
31	36.0	40.3(4)	1.5	168.9(9)
Packing S.N.B.(2), 92.4 cm, 562 µmole of silver nitrate, 6.09 µmole cm^{-1}. Sample size of ammonia, (412 - 418)µmole				
33	21.0	6.7(3)	-	93.4(1)
34	21.0	6.7(3)	-	94.8(7)

Table 4.7.5 continued

Expt. no.	Column temp. °C	Flow-rate $cm^3\ min^{-1}$	$10^3.D_1$ atm.	$10^3.p_d$ atm.
35	21.0	26.8(8)	1.0	102.9(4)
36	21.0	26.8(8)	1.2	103.9(9)
37	21.0	40.3(7)	0.8	102.7(9)
38	21.0	40.3(7)	0.8	101.9(0)
39	24.0	7.2(4)	-	105.2(1)
40	24.0	7.2(4)	-	104.7(9)
41	24.0	26.7(2)	1.9	117.5(7)
42	24.0	26.7(2)	2.3	117.2(3)
43	24.0	45.2(0)	1.9	113.3(5)
44	24.0	45.2(0)	1.9	113.1(0)
45	28.0	7.4(9)	-	123.4(6)
46	28.0	7.4(9)	-	122.4(9)
47	28.0	25.0(1)	1.7	137.7(4)
48	28.0	25.0(1)	1.6	136.4(4)
49	28.0	43.6(1)	1.3	131.3(8)
50	28.0	43.6(1)	1.3	130.4(8)
51	32.0	6.2(2)	-	147.2(1)
52	32.0	6.2(2)	-	148.3(2)
53	32.0	25.1(2)	1.9	153.0(1)
54	32.0	25.1(2)	0.9	152.8(6)
55	32.0	40.5(4)	0.7	151.5(1)
56	32.0	40.5(4)	0.7	149.6(9)
57	36.0	5.8(3)	-	168.4(2)
58	36.0	5.8(3)	-	168.3(1)
59	36.0	27.1(5)	1.2	173.9(3)
60	36.0	27.1(5)	1.5	175.0(1)
61	36.0	40.2(2)	2.5	169.9(9)
62	36.0	40.2(2)	1.0	171.1(5)
Packing S.N.B.(3), 92.6 cm, 306 µmole of silver nitrate, 3.31 µmole cm^{-1}. Sample size of ammonia, (412 - 418) µmole				
64	21.0	6.2(4)	3.6	107.2(1)
65	21.0	6.2(4)	3.6	107.3(3)
66	21.0	21.6(9)	0.9	107.8(1)
67	21.0	21.6(9)	1.4	108.2(4)
68	21.0	38.5(2)	1.0	104.7(7)
69	21.0	38.5(2)	1.4	104.7(7)
70	24.0	7.4(7)	3.4	120.2(0)
71	24.0	7.4(7)	3.5	120.1(1)
72	24.0	20.8(3)	2.5	120.0(2)
73	24.0	20.8(3)	2.2	119.9(3)
74	24.0	38.8(5)	1.9	117.4(8)
75	24.0	38.8(5)	1.6	117.3(2)

Table 4.7.5 continued

Expt. no.	Column temp. °C	Flow-rate $cm^3\ min^{-1}$	$10^3.D_1$ atm.	$10^3.p_d$ atm.
76	28.0	6.8(9)	2.5	140.9(3)
77	28.0	6.8(9)	2.7	140.8(6)
78	28.0	20.2(0)	1.0	140.0(3)
79	28.0	20.2(0)	1.1	139.8(6)
80	28.0	38.2(1)	1.1	135.5(4)
81	28.0	38.2(1)	0.8	135.0(5)
82	32.0	5.8(5)	1.6	162.9(2)
83	32.0	5.8(5)	1.6	162.5(4)
84	32.0	20.0(8)	1.1	158.8(8)
85	32.0	20.0(8)	1.5	158.7(2)
86	32.0	39.7(2)	1.7	153.8(1)
87	32.0	39.7(2)	1.6	152.9(4)
88	36.0	6.1(1)	1.5	183.2(1)
89	36.0	6.1(1)	1.5	184.6(2)
90	36.0	20.2(2)	1.9	178.1(0)
91	36.0	20.2(2)	1.9	178.1(0)
92	36.0	39.2(5)	2.2	174.2(5)
93	36.0	39.2(5)	2.3	172.7(7)
Packing S.N.B.(4), 92.5 cm, 108 µmole of silver nitrate, 1.17 µmole cm^{-1}. Sample size of ammonia, (412 - 418)µmole.				
95	21.0	6.9(4)	4.6	104.3(0)
96	21.0	6.9(4)	4.9	104.3(1)
97	21.0	20.6(1)	4.4	102.2(5)
98	21.0	20.6(1)	5.1	102.4(2)
99	21.0	38.6(1)	5.2	99.3(9)
100	21.0	38.6(1)	5.1	99.8(2)
101	24.0	7.0(3)	6.1	116.8(3)
102	24.0	7.0(3)	6.1	116.2(4)
103	24.0	21.4(5)	6.4	114.1(9)
104	24.0	21.4(5)	6.4	115.3(7)
105	24.0	37.1(7)	5.9	112.5(9)
106	24.0	37.1(7)	5.9	112.2(5)
Packing S.N.B(5), 92.2cm, 145 µmole of silver nitrate, 1.57 µmole cm^{-1}. Sample size of ammonia, (609 - 613) µmole.				
108	28.0	7.6(9)	3.2	136.0(3)
109	28.0	7.6(9)	3.3	137.7(4)
110	28.0	18.8(7)	4.7	136.5(2)
111	28.0	18.8(7)	5.7	136.0(3)
112	28.0	48.0(6)	6.0	135.0(5)
113	28.0	48.0(6)	6.5	134.8(0)
114	32.0	8.2(1)	4.6	157.5(3)
115	32.0	8.2(1)	4.6	157.5(3)
116	32.0	23.1(0)	5.5	156.8(2)

Table 4.7.5 continued

Expt. no.	Column temp. °C	Flow-rate $cm^3\ min^{-1}$	$10^3.D_1$ atm.	$10^3.p_d$ atm.
117	32.0	23.1(0)	5.9	157.1(3)
118	32.0	43.4(8)	5.9	158.4(0)
119	32.0	43.4(8)	6.3	158.4(8)
120	36.0	6.5(2)	4.0	178.9(5)
121	36.0	6.5(2)	4.1	179.7(2)
122	36.0	21.4(6)	5.3	177.5(6)
123	36.0	21.4(6)	5.2	179.1(0)
124	36.0	48.0(6)	4.6	176.7(9)
125	36.0	48.0(6)	4.8	176.7(9)
Packing S.N.B.(1), 92.6 cm, 650 μmole of silver nitrate, 7.02 μmole cm^{-1}. Sample size of ammonia, (826 - 829) μmole.				
126	21.0	7.3(4)	3.5	104.6(0)
127	24.0	7.4(1)	3.5	116.7(0)
128	28.0	7.2(6)	3.3	135.6(2)
129	32.0	7.1(3)	3.8	157.0(5)
130	36.0	6.7(8)	4.7	179.1(8)

Table 4.7.5 calls for the following comments.

(a) packings S.N.B.(1) and S.N.B.(2) gave chromatograms of the type shown in figs. 31 and 33 (Expt. 14) for the lowest flow-rates. This indicated that all the ammonia was converted from zone I to zone II before the ammonia band reached the column exit. Band broadening of zone II then occurred (see 2.2) resulting in insufficient ammonia being present in any section of the column occupied by the band, consequent to which the plateau height could not be maintained. This is indicated by the low values of the dissociation pressures obtained for packings S.N.B.(1) and S.N.B.(2) at the lowest flow-rates. For packing S.N.B.(2) the values of the dissociation pressures at the lowest flow-rates are somewhat higher than for S.N.B.(1), suggesting that since the complete conversion of zone I to zone II must have occurred nearer the

column exit of S.N.B.(2) than of S.N.B.(1), because of the lower silver concentration in the former, less band spreading occurred, with correspondingly increased plateau heights.

(b) packing S.N.B.(3) shows distinctly higher dissociation pressure values than the other packings. The reason for this is unknown, but possible contamination of the packing may be the cause.

(c) the general scatter of the dissociation pressure values with silver concentration and flow-rate is much less than that for the decayed plateau systems, indicating a high rate of decomposition of the complex. There is however some drop in the dissociation pressure values with the higher flow-rates, indicating that the decomposition rate of the complex is not so high that it can meet all requirements.

(d) the values of the dip D_1, due to delayed decomposition of the complex, again appear in a haphazard fashion relative to the experimental variables.

Table 4.7.6 Silver nitrate in benzonitrile - statistical reflection of the rate dependence of the dissociation pressures

Column temp. °C	$10^3.\overline{p_d}$ atm.	$10^3.\sigma$ atm.	$\frac{10^2.\sigma}{\overline{p_d}}$
21.0	102.1(6)	1.7(7)	1.73
24.0	114.6(5)	2.5(0)	2.18
28.0	134.0(9)	3.0(8)	2.30
32.0	154.0(9)	3.6(1)	2.34
36.0	174.8(4)	3.8(9)	2.22

The mean values of the dissociation pressures shown in table 4.7.6. do not include any values from packing S.N.B.(3), or the values of packings S.N.B.(1) and S.N.B.(2) at the lowest

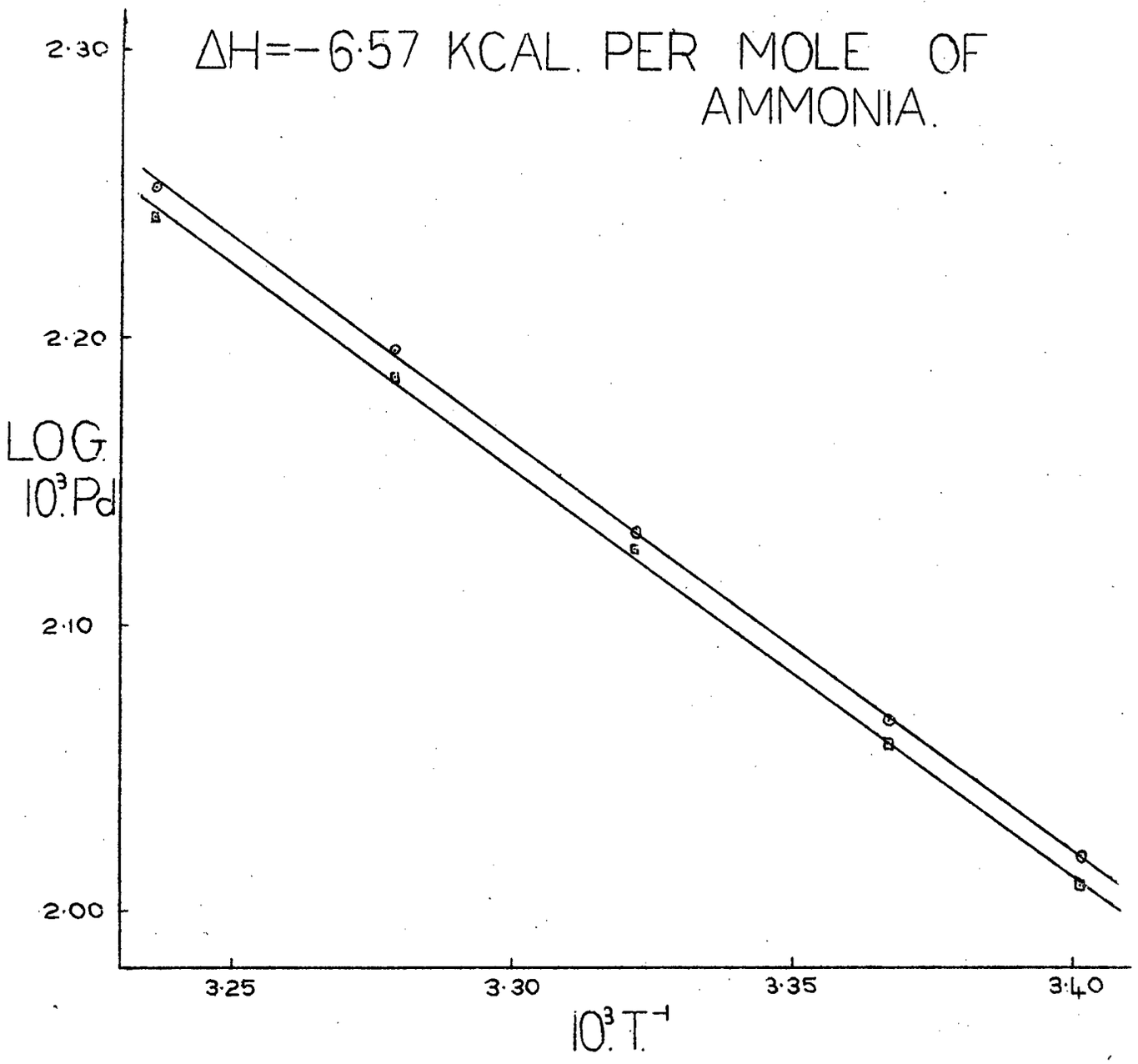

FIGURE 36. SILVER NITRATE IN BENZONITRILE. TEMPERATURE PLOTS OF THE DISSOCIATION PRESSURES.

flow-rates.

The small values of the coefficients of variation reflect statistically the high decomposition rate of the complex.

Fig. 36 shows the dissociation pressure temperature plots. The lower line is the graph of the mean values, the upper line is the plot of the dissociation pressures of packing S.N.B.(1) at the lowest flow-rates and large sample sizes ($\sim$827 μmole). The overall heat of reaction, ΔH, was obtained from the upper graph. The similarity in the slopes of the lines again indicate that the slopes are nearly independent of rate-effects.

Comparison of the overall heat of reaction with the heats of the stages (eqn.(41) of 2.5.4) leads to

$y\Delta H/\text{Kcal (mole silver)}^{-1} = 4.(-6.57) = -26.28$

$\Delta H_2 + y\Delta H_1/\text{Kcal (mole silver)}^{-1} = -22.19 + 4.(-1.81) = -29.43$

4.7.7 Stoichiometric interpretation

The experimental data yielded by this system, indicate that formation of the following complexes

$$AgNO_{3(l)} + 1.5\ NH_{3(l)} \rightleftharpoons AgNO_3(NH_3)_{1.5(s)}$$

$$AgNO_3(NH_3)_{1.5(s)} + 4\ NH_{3(l)} \rightleftharpoons AgNO_3(NH_3)_{5.5(s)}$$

4.7.8 Tensimetric determination of the equilibrium function

In order to verify the chromatographic method of determining the equilibrium function, the tensimeter described in 3.1.6 was used. The experimental procedure described in 3.1.6 was carried out on a solution of silver nitrate in benzonitrile. The amounts of material used and results

obtained were as follows:

(a) amount of silver nitrate dissolved in 11.42(8) cm^3 of benzonitrile (24.9°C) = 310 μmole.

(b) total amount of ammonia injected into tensimeter = 3897 μmole.

(c) total amount of ammonia absorbed in the liquid phase = 3045 μmole.

(d) amount of ammonia in the liquid phase assumed to be associated with complex I = 1.5 x 310 = 465 μmole.

(e) amount of ammonia associated with complex II = $(3045 - 465) \times \frac{\text{"\% conversion"}}{100}$

(f) % conversion = 39%

(g) the value of F (K) at 24.9°C was found to be 11.7 x 10^3 $litre^4$ $mole^{-4}$, as compared with 8.6(5) x 10^3 $litre^4$ $mole^{-4}$ obtained from fig. 35.

The agreement is as good as can be expected considering the crudity of the tensimetric technique.

4.8 Silver nitrate in benzyl cyanide

This system absorbed ammonia due to the formation of complex I, and thereafter gave chromatograms showing two undecayed plateaux, which indicated the formation of more than one complex having a detectable dissociation pressure.

4.8.1 The packings

The packings turned pale mauve shortly after preparation, and showed no further colour change on the addition of ammonia. The packing characteristics are shown in table 4.8.1.

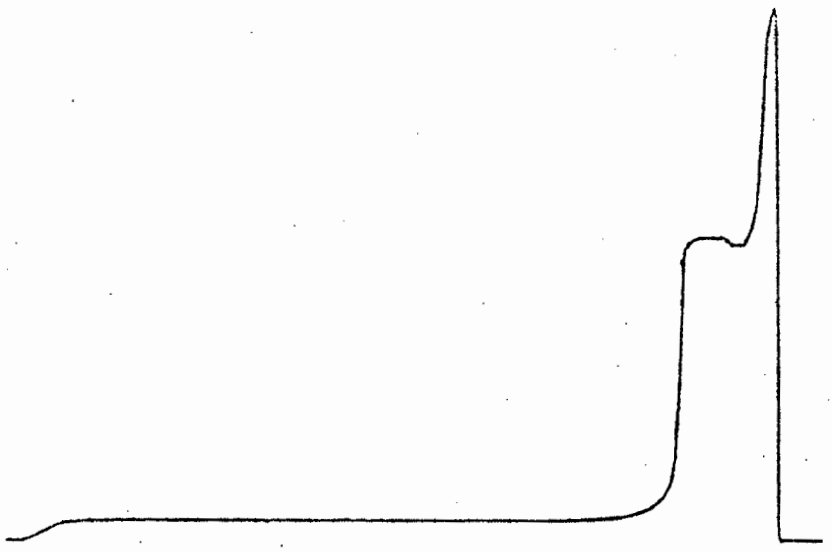

EXPT. 36 665 μMOLE.

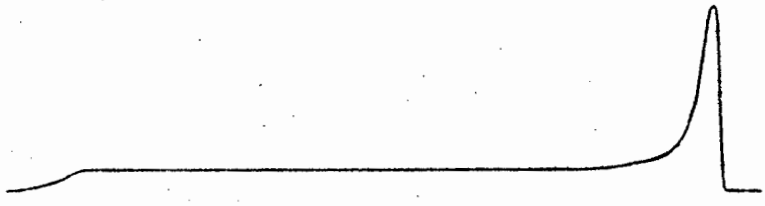

EXPT. 36(A) 280 μMOLE.

FIGURE 37. SILVER NITRATE IN BENZYL CYANIDE.—EFFECT OF SAMPLE SIZE. PACKING S.N.B.C.(2)., FLOW-RATE, 21·5(7) $CM.^3$ $MIN.^{-1}$, COLUMN TEMPERATURE, 21·0°C.

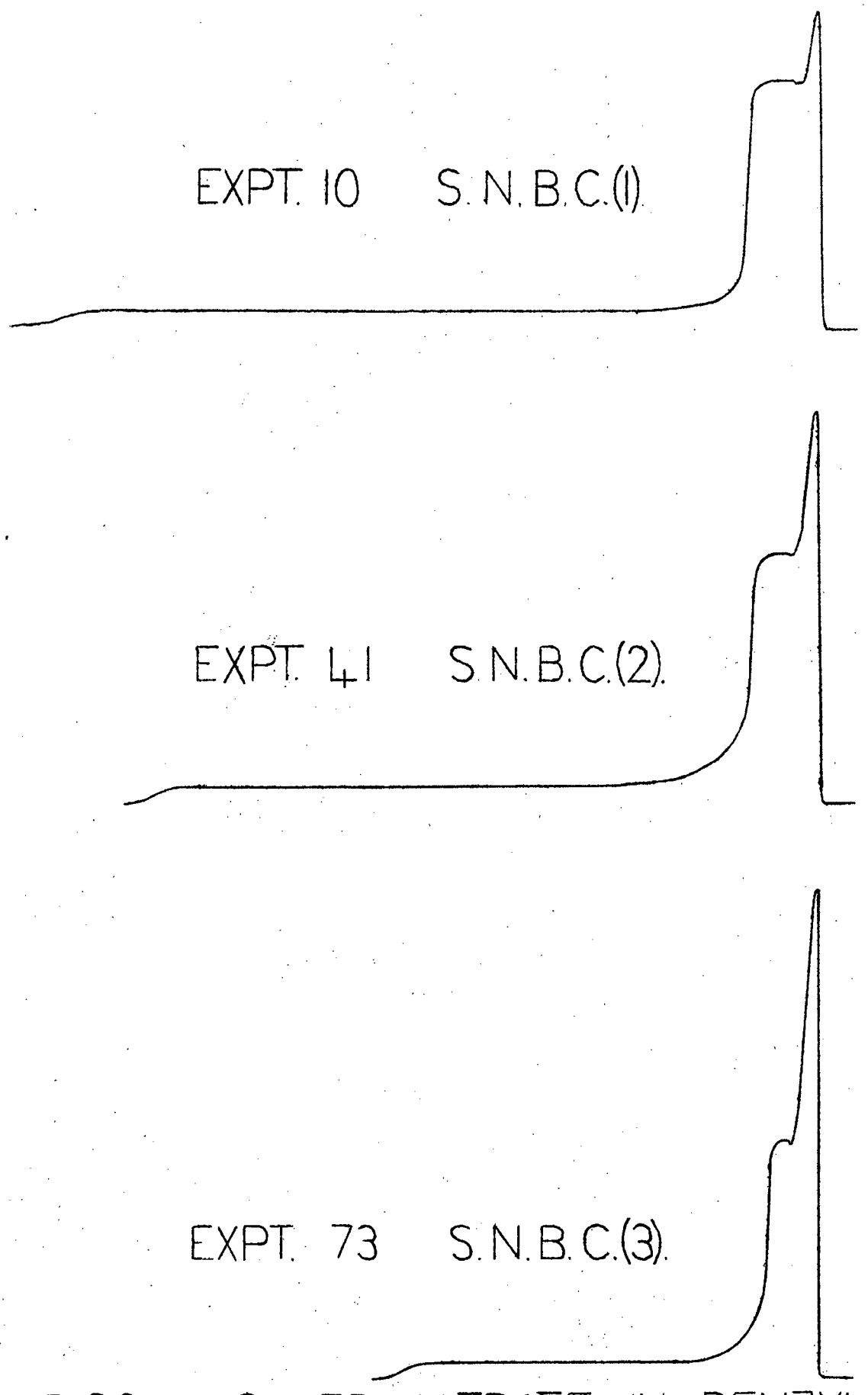

FIGURE 38. SILVER NITRATE IN BENZYL CYANIDE—EFFECT OF SILVER CONCENTRATION. SAMPLE SIZE, (665–670) μMOLE, COLUMN LENGTH, (91·6–93·9) CM, FLOW-RATE, (17·2(4)–19·2(3)) CM^3 $MIN.^{-1}$, COLUMN TEMPERATURE, 24·0°C.

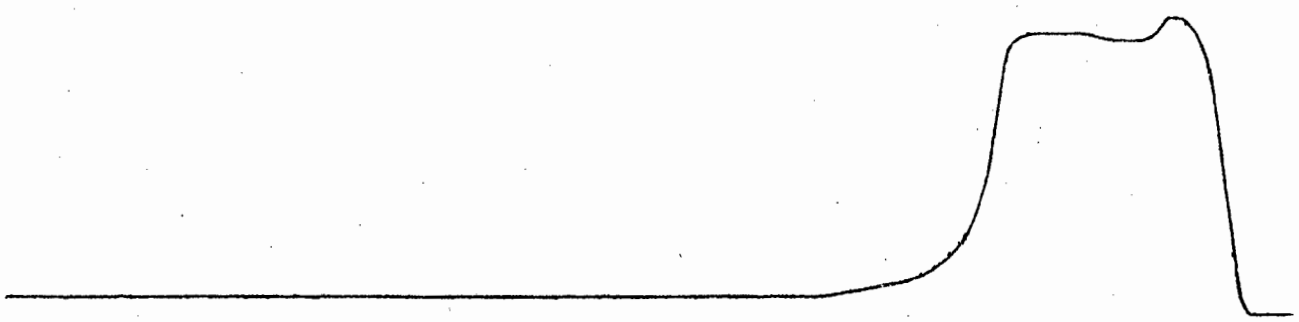

EXPT. 2 FLOW-RATE, 8·2(0) CM^3 MIN^{-1}

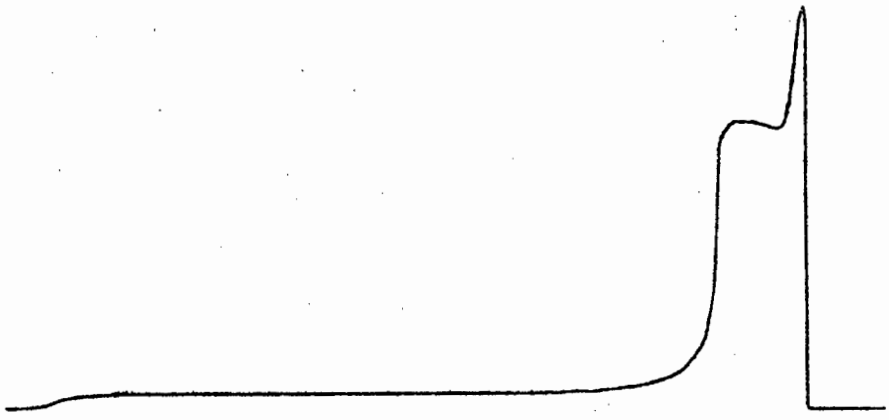

EXPT. 4 FLOW-RATE, 22·2(9) CM^3 MIN^{-1}

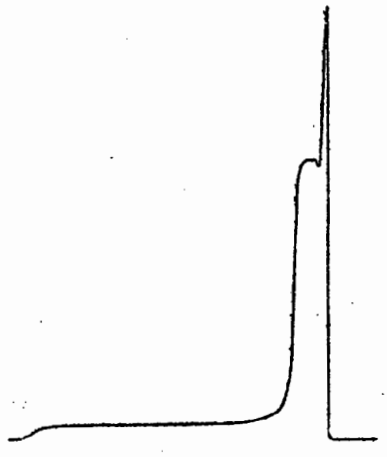

EXPT. 7 FLOW-RATE, 55·7(1) CM^3 MIN^{-1}

FIGURE 39. SILVER NITRATE IN BENZYL CYANIDE.—EFFECT OF FLOW-RATE. PACKING S.N.B.C.(1). SAMPLE SIZE, (664–667) μMOLE, COLUMN TEMPERATURE, 21·0°C.

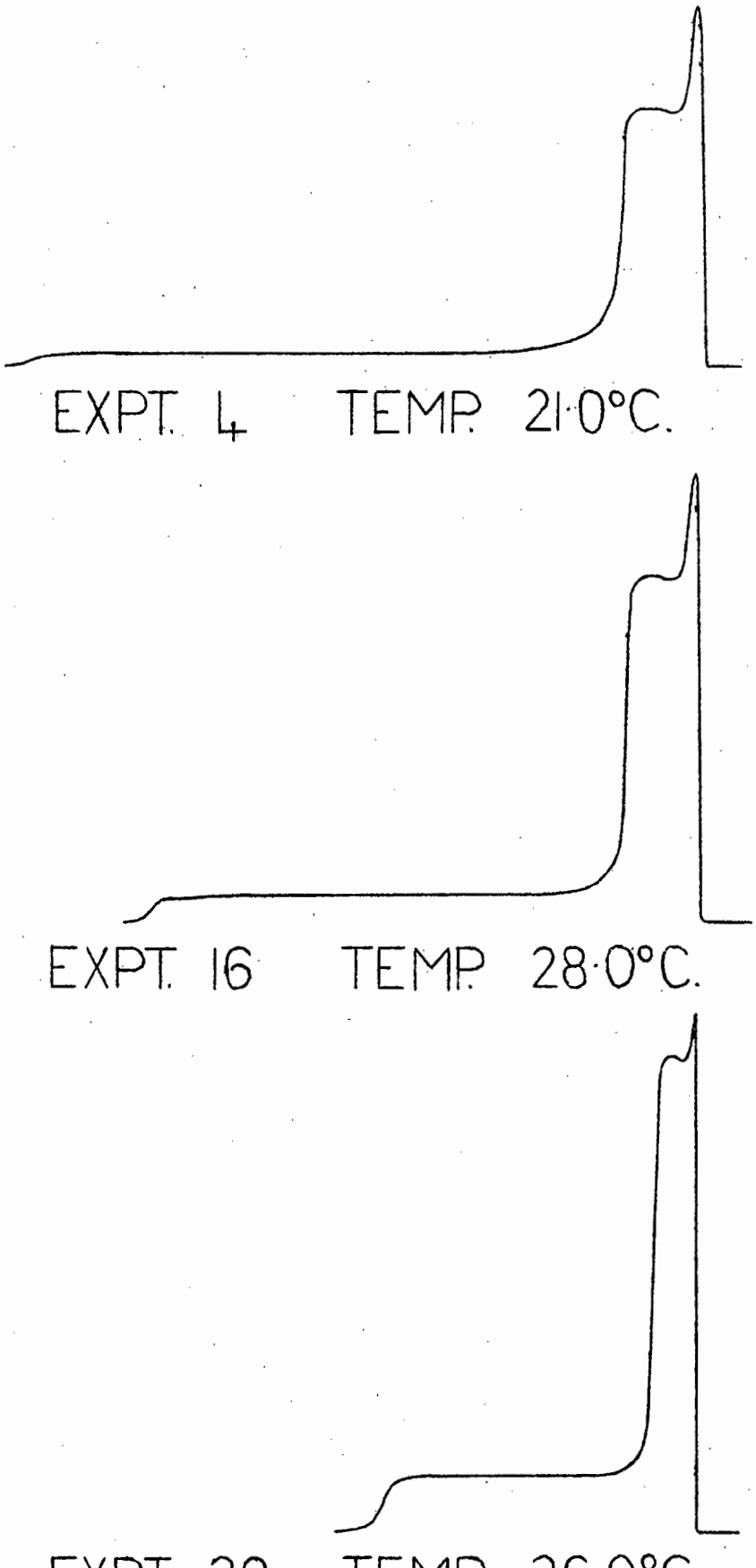

FIGURE 4.0. SILVER NITRATE IN BENZYL CYANIDE.—EFFECT OF COLUMN TEMPERATURE. PACKING S.N.B.C.(1). FLOW-RATE, (21·7(2)–22·2(9)) CM^3 MIN^{-1}. SAMPLE SIZE, (663–669) μMOLE.

Table 4.8.1 Column packings of silver nitrate in benzyl cyanide

Packing	Column length cm	10^2.s (at 25°C) $cm^3\ gm^{-1}$	Silver conc. $\mu mole\ cm^{-3}$ (at 25°C)
S.N.B.C.(1)	92.6	2.70	461
S.N.B.C.(2)	91.6	2.71	303
S.N.B.C.(3)	93.9	2.50	187

4.8.2. The initial absorption

The following initial absorptions (moles of ammonia per mole of silver) were measured

Packing	S.N.B.C.(1)	1.42
	S.N.B.C.(2)	1.53
	S.N.B.C.(3)	1.41

4.8.3 The chromatograms

The two plateau chromatograms shown in figs. 37 to 40, exhibit the same predicted change in shape with the column variables as shown by the chromatograms of the other systems. The undecayed plateaux indicate fast decomposition rates of the complexes. The higher plateau shows the usual dip effect, which is not manifested at all by the lower plateau.

The lower plateau is treated in the usual quantitative fashion, but this treatment cannot be applied to the higher plateau (see 4.8.7).

4.8.4 The equilibrium function, results and temperature plot for the lower plateau

Although the lower plateau showed no decay, there is a somewhat larger scatter of the equilibrium function values than

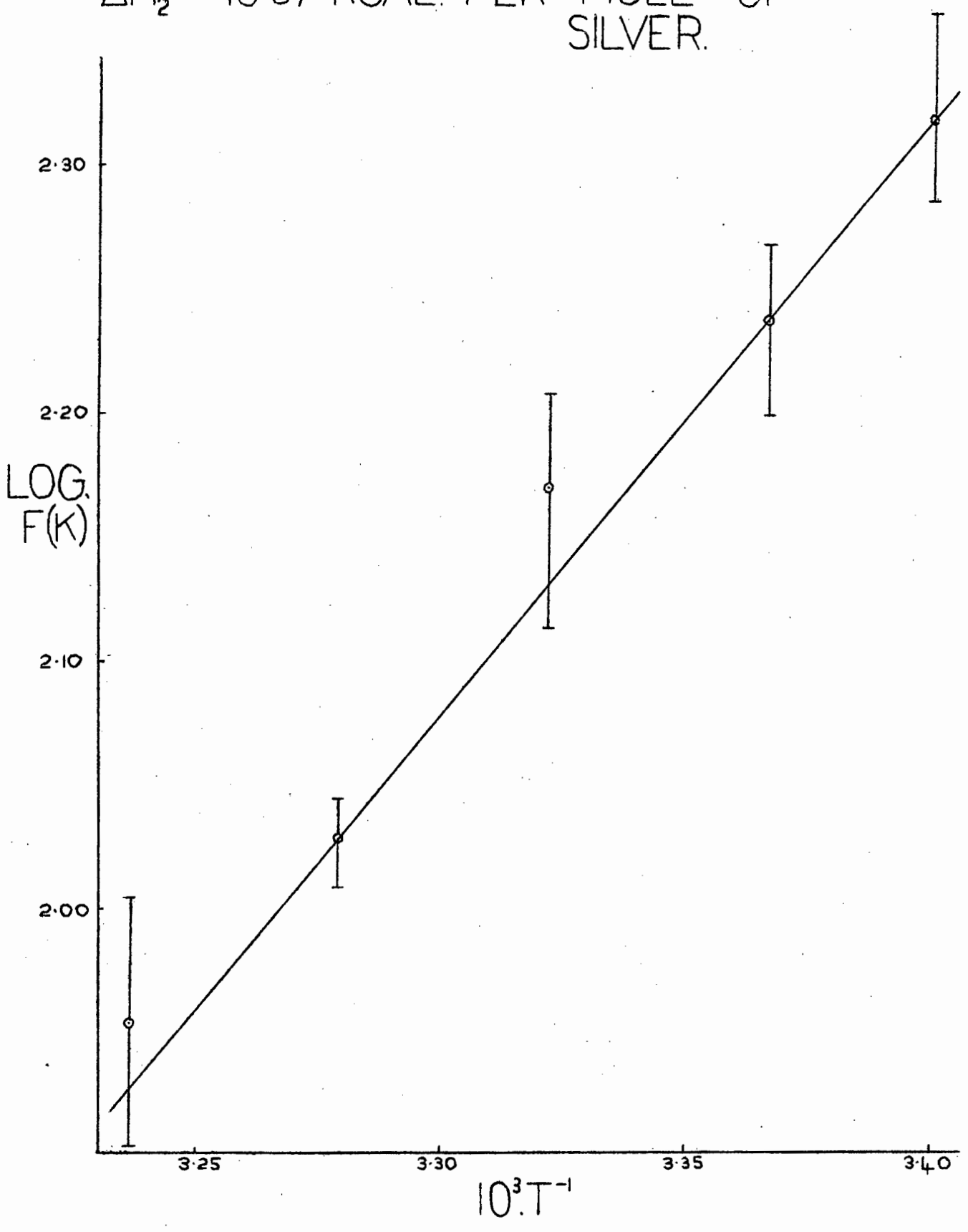

FIGURE 4.1. SILVER NITRATE IN BENZYL CYANIDE. TEMPERATURE PLOT OF THE EQUILIBRIUM FUNCTION OF THE LOWER PLATEAU.

for the benzonitrile system. This is due to the fact that a small error in locating the rear end of zone II(a) necessarily meant an enhanced error in the determination of the unreacted amount of ammonia since the area of zone II(b) is small.

The values of the equilibrium function are listed in table 4.8.2 and were obtained for y = 1. The heat of reaction of complex II, ΔH_2, was determined from the temperature plot of the equilibrium function shown in fig. 41.

Table 4.8.2 Silver nitrate in benzyl cyanide - results and temperature dependence of the equilibrium function

Packing S.N.B.C.	Column temp. °C	Molar ratio (R)	% conversion	$10^{-2}.F(K)$ litre $mole^{-1}$
(1)	21.0	0.44	98.1(5)	2.0(1)
(2)	21.0	0.47	96.9(7)	1.9(3)
(3)	21.0	0.74	93.1(2)	2.3(0)
(1)	24.0	0.41	97.7(7)	1.5(8)
(2)	24.0	0.48	96.6(3)	1.7(6)
(3)	24.0	0.78	91.0(5)	1.8(6)
(1)	28.0	0.39	97.3(8)	1.3(0)
(2)	28.0	0.61	95.0(6)	1.5(1)
(3)	28.0	0.77	90.1(0)	1.6(2)
(1)	32.0	0.40	96.9(0)	1.1(1)
(2)	32.0	0.61	93.4(0)	1.0(9)
(3)	32.0	0.82	85.2(1)	1.0(2)
(1)	36.0	0.38	95.9(0)	0.8(0)
(2)	36.0	0.69	91.7(5)	1.0(1)
(3)	36.0	0.82	83.8(1)	0.8(6)

The equilibrium function values were found to vary in the manner predicted in 2.5.2 with assumed y values as indicated in table 4.8.3.

Table 4.8.3 Silver nitrate in benzyl cyanide - variation of F'(K) with assumed y values

Packing S.N.B.C.	δ	$\frac{(n_I\, y - \Delta)}{(n_I(y+\delta) - \Delta)}$	$\left[\frac{n_{NH_3} - \Delta}{V_f}\right]^{-\delta}$ litre$^{\delta}$ mole$^{-\delta}$	F'(K) (at 21.0°C) litre$^{y+\delta}$ mole$^{-(y+\delta)}$
(1)	0	1	1	2.0(1) x 10^2
(2)	0	1	1	1.9(3) x 10^2
(3)	0	1	1	2.3(0) x 10^2
(1)	+1	0.36	269	19.8 x 10^3
(2)	+1	0.35	231	15.7 x 10^3
(3)	+1	0.24	106	5.8 x 10^3
(1)	+2	0.22	7.21 x 10^4	32.4 x 10^5
(2)	+2	0.21	5.32 x 10^4	22.0 x 10^5
(3)	+2	0.14	1.12 x 10^4	3.4(9) x 10^5

4.8.5 Heat of solution of ammonia in benzyl cyanide

Table 4.8.4 shows the temperature dependence of the partition coefficient, from which the heat of solution of ammonia in benzyl cyanide was determined and found to be - 1.78 Kcal per mole of ammonia.

Table 4.8.4 Effect of temperature on the partition coefficient

Column temp. °C	t_r min.	t_g min.	$t_r - t_g = t_f$ min.	$V^o_R{}'$ cm^3	V_f cm^3	K
24.8	4.4(0)	1.2(5)	3.1(5)	51.3(6)	1.85(5)	(27.6(9))
28.0	4.6(3)	1.2(3)	3.4(0)	56.2(4)	1.86(0)	30.2(3)
32.0	4.5(7)	1.2(4)	3.3(3)	53.6(0)	1.86(6)	28.7(2)
36.0	4.4(5)	1.2(5)	3.2(0)	52.4(0)	1.87(2)	27.9(9)

4.8.6 Dissociation pressures, results and temperature plot for the lower plateau

Table 4.8.5 lists the dissociation pressure results obtained for the lower plateau.

Table 4.8.5 Silver nitrate in benzyl cyanide - effect of experimental variables on the dissociation pressures of the lower plateau

Expt. no.	Column temp. °C	Flow-rate $cm^3\ min^{-1}$	$10^3.p_d$ atm.
Packing S.N.B.C.(1), 92.6 cm, 571 µmole of silver nitrate, 6.16 µmole cm^{-1}. Sample size of ammonia, (663 - 670) µmole.			
2	21.0	8.2(0)	6.4(2)
3	21.0	8.2(0)	6.7(7)
4	21.0	22.2(9)	6.8(6)
5	21.0	22.2(9)	6.1(6)
6	21.0	55.7(1)	6.9(4)
7	21.0	55.7(1)	6.2(5)
8	24.0	7.6(3)	8.1(0)
9	24.0	7.6(3)	7.6(0)
10	24.0	19.2(3)	8.1(0)
11	24.0	19.2(3)	7.6(8)
12	24.0	56.4(6)	8.1(0)
13	24.0	56.4(6)	7.6(0)
14	28.0	6.4(1)	10.2(8)
15	28.0	6.4(1)	10.4(4)
16	28.0	21.7(2)	10.8(5)
17	28.0	21.7(2)	10.4(4)
18	18.0	54.5(4)	10.7(7)
19	28.0	54.5(4)	10.6(1)
20	32.0	7.7(0)	14.5(7)
21	32.0	7.7(0)	14.0(2)
22	32.0	20.2(8)	15.0(5)
23	32.0	20.2(8)	14.6(5)
24	32.0	54.4(1)	15.0(5)
25	32.0	54.4(1)	14.7(3)
26	36.0	6.0(8)	20.6(9)
27	36.0	6.0(8)	20.1(5)
28	36.0	21.8(7)	20.5(4)
29	36.0	21.8(7)	19.7(6)
30	36.0	50.8(9)	20.8(4)
31	36.0	50.8(9)	20.1(5)
Packing S.N.B.C.(2), 91.6 cm, 431 µmole of silver nitrate, 4.70 µmole cm^{-1}. Sample size of ammonia, (663 - 670)µmole.			
33	21.0	5.2(7)	6.9(4)
34	21.0	5.2(7)	6.3(4)
35	21.0	21.5(7)	6.6(0)
36	21.0	21.5(7)	6.4(2)
37	21.0	55.6(9)	6.6(0)
38	21.0	55.6(9)	5.9(0)

Table 4.8.5 continued

Expt. no.	Column temp. °C	Flow-rate $cm^3\ min^{-1}$	$10^3.p_d$ atm.
39	24.0	7.3(6)	[7.0(9)]
40	24.0	7.3(6)	[7.0(9)]
41	24.0	17.3(2)	7.9(3)
42	24.0	17.3(2)	7.7(6)
43	24.0	60.8(3)	7.9(3)
44	24.0	60.8(3)	7.6(0)
45	28.0	6.4(6)	10.6(1)
46	28.0	6.4(6)	10.3(6)
47	28.0	38.0(3)	10.6(1)
48	28.0	38.0(3)	10.3(6)
49	28.0	59.1(9)	10.6(1)
50	28.0	59.1(9)	10.3(6)
51	32.0	8.9(3)	14.5(7)
52	32.0	8.9(3)	14.8(1)
53	32.0	34.8(9)	14.7(3)
54	32.0	34.8(9)	14.0(2)
55	32.0	57.8(1)	14.8(1)
56	32.0	57.8(1)	14.3(4)
57	36.0	8.7(1)	20.7(7)
58	36.0	8.7(1)	19.9(2)
59	36.0	34.1(4)	20.0(7)
60	36.0	34.1(4)	19.3(8)
61	36.0	54.5(8)	20.4(6)
62	36.0	54.5(8)	19.3(8)
Packing S.N.B.C.(3), 93.9 cm, 211 μmole of silver nitrate, 2.25 μmole cm^{-1}. Sample size of ammonia, (663 - 670) μmole.			
64	21.0	8.7(5)	6.5(9)
65	21.0	8.7(5)	6.5(1)
66	21.0	32.9(3)	6.6(8)
67	21.0	32.9(3)	6.3(4)
68	21.0	51.6(8)	7.0(3)
69	21.0	51.6(8)	6.7(7)
70	24.0	7.5(1)	8.1(9)
71	24.0	7.5(1)	7.7(6)
72	24.0	17.2(4)	7.7(6)
73	24.0	17.2(4)	7.7(6)
74	24.0	52.0(2)	7.6(8)
75	24.0	52.0(2)	7.6(0)
76	28.0	9.0(6)	10.4(4)
77	28.0	9.0(6)	10.0(4)
78	28.0	30.8(2)	10.1(2)
79	28.0	30.8(2)	10.1(2)
80	28.0	50.5(9)	10.5(3)
81	28.0	50.5(9)	10.0(4)

Table 4.8.5 continued

Expt. no.	Column temp. °C	Flow-rate $cm^3\ min^{-1}$	$10^3.p_d$ atm.
82	32.0	6.5(4)	14.4(1)
83	32.0	6.5(4)	13.3(8)
84	32.0	31.2(2)	14.0(2)
85	32.0	31.2(2)	13.3(8)
86	32.0	46.7(7)	14.1(0)
87	32.0	46.7(7)	13.3(8)
88	36.0	5.5(9)	18.6(8)
89	36.0	5.5(9)	17.8(3)
90	36.0	29.5(9)	18.3(0)
91	36.0	29.5(9)	17.8(3)
92	36.0	52.2(5)	17.7(6)
93	36.0	52.2(5)	17.8(3)

The values of p_d for experiments 39 and 40 differ from the mean by more than twice the standard deviation, and are bracketed in table 4.8.5.

The values of the dissociation pressures indicate little rate-effects, except for packing S.N.B.C.(3) at the higher temperatures, where there is a drop in the values, again suggesting that the decomposition rate of the complex is not so high that it can meet all requirements. This can be seen in the increase of the coefficients of variation for the two highest temperatures shown in table 4.8.6.

Table 4.8.6 Silver nitrate in benzyl cyanide - statistical analysis of the dissociation pressure values of the lower plateau.

Column temp. °C	$10^3.\overline{p_d}$ atm.	$10^3.\sigma$ atm.	$\frac{10^2.\sigma}{\overline{p_d}}$
21.0	6.5(6)	0.3(0)	4.57
24.0	7.8(2)	0.2(1)	2.69
28.0	10.4(2)	0.2(4)	2.30
32.0	14.3(3)	0.5(5)	3.84
36.0	19.4(6)	1.1(3)	5.81

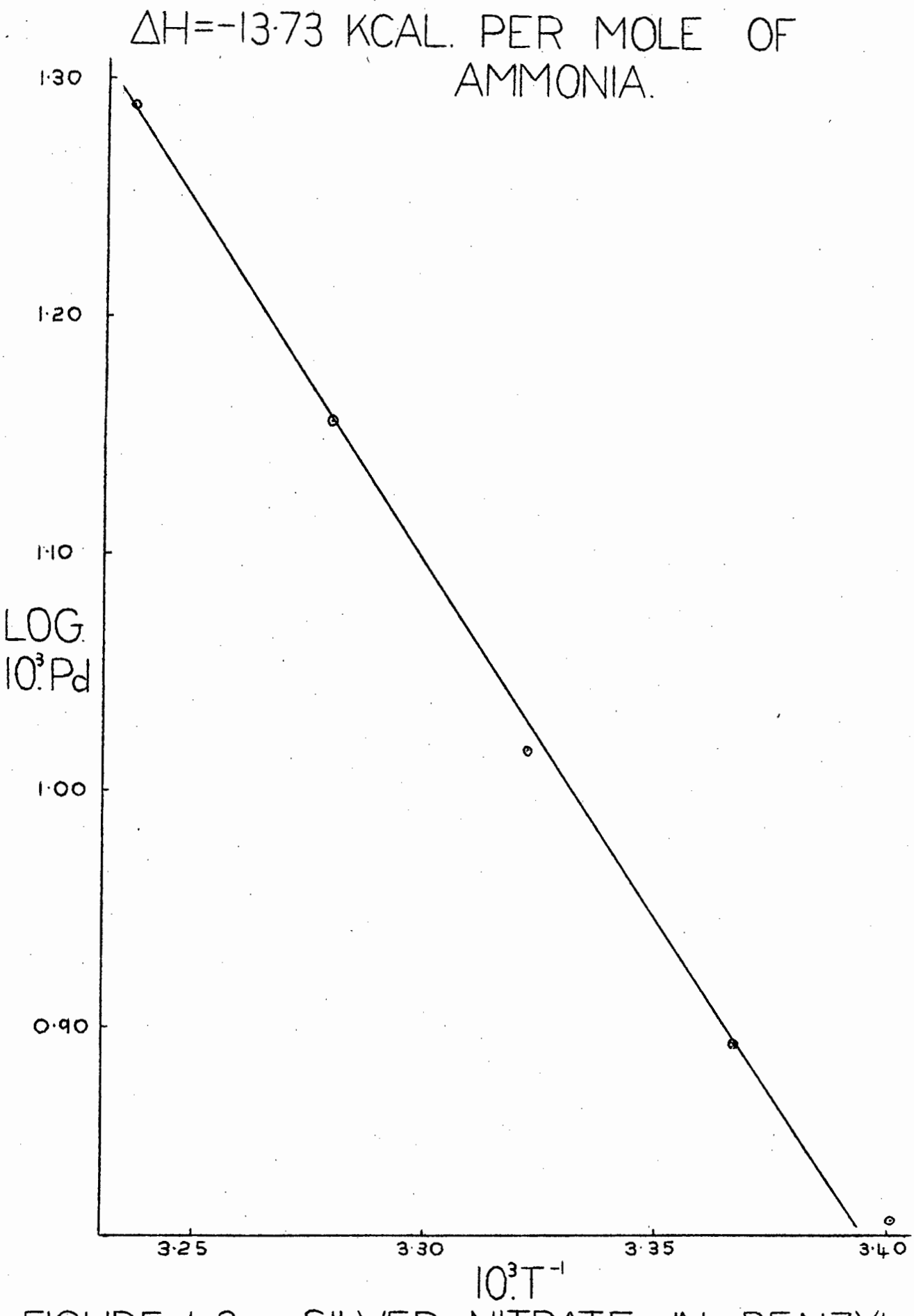

FIGURE 42. SILVER NITRATE IN BENZYL CYANIDE. TEMPERATURE PLOT OF THE DISSOCIATION PRESSURE OF THE LOWER PLATEAU

The large coefficient of variation obtained at 21.0°C is not due to rate-effects (as can be seen from the p_d values in table 4.8.5) but to large experimental scatter of the normal type.

The temperature plot of the dissociation pressures shown in fig. 42 was obtained from the mean values.

Comparison of the overall heat of reaction with the heats of the stages (eqn. (41) of 2.5.4) leads to :

$y\Delta H$/Kcal (mole silver)$^{-1}$ = - 13.73

$\Delta H_2 + y\Delta H_1$/Kcal (mole silver)$^{-1}$ = - 10.87 + (-1.78) = - 12.65

4.8.7 The higher plateau

The appearance of two plateau chromatograms preceded by the usual initial absorption of ammonia, indicates that one of the following processes occurs in the column.

(a) $NH_{3(g)} \rightleftharpoons NH_{3(l)}$

$AgNO_{3(l)} + 1.5\ NH_{3(l)} \rightleftharpoons AgNO_3(NH_3)_{1.5(s)}$

followed by the successive reactions

$AgNO_3(NH_3)_{1.5(s)} + NH_{3(l)} \rightleftharpoons AgNO_3(NH_3)_{2.5(s)}$ - lower plateau

$AgNO_3(NH_3)_{2.5(s)} + yNH_{3(l)} \rightleftharpoons AgNO_3(NH_3)_{(2.5+y)(s)}$ - higher plateau

or (b) $NH_{3(g)} \rightleftharpoons NH_{3(l)}$

$AgNO_{3(l)} + 1.5\ NH_{3(l)} \rightleftharpoons AgNO_3(NH_3)_{1.5(s)}$

followed by the competitive reactions

$AgNO_3(NH_3)_{1.5(s)} + NH_{3(l)} \rightleftharpoons AgNO_3(NH_3)_{2.5(s)}$ - lower plateau

$AgNO_3(NH_3)_{1.5(s)} + yNH_{3(l)} \rightleftharpoons AgNO_3(NH_3)_{(1.5+y)(s)}$ - higher plateau

Table 4.8.7 lists the values of the dissociation pressures obtained for the higher plateau, together with the

values of the dip D_1 due to delayed decomposition of the solid complex.

Table 4.8.7 Silver nitrate in benzyl cyanide - effect of experimental conditions on the dissociation pressures of the higher plateau

Expt. no.	Column temp. °C	Flow-rate $cm^3\ min^{-1}$	$10^3.D_1$ atm.	$10^3\ p_d$ atm.
Packing S.N.B.C.(1), 92.6 cm, 571 µmole of silver nitrate, 6.16 µmole cm^{-1}. Sample size of ammonia, (663 - 670) µmole				
2	21.0	8.2(0)	0.9	101.8(2)
3	21.0	8.2(0)	2.4	101.7(3)
4	21.0	22.2(9)	1.9	97.8(2)
5	21.0	22.2(9)	1.7	99.2(1)
6	21.0	55.7(1)	2.4	98.0(8)
7	21.0	55.7(1)	2.6	98.4(3)
8	24.0	7.6(3)	0.9	110.8(2)
9	24.0	7.6(3)	0.8	109.1(3)
10	24.0	19.2(3)	2.1	110.0(6)
11	24.0	19.2(3)	1.8	110.8(2)
12	24.0	56.4(6)	1.6	105.8(4)
13	24.0	56.4(6)	1.6	107.0(2)
14	28.0	6.4(1)	1.8	126.4(8)
15	28.0	6.4(1)	1.6	129.6(6)
16	28.0	21.7(2)	2.4	126.6(4)
17	28.0	21.7(2)	2.4	126.6(4)
18	28.0	54.5(4)	2.4	123.7(1)
19	28.0	54.5(4)	2.3	124.9(3)
20	32.0	7.7(0)	2.5	148.9(0)
21	32.0	7.7(0)	1.5	149.9(3)
22	32.0	20.2(8)	2.7	146.2(8)
23	32.0	20.2(8)	2.4	147.0(0)
24	32.0	54.4(1)	2.3	140.9(8)
25	32.0	54.4(1)	1.7	141.3(7)
26	36.0	6.0(8)	3.4	168.3(0)
27	36.0	6.0(8)	2.2	171.5(4)
28	36.0	21.8(7)	4.2	167.5(2)
29	36.0	21.8(7)	2.9	169.2(2)
30	36.0	50.8(9)	3.9	[162.1(2)]
31	36.0	50.8(9)	1.7	[162.4(3)]
Packing S.N.B.C.(2), 91.6 cm, 431 µmole of silver nitrate, 4.70 µmole cm^{-1}. Sample size of ammonia, (663 - 670) µmole				
33	21.0	5.2(7)	1.0	98.7(8)
34	21.0	5.2(7)	2.3	100.5(1)
35	21.0	21.5(7)	3.5	98.9(5)

Table 487 continued

Expt. no.	Column temp. °C	Flow-rate $cm^3\ min^{-1}$	$10^3.D_1$ atm.	$10^3 p_d$ atm.
36	21.0	21.5(7)	2.5	98.0(0)
37	21.0	55.6(9)	2.4	97.1(3)
38	21.0	55.6(9)	1.7	95.8(3)
39	24.0	7.3(6)	0.8	110.5(6)
40	24.0	7.3(6)	0.3	110.5(6)
41	24.0	17.3(2)	-	108.4(1)
42	24.0	17.3(2)	0.4	108.6(2)
43	24.0	60.8(3)	-	104.6(6)
44	24.0	60.8(3)	-	105.7(5)
45	28.0	6.4(6)	-	125.7(5)
46	28.0	6.4(6)	-	128.8(5)
47	28.0	38.0(3)	0.9	127.0(5)
48	28.0	38.0(3)	0.9	129.1(7)
49	28.0	59.1(9)	0.8	125.0(1)
50	28.0	59.1(9)	1.0	127.0(5)
51	32.0	8.9(3)	-	149.3(7)
52	32.0	8.9(3)	0.6	149.3(7)
53	32.0	34.8(9)	1.1	147.7(9)
54	32.0	34.8(9)	0.9	147.2(3)
55	32.0	57.8(1)	0.9	143.7(5)
56	32.0	57.8(1)	0.8	141.8(5)
57	36.0	8.7(1)	0.6	172.4(6)
58	36.0	8.7(1)	0.4	172.9(3)
59	36.0	34.1(4)	1.7	172.0(8)
60	36.0	34.1(4)	1.4	172.3(1)
61	36.0	54.5(8)	1.6	166.8(3)
62	36.0	54.5(8)	1.5	165.5(9)
Packing S.N.B.C.(3), 93.9 cm., 211 µmole of silver nitrate, 2.25 µmole cm^{-1}. Sample size of ammonia (663 - 670) µmole				
64	21.0	8.7(5)	2.4	101.8(9)
65	21.0	8.7(5)	2.3	102.1(6)
66	21.0	32.9(3)	2.5	101.7(3)
67	21.0	32.9(3)	2.6	101.0(4)
68	21.0	51.6(8)	1.4	99.1(3)
69	21.0	51.6(8)	1.4	99.4(7)
70	24.0	7.5(1)	-	110.4(0)
71	24.0	7.5(1)	0.7	110.7(3)
72	24.0	17.2(4)	0.3	109.0(4)
73	34.0	17.2(4)	0.8	110.4(0)
74	24.0	52.0(2)	-	106.3(4)
75	24.0	52.0(2)	0.3	107.0(2)

Table 4.8.7 continued

Expt. no.	Column temp. °C	Flow-rate $cm^3\ min^{-1}$	$10^3.D_1$ atm.	$10^3.p_d$ atm.
76	28.0	9.0(6)	-	126.2(4)
77	28.0	9.0(6)	-	127.9(5)
78	28.0	30.8(2)	0.4	127.1(1)
79	28.0	30.8(2)	0.4	127.1(3)
80	28.0	50.5(9)	0.7	125.5(0)
81	28.0	50.5(9)	0.8	126.4(8)
82	32.0	6.5(4)	-	149.8(0)
83	32.0	6.5(4)	-	149.8(5)
84	32.0	31.2(2)	0.8	149.9(3)
85	32.0	31.2(2)	0.9	150.4(8)
86	32.0	46.7(7)	1.0	147.3(9)
87	32.0	46.7(7)	1.1	148.1(8)
88	36.0	5.5(9)	-	172.2(3)
89	36.0	5.5(9)	0.7	172.2(3)
90	36.0	29.5(9)	1.5	173.5(5)
91	36.0	29.5(9)	1.5	174.1(6)
92	36.0	52.2(5)	-	169.0(7)
93	36.0	52.2(5)	1.4	171.0(0)
Packing S.N.B.C.(1), 92.6 cm., 571 µmole of silver nitrate, 616 µmole cm^{-1}. Sample size of ammonia, ~1600 µmole.				
94	24.0	4.2(1)	2.5	111.4(1)
95	32.0	4.5(6)	0.4	152.0(6)
96	36.0	4.5(0)	0.7	175.4(8)

The values of the dissociation pressures reveal little rate-effects except at the higher flow-rates. This is shown in table 4.8.8 by the small values obtained for the coefficients of variation.

Table 4.8.8 Silver nitrate in benzyl cyanide - statistical analysis of the dissociation pressure

Column temp. °C	$10^3.\overline{p_d}$ atm.	$10^3.6$ atm.	$\frac{10^2.6}{\overline{p_d}}$
21.0	99.5(4)	1.8(8)	1.89
24.0	108.6(8)	2.0(8)	1.91
28.0	126.7(4)	1.5(2)	1.20
32.0	147.1(9)	3.1(4)	2.13
36.0	170.6(9)	2.5(8)	1.51

The values of the dissociation pressures for experiments 30 and 31 differ from the mean by more than twice the standard deviation, and are bracketed in table 4.8.7.

The values of the dissociation pressures of the higher plateau of the benzyl cyanide, and single plateau of the benzonitrile systems are very similar. However the values for the latter solvent are distinctly higher than for the former. This may be due to either or both of the following reasons

(a) the different solvents may account for the difference in the plateau heights.

(b) the fact that successive or competitive reactions occur in the benzyl cyanide solvent indicates that equation (22) has to be modified as follows:

(1) for a successive reaction (22) becomes

$$\overline{V_t}\left[\overline{NH_{3(g)}}\right] = \frac{(k_6 S_{III} - k_5 S_{II}\left[\overline{NH_{3(l)}}\right]^y + k_4 S_{II} - k_3 S_I\left[\overline{NH_{3(l)}}\right])V_g \cdot L_1}{L} \quad \ldots\ldots\ldots\ldots\ldots\ldots (42)$$

(2) for a competitive reaction (22) becomes

$$\overline{V_t}\left[\overline{NH_{3(g)}}\right] = \frac{(k_6 S_{III} - k_5 S_I\left[\overline{NH_{3(l)}}\right]^y + k_4 S_{II} - k_3 S_I\left[\overline{NH_{3(l)}}\right])V_g \cdot L_1}{L} \quad \ldots\ldots\ldots\ldots\ldots\ldots (43)$$

where S_{II} = surface area of solid complex responsible for the lower plateau

and S_{III} = surface area of solid complex responsible for the higher plateau.

Consider the case of the successive reaction. When the ammonia gas pressure is greater than the dissociation pressure

of complex III,

$(k_5 S_{II}[NH_{3(l)}]^y - k_6 S_{III}) > 0$, and $(k_3 S_I[NH_{3(l)}] - k_4 S_{II}) > 0$,

otherwise no appreciable amounts of the complexes would form. When the higher plateau appears,

$(k_5 S_{II}[NH_{3(l)}]^y - k_6 S_{III}) < 0$, but $(k_3 S_I[NH_{3(l)}] - k_4 S_{II}) > 0$

If $(k_3 S_I[NH_{3(l)}] - k_4 S_{II})$ is designated G, equation (42) becomes (when complex III is dissociating)

$$\overline{V_t}[NH_{3(g)}] = \frac{(k_6 S_{III} - k_5 S_{II}[NH_{3(l)}]^y - G)V_g \cdot L_1}{L} \quad \ldots\ldots\ldots (44)$$

Similarly for the case of the competitive reaction (43) becomes

$$\overline{V_t}[NH_{3(g)}] = \frac{(k_6 S_{III} - k_5 S_I[NH_{3(l)}]^y - G)\, V_g \cdot L_1}{L} \quad \ldots\ldots\ldots (45)$$

Both equations (44) and (45) indicate the possible reason for the lowered ammonia gas concentration by the inclusion of the negative G term.

In practice this means that three processes are competing for the unreacted liquid phase ammonia, viz., the reaction forming complex II, the reaction forming the dissociating complex III, and the transfer of ammonia from the liquid to the gas phase. Thus the net concentration of ammonia available for the phase transfer reaction is not sufficiently high to maintain the true plateau level, despite the fast decomposition rate of complex III.

Further support for the explanation (b) is provided by the increased dissociation pressure values obtained at extremely high sample sizes for packing S.N.B.C.(1) and shown by experiments 94, 95 and 96 in table 4.8.7. The extremely high amount of complex formed under such conditions suggests

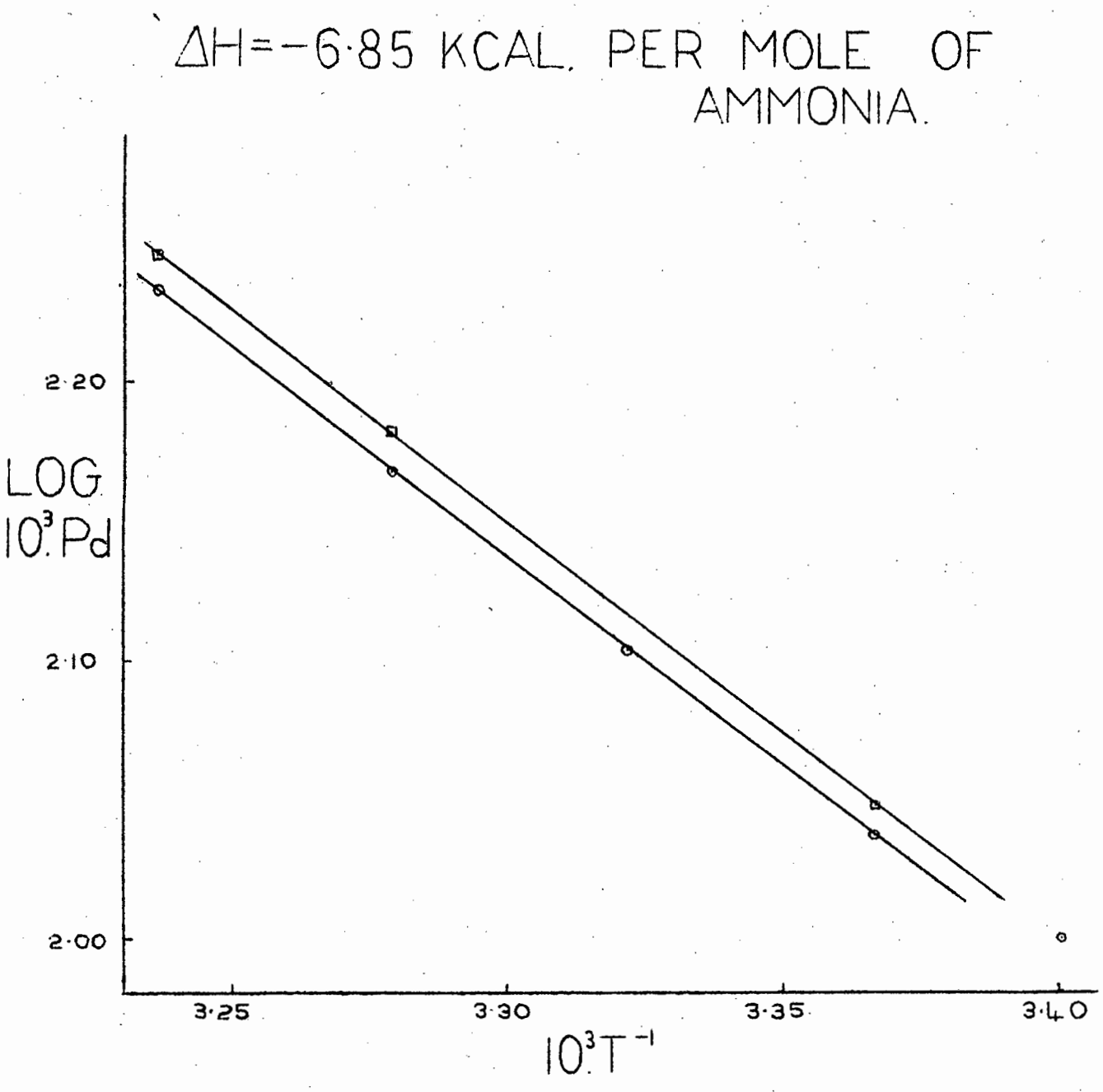

FIGURE 43. SILVER NITRATE IN BENZYL CYANIDE. TEMPERATURE PLOTS OF THE DISSOCIATION PRESSURES OF THE HIGHER PLATEAU.

a fast enough decomposition rate, (in spite of the successive or competitive reactions) which can maintain the increased upper plateau levels.

The quantitative treatment of the higher plateau can be carried out in the usual way, but the evaluation of the equilibrium function cannot be made, as the amount of complex II (in the case of the successive reaction) or complex I (in the case of the competitive reaction) associated with each of the reactions cannot be determined. This is due to the fact that the extrapolated quantities obtained for complex III are those under successive or competitive reaction conditions, while the extrapolated quantities for complex II (which emerges from the column once all of complex III has been eluted) are those obtained in the absence of successive or competing reactions.

The temperature plot of the dissociation pressures are shown in fig. 43. The lower graph is that obtained from the mean values (ΔH = - 6.82 Kcal), while the upper line is obtained from the high sample size results of experiments 94, 95 and 96 (ΔH = - 6.85 Kcal).

4.8.8 Stoichiometric interpretation

The experimental data obtained for this system indicate the occurrence of either of the processes shown in 4.8.7, p.96.

4.9 Ageing effects

After approximately two months storage in a dark cupboard, a solution of silver nitrate in benzonitrile was found to contain a precipitate of silver. A solution of silver nitrate in benzyl cyanide gave no precipitation but the colourless solution turned dark brown. A column

containing a low concentration of silver nitrate in benzonitrile (packing S.N.B.(4), 4.7.4) became inactive relative to the formation of plateau type chromatograms after about two months.

Thus it seems that some of these silver-organic solutions are unstable and give slow precipitation of the silver. The addition of ammonia causing the formation of solid complex I seems to prevent the precipitation of silver. However in a column such as S.N.B.(4) which had been treated with ammonia but allowed to stand unused for some time, slow decomposition of complex I would result, with subsequent precipitation of the silver.

Whether the silver precipitates out of solution, can be tested by determining the equilibrium function at some temperature, for a particular packing, at different time intervals, and seeing if there is any trend obtained in the equilibrium function values.

4.10 The toluidine isomers

It was found by du Plessis, when investigating the solubility of ammonia in various organic liquids, that m-toluidine showed abnormally high retention volumes for ammonia, which he attributed to possible hydrogen bonding between the nitrogen atoms of the two compounds[97].

It was decided to investigate this possible hydrogen bonding effect by comparing the solubility of ammonia in the toluidine isomers.

As p-toluidine solidifies at about 42°C, it was dissolved in benzonitrile, and the heats of solution of ammonia in benzonitrile/p-toluidine mixtures of various

compositions were determined over a temperature range of about 24° to 36°C. The heat of solution of ammonia in pure p-toluidine was found by extrapolating the plot of the heat of solution of ammonia as a function of molar percentage p-toluidine in the mixture to 100 mole percent.

The experimental points of the last mentioned plot were scattered, and to check whether a linear plot was justified, the other isomers (liquids) were mixed with benzonitrile and similar measurements and plots were made. The m-toluidine/ benzonitrile plot gave a straight line, but the o-toluidine/ benzonitrile plot did not. Linear plots were however made, as the variations in the values of the points showing a scatter about the straight line graphs were small, and were attributed to normal experimental errors, especially with the approximations made in the chromatographic method.

4.10.1 The packings

Table 4.10.1 gives details of the column packings used. All columns were approximately 90 cm in length.

Table 4.10.1 Column packings of the toluidine isomers

Packing	10^2.s (at 25°C) cm^3 gm^{-1}	Mole % benzonitrile in liquid phase
o - T.B.	2.86	41.23
o - T.	2.92	0
m - T.B.	3.02	50.49
m - T.	2.97	0
p - T.B(1)	2.84	65.06
p - T.B(2)	2.79	26.80

4.10.2 Results

Table 4.10.2 gives the results obtained. The value of the heat of solution of ammonia in pure benzonitrile was taken from 4.7.5 when drawing the necessary graphs.

Table 4.10.2 Results for the toluidine isomers

Column temp. °C	t_r min.	t_g min.	$t_r - t_g = t_f$ min.	$V^{o}_{R}{}'$ cm^3	V_f cm^3	K
Packing o-T.B. ΔH_1 = - 1.92 Kcal per mole of ammonia.						
25.9	6.6(9)	1.4(0)	5.2(9)	61.3(0)	1.89(3)	32.3(8)
29.0	6.8(4)	1.4(1)	5.4(2)	60.4(5)	1.89(8)	31.8(5)
32.0	6.6(4)	1.4(0)	5.2(4)	58.7(7)	1.90(3)	30.8(8)
36.0	5.9(1)	1.2(5)	4.6(6)	61.3(4)	1.91(0)	(32.1(2))
Packing o-T. ΔH_1 = - 2.21 Kcal per mole of ammonia.						
24.7	5.3(7)	1.3(4)	4.0(3)	59.8(8)	1.53(8)	38.9(3)
28.0	5.2(7)	1.4(1)	3.8(6)	55.3(5)	1.54(2)	35.9(0)
32.0	4.1(3)	1.0(8)	3.0(5)	55.1(6)	1.54(8)	35.6(3)
36.0	4.0(2)	1.1(1)	2.9(1)	52.7(4)	1.55(3)	33.9(6)
Packing m-T.B. ΔH_1 = - 2.38 Kcal per mole of ammonia						
24.6	6.5(0)	1.4(5)	5.0(5)	58.9(2)	1.34(8)	(43.7(1))
28.0	5.9(6)	1.2(5)	4.7(1)	65.3(5)	1.35(2)	48.3(4)
32.0	5.4(8)	1.1(7)	4.3(1)	61.6(3)	1.35(6)	45.4(5)
36.0	5.4(8)	1.2(3)	4.2(5)	59.0(1)	1.36(0)	43.3(9)
Packing m-T. ΔH_1 = - 2.95 Kcal per mole of ammonia.						
24.8	3.6(6)	0.8(8)	2.7(8)	61.6(8)	1.22(6)	50.3(1)
28.0	3.6(7)	0.9(4)	2.7(3)	58.6(2)	1.22(9)	47.6(9)
32.0	3.5(4)	0.9(4)	2.6(0)	55.2(0)	1.23(4)	44.7(3)
36.0	3.7(2)	0.9(7)	2.7(5)	57.9(2)	1.23(8)	(46.7(8))
Packing p-T.B.(1). ΔH_1 = - 1.97 Kcal per mole of ammonia						
24.9	5.6(3)	1.8(6)	3.7(7)	37.5(5)	1.25(4)	(29.9(5))
28.0	3.6(0)	1.3(0)	2.3(0)	32.3(0)	1.25(7)	25.7(0)
32.0	3.5(3)	1.3(3)	2.2(0)	30.9(5)	1.26(1)	24.5(5)
36.0	3.0(9)	1.1(8)	1.9(1)	29.9(8)	1.26(5)	23.7(0)
Packing p-T.B.(2). ΔH_1 = - 2.15 Kcal per mole of ammonia						
24.8	4.1(1)	1.2(5)	2.8(6)	36.5(8)	1.17(2)	31.2(1)
28.0	3.2(0)	1.0(2)	2.1(8)	35.4(6)	1.17(6)	30.1(5)
32.0	2.9(5)	0.8(9)	2.0(6)	34.2(2)	1.18(0)	29.0(0)
36.0	3.0(0)	0.94	2.0(6)	32.8(3)	1.18(5)	27.7(0)

The heat of solution of ammonia in pure p-toluidine, ΔH_1 (extrapolated value) = - 2.29 $\pm$ 0.05 Kcal per mole of ammonia.

4.10.3 Discussion of results

Hydrogen bonding between the amino groups of the toluidine isomers and ammonia can occur by either of the following processes

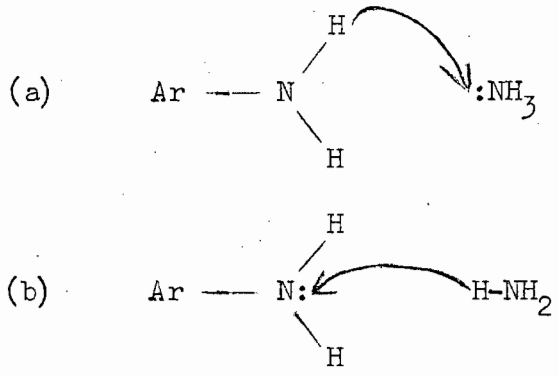

Whether process (a) or (b) occurs depends upon the relative electron densities of the nitrogen atoms of the respective compounds. Values of the acidic dissociation constants (K_a) of the toluidine isomers and ammonia in aqueous solution[98] shown in table 4.10.3 suggest that process (a) is far more likely to occur than process (b).

Table 4.10.3 Acidic strengths of the toluidine isomers and ammonia

Substance	$10^5 . K_a$ (at 25.0°C)	ΔH_1 Kcal
o - T	4.07	-2.21
m - T	2.04	-2.95
p - T	0.85	-2.29
NH_3	5.62×10^{-5}	-

Thus the solubility of ammonia in the toluidine isomers should increase with increasing K_a values of the isomers, and a similar increase should be found in the magnitudes of ΔH_1. However the value of ΔH_1 for o-toluidine does not obey the expected trend, and this is attributed to steric effects, the

proximity of the methyl group hindering the H ..... N bond association of ammonia with the amino group. Therefore, despite o-toluidine being the most acidic of the isomers, the solubility of ammonia in o-toluidine is reduced with a corresponding drop in the value of ΔH_1.

If process (b) occurred this steric effect would be expected to a lesser degree, as it only requires the "closest approach" of a peripheral hydrogen of the ammonia molecule to effect the N ..... H bond association.

SECTION 5

CONCLUSION

In the first part of this section, the results of the various salt-solvent systems are correlated and the work done discussed, while in the second part proposals for future work are suggested.

5.1 Correlation of results, and discussion of the work done

The quantitative methods applied to the plateau type chromatograms have led to results similar to those expected on theoretical grounds, and which are summarised in table 5.1.1.

Table 5.1.1 Correlated salt-solvent results

Salt-solvent system	$10^3 . p_d$ (at 32.0°C) atm.	ΔH Kcal per mole of ammonia	$NH_3 : AgX(NH_3)_x$ =y
S.N.B.C. (lower plateau)	14.3(3)	-13.73	1
S.P.T.	83.0(1)	- 8.41	2
S.P.F.	87.2(4)	- 7.51	3
S.N.B.	157.0(5)	- 6.57	4
S.N.B.C. (higher plateau)	152.0(6)	- 6.85	?

Gas-liquid chromatography thus provides a means not only of detecting the formation of solid ammine complexes, but also of elucidating the processes which occur, perhaps not completely but to a very considerable degree. The key to the study of these complexes lies in the unique shape of their chromatograms, and kinetic considerations as well as phase rule interpretation of the plateau portion of these chromatograms, have not only yielded quantitative information on the complexes, but have accounted for rate-effects exhibited by the chromatograms.

Firstly, the solvent plays an extremely important part in complex formation. Its presence radically affects the

5.2 Proposals for future work

Two proposals are made :

(a) investigation of the importance of the solvent can be made by studying closely related solvent types, such as the homologues of benzonitrile, and the tolunitriles.

(b) the accurate quantitative analysis of the chromatograms is subject to the uncertainty in the location of the dividing line between zone II(a) and II(b), especially where rate-effects are manifested. Furthermore, an extremely large number of area measurements and calculations are required in determining F(K) which makes the method both laborious and time consuming.

It is believed that an alternative procedure may be applied to the study of these complexes, based on the work of Muhs and Weiss[33], described in 1.2. Their equation (eqn. (1), p.5) derived for homogeneous liquid phase complexing reactions can be modified for solid ammine complex formation to

$$V_f K' = V_f \cdot K + K \cdot F(K) \cdot (n_I)^q \quad \ldots\ldots\ldots\ldots\ldots\ldots\ldots\ldots \quad (46)$$

where $F(K) = \frac{k_3}{k_4} \cdot \frac{(C_I)^q}{C_{II}} = \frac{n_{II}}{(n_I - qn_{II})^q \left[\frac{n_{NH_3} - n_{II}}{V_f}\right]} \quad \ldots\ldots \quad (47)$

and q = molar ratio of silver to ammonia (i.e., $q = (y)^{-1}$).

Since $(n_I - qn_{II}) \simeq n_I$ (see appendix II, p.120)

(47) becomes

$$F(K) = \frac{n_{II}}{(n_I)^q \left[\frac{n_{NH_3} - n_{II}}{V_f}\right]}$$

and this form of F(K) is used in deriving (46).

The experimental procedure would consist of injecting a very small amount of ammonia into the column (all of the silver having already been converted into the complex I form) resulting in a normal type elution curve having a peak maximum whose retention volume would be some function of the complexing process, and would obey equation (13).

When there are rate-controlling steps present in the complexing process, the retention volume of the peak maximum of the chromatogram should become flow-rate dependent and equation (46) must be modified to

$$V_f K' = V_f \cdot K + K \cdot F(K) \cdot (n_I)^q - \frac{K \overline{V_t}'}{k_4 C_{II} \Delta V_g} \quad \ldots\ldots\ldots\ldots\ldots (48)$$

where ΔV_g = average interstitial volume of column occupied by the ammonia band

and $\overline{V_t}'$ = average volumetric flow-rate of carrier gas in the column.

(The derivation of (48) is given in appendix II)

Two cases may be discerned:

(1) when the rate of formation of the complex is slow, $V^o_R{}'$ (retention volume of the maximum peak height) will decrease with increasing flow-rate, and a plot of $V_f K'$ as a function of flow-rate should give a curve having a limiting maximum value of $V_f K'$ at zero flow-rate.

(2) when the rate of decomposition of the complex is slow, $V^o_R{}'$ will increase with increasing flow-rate, and the plot of $V_f K'$ as a function of flow-rate should give a curve having a limiting minimum value of $V_f K'$ at zero flow-rate.

Once K' at zero flow-rate is obtained, equation (46) is utilized, and a plot of $V_f \cdot K'$ against $(n_I)^q$ for a series of

columns differing widely in silver content should give a straight line for the correct insertion of the value of q. No salting-out effect should be observed, because all the silver salt is in the solid complex I form. F(K) can then be obtained from the slope.

If more than one complex is formed, as for example in the S.N.B.C. system, (46) becomes, for successive reactions,

$$V_f K' = V_f \cdot K + K \cdot F(K_1) \cdot (n_I)^{q_1} + K \cdot F(K_1) \cdot F(K_2) \cdot (n_I)^{q_1 - q_2}$$

and for competitive reactions,

$$V_f K' = V_f \cdot K + K \cdot F(K_1) (n_I)^{q_1} + K \cdot F(K_2) (n_I)^{q_2}$$

Where rate-effects occur in systems forming two or more complexes having discernible p_d values, the necessary formulae can be derived on the basis of the treatment given for equation (48) in appendix II.

BIBLIOGRAPHY

(1) "Principles and Practice of Gas Chromatography", John Wiley and Sons, Inc., New York, (ed. R.L. Pecsok). 1959, p.1.

(2) Keulemans, A.I.M., "Gas Chromatography", Reinhold Publishing Corporation, New York, 1959, p.9.

(3) Martin, A.J.P., and Synge, R.L.M., Biochem. J. (1941), 35, 1358.

(4) James, A.T., and Martin A.J.P., ibid., (1952), 50, 679.

(5) Tiselius, A., Arkiv. Kemi. Min. Geol. (1943), 16A, 11.

(6) Claesson, S., Disc. Faraday Soc., (1949), 7, 34.

(7) James, D.H., and Phillips, C.S.G., J. Chem. Soc., (1953), 1600.

(8) Griffiths, J.H., and Phillips, C.S.G., ibid., (1954), 3446.

(9) Claesson, S., Arkiv. Kemi. Min. Geol. (1946), 23A, 133.

(10) Turner, N.C., Natl. Petrol. News, (1943), 35, 234.

(11) Niegisch, W.D., and Stahl, W.H., Food Research, (1956), 21, 657.

(12) van Deemter, J.J., Zuiderweg, F.J., and Klinkenberg, A., Chem. Eng. Sci., (1956), 5, 271.

(13) Golay, M., Anal. Chem., (1957), 29, 928.

(14) Golay, M., "Gas Chromatography", Butterworths Scientific Publications, London, 1958, p.36.

(15) Golay, M., ibid., p.53.

(16) Karchmer, J.H., Anal. Chem., (1959), 31, 1377.

(17) Janak, J., and Komers, R., "Gas Chromatography", Butterworths Scientific Publications, London, 1958, p. 343.

(18) James, A.T., J. Chromatog., (1959), 2, 552.

(19) Beaven, G.H., James, A.T., and Johnson, E.A., Nature, (1957), 179, 490.

(20) Langer, S.H., Zahn, C., and Pantazoplos, G., J. Chromatog., (1960), 3, 154.

(21) Janak, J., and Hrivnac, M., ibid., (1960), 3, 297.

(22) Maczek, A.O.S., and Phillips, C.G.S., "Gas Chromatography", Butterworths Scientific Publications, London, 1960, p.284.

(23) Barber, D.W., Phillips, C.S.G., Tusa, G.F., and Verdin, A., J. Chem. Soc. (1959), 1, 18.

(24) Cartohi, G.P., Lowrie, R.S., Phillips, C.G.S., and Venanzi, L.M., "Gas Chromatography", Butterworths Scientific Publications, London, 1960, p.273.

(25) Bradford, B.W., Harvey, D., and Chalkley, D.E., J. Inst. Petrol. (1955) 41, 80.

(26) Gil-Av, E., Herling, J., and Shabtai, J., J. Chromatog., (1958), 1, 508.

(27) Shabtai, J., Herling, J., and Gil-Av. E., ibid., (1959), 2, 406.

(28) Rijnders, G.W.A., Chem. Weekblad, (1958), 54, 669.

(29) Tenny, H.M., Anal. Chem., (1958), 30, 2.

(30) van de Craats, Analyt. Chim. Acta., (1956), 14, 136.

(31) Phillips, C., "Gas Chromatography", Academic Press Inc., New York, 1958, p.58.

(32) Bednas, M.E., and Russel, D.S., Can. J. Chem. (1958), 36, 1272.

(33) Muhs, M.A., and Weiss, F.T., J. Am. Chem. Soc. (1962), 84, 4697.

(34) Gil-Av., E., and Herling, J., J. Phys Chem. (1962), 66, 1208.

(35) Gil-Av., E., and Herzberg-Minzly, Y., Proc. Chem. Soc. (London), (1961), 316.

(36) Kokes, R.J., Tobin Jr., H., and Emmett, P.H., J. Am. Chem. Soc., (1955), 77, 5860.

(37) Keith Hall, W., and Emmett, P.H., ibid., (1957), 79, 2091.

(38) Keith Hall, W., and Emmett, P.H., J. Phys. Chem. (1959), 63, 1102.

(39) Keulemans, A.I.M., and Voge, H.H., ibid., (1959), 63, 476.

(40) Greene, S.A., J. Chem. Ed. (1957), 34, 194.

(41) Hewitt, G.C., and Whitham, B.T., Analyst, (1961), 86, 643.

(42) Tamaru, K., Nature (1959), 183, 319.

(43) Bassett, D.W., and Habgood, H.W., J. Phys. Chem. (1960), 64, 769.

(44) Derby, I.H., and Yngve, V., J. Am. Chem. Soc. (1916), 38, 1439.

(45) Caven, R.M., and Ferguson, J., J. Chem., Soc., (1922), 121, 1408.

(46) Gillespie, L.J., and Lurie, E., J. Am. Chem. Soc., (1931), 53, 2978.

(47) Hart, A.B., and Partington, J.R., J. Chem. Soc., (1943) 104.

(48) Fowles, G.W.A., and Pollard, F.H., ibid., (1952), 4938.

(49) Allen, J.A., and Scaife, D.E., J. Phys.Chem. (1953), 57, 863.

(50) Watt, G.W. and McBride, W.R., J. Am. Chem. Soc., (1955), 77, 1317.

(51) Miller, D.B., and Sisler, H.H., ibid., (1955), 77, 4998.

(52) Keefer, R.M., Andrews, L.J., and Kepner, R.E., ibid., (1949), 71, 3906.

(53) Cope, A.C., and Kintner, M.R., ibid., (1950), 72, 630.

(54) Cope, A.C., and Hochstein, F.A., ibid., (1950), 72, 2515.

(55) Cope, A.C., Mclean, D.C., and Nelson, N.A., ibid., (1955), 77, 1628.

(56) Cope, A.C., and Moore, W.R., ibid., (1955), 77, 4939.

(57) Jones, W.O., J. Chem. Soc., (1954), 312, 1808.

(58) Slade Jr., P.E., and Jonassen, H.B., J. Am. Chem. Soc., (1957), 79, 1277.

(59) Traynham, S.G., and Olechowski, J., ibid, (1959), 81, 571.

(60) Abel, E.W., Bennet, M.A., and Wilkinson, G., J. Chem. Soc., (1959), 3178.

(61) Traynham, J.G., J. Org. Chem., (1961), 26, 4694.

(62) Kraus, J.W., and Stern, E.W., J. Am. Chem. Soc., (1962), 84, 2893.

(63) du Plessis, L.A., Ph.D. Thesis, University of Cape Town, (1959), p.74.

(64) du Plessis, L.A., ibid.

(65) du Plessis, L.A. and Spong, A.H., J. Chem. Soc., (1959), 2027.

(66) Keulemans, A.I.M., "Gas Chromatography", Reinhold Publishing Corporation, New York, 1959, Chapter 5.

(67) Porter, P.E., Deal, C.H., and Stross, F.H., J. Am. Chem. Soc., (1956), 78, 2999.

(68) Littlewood, A.B., Phillips, C.S.G., and Price, D.T., J. Chem. Soc., (1955), 1480.

(69) Hardy, C.J., J. Chromatog., (1959), 2, 490.

(70) Kwantes, A., and Rijnders, G.W.A., "Gas Chromatography", Butterworths Scientific Publications, London, 1958, p.125.

(71) Adlard, E.R., Khan, M.A., and Whitham, B.T., ibid., London, 1960, p.251.

(72) Everett, D.H., and Stoddart, C.T.H., Trans. Faraday Soc., (1961), 57, 746.

(73) "Gas Chromatography", Butterworths Scientific Publications, London, 1960, p.427.

(74) Ambrose, D., Keulemans, A.I.M., and Purnell, J.H., Anal. Chem., (1958), 30, 1582.

(75) Hoare, M.R. and Purnell, J.H., Trans. Faraday Soc., (1956), 52, 222.

(76) Hoare, M.R., and Purnell, J.H., Research, (1955), 8, S41.

(77) Pollard, F.H. and Hardy, C.J., "Vapour Phase Chromatography", Butterworths Scientific Publications, London, 1957, p.115.

(78) Pyke, B.H., and Swinbourne, E.S., Australian J. Chem., (1959), 12, 104.

(79) Keulemans, A.I.M., "Gas Chromatography", Reinhold Publishing Corporation, New York, 1959, p.188.

(80) Bohemen, J., and Purnell, J.H., "Gas Chromatography", Butterworths Scientific Publications, London, 1958, p.6.

(81) Bethea, R.M. and Smutz, M., Anal. Chem. (1959), 31, 1211.

(82) Bayer, E., "Gaschromatographie", Springer - Verlag, Berlin, Gottingen, Heidelberg, 1959, p.31.

(83) du Plessis, L.A., Ph.D. thesis, University of Cape Town, 1959, p.107, 116.

(84) du Plessis, L.A., ibid., p.16.

(85) du Plessis, L.A., ibid, p.19, 20.

(86) du Plessis, L.A., ibid., p.68.

(87) James, D.H. and Phillips, C.S.G., J. Sci. Instrum. (1952), 29, 362.

(88) Keulemans, A.I.M., "Gas Chromatography", Reinhold Publishing Corporation, New York, 1959, p.59.

(89) van de Craats, F., "Gas Chromatography", Butterworths Scientific Publications, London, 1958, p.251.

(90) "International Critical Tables", (first edition), Vol. III, 1928, p.28.

(91) Findlay, A., "Practical Physical Chemistry", Longmans, Green and Co., London, p.71 - 74.

(92) du Plessis, L.A., Ph. D. thesis, University of Cape Town, 1959, p.37.

(93) Littlewood, A.B. "Gas Chromatography", Butterworths Scientific Publications, London, 1958, p.23.

(94) Stability Constants, Part 1, Organic Ligands. The Chem. Soc. London, Special Publication No. 6, p.54.

(95) "Principles and Practice of Gas Chromatography", John Wiley and Sons, Inc., New York, (ed. R.L. Pecsok), p.41.

(96) Ambrose, D., and Ambrose, D.A., "Gas Chromatography", George Newnes, Ltd., London, 1961, p.99.

(97) du Plessis, L.A., Ph.D. thesis, University of Cape Town, 1959, p.46.

(98) Conway, B.E., "Electrochemical Data", Elsevier Publishing Company, London, 1952, p.186, 188.

APPENDIX I

Table I shows the values of y obtained for the S.N.B. system by du Plessis' method. All other systems showed similar results.

Table I Determination of y by du Plessis' method

Expt. no.	Packing S.N.B.	Flow-rate $cm^3\ min^{-1}$	y
Sample size of ammonia, (412 - 418) µmole, column temperature, 21.0°C			
2	(1)	6.9(3)	0.75
4	(1)	23.5(5)	0.72
7	(1)	38.2(4)	0.72
34	(2)	6.7(3)	0.85
35	(2)	26.8(8)	0.84
37	(2)	40.3(7)	0.83
64	(3)	6.2(4)	1.44
66	(3)	21.6(9)	1.43
69	(3)	38.5(2)	1.39
96	(4)	6.9(4)	3.34
98	(4)	20.6(1)	3.33
100	(4)	38.6(1)	3.30

APPENDIX II

Equation (48) can be derived by considering the following process occurring in the chromatographic column :

$$NH_{3(g)} \underset{k_2}{\overset{k_1}{\rightleftharpoons}} NH_{3(l)} \quad \ldots\ldots\ldots\ldots\ldots\ldots\ldots\ldots\ldots\ldots\ldots\ldots (B)$$

$$q\,AgX'_{(s)} + NH_{3(l)} \underset{k_4}{\overset{k_3}{\rightleftharpoons}} (AgX'_{(q)} \cdot NH_3)_{(s)} \quad \ldots\ldots\ldots\ldots\ldots\ldots\ldots (C)$$

where $AgX'_{(s)} = AgX(NH_3)_x$

Reaction (B) is considered instantaneous, while one of the stops of (C) is rate-controlling.

A material balance of ammonia in the gas phase gives

$$\frac{d[NH_{3(g)}]}{dt} = -k_1[NH_{3(g)}] + k_2[NH_{3(l)}] - \frac{[NH_{3(g)}]\overline{V_t'}}{\Delta V_g} \quad \ldots\ldots (49)$$

For the liquid phase

$$\frac{d[NH_{3(l)}]}{dt} = -k_3[NH_{3(l)}](S_I)^q + k_4 S_{II} + k_1[NH_{3(g)}] - k_2[NH_{3(l)}] \quad \ldots\ldots (50)$$

$$\text{now} \quad \frac{d[NH_{3(l)}]}{dt} = \frac{d}{dt}\left([NH_{3(g)}]\cdot\frac{[NH_{3(l)}]}{[NH_{3(g)}]}\right) = K\,\frac{d[NH_{3(g)}]}{dt} \quad \ldots\ldots\ldots\ldots (51)$$

Substituting (49) and (50) in (51) yields

$$K\left(-k_1[NH_{3(g)}] + k_2[NH_{3(l)}] - \frac{[NH_{3(g)}]\overline{V_t'}}{\Delta V_g}\right) = -k_3[NH_{3(l)}](S_I)^q + k_4 S_{II} + k_1[NH_{3(g)}] - k_2[NH_{3(l)}] \quad \ldots\ldots\ldots\ldots\ldots\ldots\ldots\ldots (52)$$

Rearranging (52)

$$[NH_{3(l)}](K+1)(-k_1 + k_2 K) - \frac{[NH_{3(g)}]K\,\overline{V_t'}}{\Delta V_g} = -k_3[NH_{3(l)}](S_I)^q + k_4 S_{II} \quad \ldots\ldots\ldots\ldots\ldots\ldots\ldots\ldots\ldots\ldots\ldots\ldots\ldots\ldots\ldots\ldots\ldots\ldots (53)$$

Now $-k_1 + k_2K = -k_1 + k_2 \cdot \frac{k_1}{k_2} = 0$

Thus dividing (53) by $\boxed{\overline{NH_{3(g)}}}$

$$-\frac{K\,\overline{V_t}'}{\Delta V_g} = -k_3 \cdot K \cdot (C_I)^q (n_I - qn_{II})^q + k_4 \cdot K \cdot C_{II} F(K)_{app.} \cdot (n_I - qn_{II})^q \quad ..(54)$$

where $F(K)_{app.}$ is the apparent flow dependent equilibrium function of reaction (C), due to the fact that one of the steps of reaction (C) is rate-controlling, and is defined as

$$F(K)_{app.} = \frac{n_{II}}{(n_I - qn_{II})^q \left[\frac{n_{NH_3} - n_{II}}{V_f}\right]} = \frac{n_{II}}{(n_I - qn_{II})^q \boxed{\overline{NH_{3(l)}}}} \quad .....(55)$$

Now $(n_I - qn_{II}) \simeq n_I$ to an extremely good approximation as the amount of complex II formed in the column by the small amount of ammonia injected, will be negligible compared with the amount of complex I present in the column.

Rearranging (54) thus gives

$$F(K)_{app.} = \frac{k_3 \cdot K \cdot (C_I)^q (n_I)^q - \frac{K\,V_t'}{\Delta V_g}}{k_4 \cdot K \cdot C_{II} (n_I)^q} \quad .....(56)$$

and (55) reduces to

$$F(K)_{app.} = \frac{n_{II}}{(n_I)^q \boxed{\overline{NH_{3(l)}}}} \quad .....(57)$$

At zero flow-rate (56) reduces to $\frac{k_3}{k_4} \cdot \frac{(C_I)^q}{C_{II}} = F(K)$

The overall partition coefficient K' at a particular flow-rate is defined as

$$K' = \frac{(NH_{3(l)} + n_{II})\ V_g}{NH_{3(g)} \cdot V_f}$$

which gives on inserting (57)

$$K' = K + \frac{K \cdot F(K)_{app.} \cdot (n_I)^q}{V_f}$$

and thus

$$V_f \cdot K' = V_f K + K \cdot F(K)_{app.} \cdot (n_I)^q \quad \ldots\ldots\ldots\ldots\ldots\ldots\ldots\ldots\ldots\ldots (58)$$

Substituting (56) in (58) yields

$$V_f \cdot K' = V_f \cdot K + K \cdot F(K) \cdot (n_I)^q - \frac{K \cdot \overline{V_t}'}{k_4 \cdot C_{II} \cdot \Delta V_g} \quad \ldots\ldots\ldots\ldots\ldots\ldots (48)$$